

AUS DER MEDIZINISCHEN KLINIK UND POLIKLINIK I LUDWIG-  
MAXIMILIANS-UNIVERSITÄT MÜNCHEN



Dissertation  
zum Erwerb des Doctor of Philosophy (Ph.D.)  
an der Medizinischen Fakultät der  
Ludwig-Maximilians-Universität zu München

***The developmental origins of macrophages define their  
metabolic and inflammatory properties***

vorgelegt von:

Sara Rahamatalla Mohamed Elhag

aus:

Alkamline, Sudan

Jahr:

2022

Mit Genehmigung der Medizinischen Fakultät der  
Ludwig-Maximilians-Universität zu München

**First evaluator:** *Prof. Dr. med. Christian Schulz*  
**Second evaluator:** *Prof. Dr. Barbara Schraml*  
**Third evaluator:** *Prof. Dr. Christian Weber*  
**Fourth evaluator:** *Priv. Doz. Dr. Anne Hilgendorff*

**Dean:** **Prof. Dr. med. Thomas Gudermann**

date of the defense:

08.04.2022

## **DEDICATION**

I dedicate this work in memory of my mother, from whom I learned to be the ambitious strong person I am. To my father for his ongoing love and support. To my beloved sisters and all my family members.

## Table of contents

Abstract .....	VI
List of Figures .....	VII
List of abbreviations .....	IX
1. Introduction and literature review .....	1
1.1 Macrophages .....	1
1.2 Origin of tissue resident macrophages .....	1
1.3 Macrophage activation .....	3
1.4 Macrophage heterogeneity and tissue microenvironment programming .....	4
1.5 Phagocytosis .....	6
1.6 Cell death .....	7
1.7 Immunometabolism and metabolic reprogramming .....	8
1.8 The inflammasomes .....	11
1.8.1 The NLRP3 inflammasome .....	11
1.9 ER-hoxb8 .....	14
1.10 Research Rational .....	14
2. Materials and methods .....	16
2.1 Table of materials and software .....	16
2.2 Experimental model and subject details .....	23
2.2.1 Mice .....	23
2.2.2 Cell lines .....	24
2.3 Methodology .....	26
2.3.1 Generation of SCF supernatant .....	26
2.3.2 Thawing and culturing HoxB8 progenitor cells .....	27
2.3.3 Determination of cell counts .....	27
2.3.4 Growth curve .....	27
2.3.5 Differentiation of ER-Hoxb8 progenitors to Macrophages .....	28
2.3.6 Detachment of differentiated adherent cells .....	28
2.3.7 Flow cytometry .....	28
2.3.8 Giemsa May-Grünwald stain .....	29
2.3.9 Immunofluorescence staining .....	29
2.3.10 Phagocytosis assay .....	29
2.3.11 Gene expression analyses .....	30

2.3.12	Lysate collection for transcriptome and proteome analyses.....	30
2.3.13	RNA sequencing and data analysis.....	30
2.3.14	Protein profiling by mass spectrometry.....	32
2.3.15	UV and FasL induced cell death assays.....	33
2.3.16	Extracellular flux XF96 Seahorse measurement .....	34
2.3.17	Multiplex immunoassays.....	35
2.3.18	Cholesterol monohydrate crystals preparation .....	36
2.3.19	Monosodium urate crystals preparation.....	36
2.3.20	IL1 $\beta$ quantification using ELISA.....	37
2.3.21	Western blotting .....	37
2.3.22	Quantification and statistical analysis .....	38
3.	Results .....	39
3.1	Characterization of E9.5 YS progenitors .....	39
3.2	Immortalization of YS and BM hematopoietic progenitors using conditional Hoxb8 .....	40
3.3	Characterization of YS and BM hoxb8 progenitors.....	41
3.4	YS and BM Hoxb8 cell lines differentiation, morphology and phagocytic capacity .....	43
3.5	BM and YS Hoxb8 macrophages response to cell death stimuli.....	48
3.6	Comparison of Transcriptome of BM and YS Hoxb8 macrophages.....	50
3.7	Proteome analysis of BM and YS Hoxb8 macrophages.....	54
3.8	Comparison of YS and BM derived macrophage energy metabolism.....	56
3.9	Cytokine secretion and Inflammasome activation .....	64
4.	Discussion.....	70
4.1	Methods .....	70
4.2	Results .....	72
5.	Conclusions.....	77
	References .....	79
	Appendix .....	90
	Acknowledgements .....	91
	Publications and scientific presentations .....	92
	Publications .....	92
	Scientific presentations .....	92
	Affidavit.....	93
	Confirmation of congruency between printed and electronic version of the doctoral thesis	94

## **Abstract**

It is established that tissue resident macrophages have mixed developmental origins in most organs. They derive in variable extent from yolk sac (YS) hematopoiesis during embryonic development. Bone marrow (BM) hematopoietic progenitors give rise to tissue macrophages in postnatal life, and their contribution increases upon organ injury.

Tissue resident macrophages are in perpetual interplay with their surroundings; thus, they are continuously reprogrammed by the microenvironment of their tissue of residence in order to serve immunologic and tissue specific functions. However, in tissue where macrophages are programmed to keep tissue homeostasis and other tissue specialized features, gene expression profiling and epigenetic landscape data revealed that heterogeneity among macrophage population exists, a property that could be attributed to distinct cells origin. Nevertheless, whether YS- and BM-derived macrophages functional properties and their contributions in their tissue of residence homeostasis or in the event microbial or inflammatory challenge varies, still remains to be shown and represents a significant question with major clinical importance.

In order to decipher cell-intrinsic macrophage programs that are independent of the tissue environment, we immortalized hematopoietic progenitors from YS and BM using conditional homeobox protein Hox-B8 (Hoxb8) and carried out an in-depth functional and molecular analysis of differentiated macrophages. While YS and BM macrophages demonstrate close similarities in cellular growth, differentiation, phagocytic properties, migration velocity and their susceptibility to cell death inducers they display differences in cell metabolism, expression of inflammatory markers, and inflammasome activation. Thus, macrophage ontogeny is associated with distinct cellular programs and immune response.

## List of Figures

Figure 1.1: Illustration summarizes the main metabolic changes in M1 and M2 macrophages. ....	10
Figure 1.2: Mechanisms of NLRP3 inflammasome activation.....	13
Figure 3.1: Flow cytometry analysis of expression patterns of early E9.5 hematopoietic cells in the YS membrane. ....	39
Figure 3.2: Gene expression comparison of YS progenitors from E9.5 yolk sac membrane to same age embryo.....	40
Figure 3.3: Gene expression analysis.....	42
Figure 3.4: Growth curve for YS and BM Hoxb8 progenitors.....	43
Figure 3.5: Bright field images of Hoxb8 cell lines during the process of macrophage differentiation..	44
Figure 3.6: macrophage morphology in May-Grünwald-Giesma stained smears. ....	45
Figure 3.7: Flow cytometry analysis of floating or adherent differentiated Hoxb8 BM cells..	46
Figure 3.8: Representative epifluorescence microscopy images of <i>Hoxb8</i> macrophages.....	46
Figure 3.9: Flow cytometry analyses of Hoxb8 progenitors in the process of differentiation towards macrophages. (d0 to d6) labelled with indicated antibodies (a representative experiment of n=3).47	
Figure 3.10: Phagocytosis assay.....	48
Figure 3.11: YS and BM macrophages response to cell death stimuli. ....	49
Figure 3.12: Principal Component Analysis (PCA) of progenitors and differentiated BM and YS under steady state and LPS and IL4 stimulation. ....	50
Figure 3.13: MA-plot of macrophage gene expression.....	51
Figure 3.14: Fold upregulation of selected genes in BM and YS-derived macrophages.....	52
Figure 3.15: Heatmap showing the top 25 upregulated genes in BM compared to YS macrophages..	53
figure 3.16 Heatmap showing the top 25 downregulated genes in BM compared to YS macrophages.	54
Figure 3.17: Proteome analysis of day 5 differentiated Hoxb8 macrophages.....	55
Figure 3.18: Top 10 upregulated proteins in BM and YS macrophages after LPS stimulation..	56
Figure 3.19: Oxygen Consumption Rate (OCR). ....	58
Figure 3.20: Mitochondrial efficiency. ....	59

Figure 3.21: ECAR linked to glycolytic activity of unstimulated and stimulated macrophages. ....	60
Figure 3.22: Comparison of total ATP Demand/turnover between BM and YS macrophages. ....	61
Figure 3.23: Partitioning of ATP production. ....	62
Figure 3.24: BM and YS macrophages metabolic switch following LPS and IL4 stimulation. ....	63
Figure 3.25: Cytokine expression analysis by Multiplex ELISA. ....	64
Figure 3.26: Measurement of IL-1 $\beta$ in cell culture supernatants after stimulation with LPS followed by MSU, CH and BIL crystals. ....	66
Figure 3.27: Quantification of NLRP3 inflammasome proteins in BM and YS macrophage cells lysate after stimulation with LPS followed by MSU crystals. ....	68
Figure 3.28: Measurement of IL-1 $\beta$ in cell culture supernatants after stimulation with <i>E. coli</i> OMVs. ....	69

## List of abbreviations

2DG	2-deoxy-glucose
AA	Antimycin A
AGM	Aorto-gonado-mesonephros
ASC	Apoptosis-associated speck-like protein containing a CARD
ATP	Adenosine triphosphate
BIL	Bilirubin
BM	Bone marrow
BSA	Bovine serum albumin
cDNA	Complementary DNA
CE	Coupling efficiency
CH	Cholesterol
CHO	Chinese hamster ovary cells
CNS	Central nervous system
cRCR	Cellular respiratory control ratio
CSF1r	Colony stimulating factor 1 receptor
DAMPs	Damage-associated molecular patterns

DNA	Deoxyribonucleic acid
DNP	2,4-Dinitrophenol
dsDNA	Double stranded DNA
E10.5	Embryonic day 10.5
E12.5	Embryonic day 12.5
E7.5	Embryonic day
E8	Embryonic day 8
E9.5	Embryonic day 9.5
ECAR	Extracellular acidification rate
ER	Endoplasmic reticulum
ER-Hoxb8	Estrogen-regulated Hoxb8
FCS	Fetal calf serum
GM-CSF	Granulocyte-macrophage colony stimulating factor
HSC	Hemopoietic stem cells
IFN- $\beta$	Interferon beta
IFN- $\gamma$	Interferon gamma
IL-10	Interleukin 10

IL-12	Interleukin 12
IL-1 $\beta$	Interleukin 1 beta
IL34	Interleukin 34
IL-4	Interleukin 4
IL-6	Interleukin 6
IL-8	Interleukin 8
LDTFs	Lineage-determining factors
LPS	Lipopolysaccharides
M-CSF	Macrophage colony stimulating factor
MHC	Major histocompatibility complex
MPS	Mononuclear Phagocyte System
MSU	Monosodium urate
NLRP3	NOD-, LRR- and pyrin domain-containing protein 3
OCR	Oxygen consumption rate
OMVs	Outer membrane vesicles
PAMP	Pathogen associated molecular pattern
PBS	Phosphate buffer saline

PDMS	Polydimethylsiloxane
PFA	Paraformaldehyde
PRR	Pattern recognition receptor
PS	Phosphatidylserine
R	Rotenone
RNA	Ribonucleic acid
SCF	Stem cell factor
TCA	Tricarboxylic acid cycle
Th1	T helper 1
Th17	T helper 17
Th2	T helper 2
TLR	Toll-like receptor
TLR4	Toll-like receptor 4
TNF	Tumor necrosis factor
TSTFs	Tissue-specific transcription factors
UV	Ultra violet

YS

Yolk sac

# **1. Introduction and literature review**

## **1.1 Macrophages**

Macrophages are important members of the innate and adaptive immunity (Junt, 2007; Thompson, 2011). Being uniquely armed with a massive pattern of receptors, high phagocytic capacity as well as the ability to release cytokines, macrophages play a key role in host defence against pathogens. For instance, their phagocytic properties are important for the clearance of dead cells and cellular debris, which contributes to the maintenance of homeostasis (Flannagan, 2012). Macrophages are diverse in their functions. Within organs, macrophages provide tissue specific functions such as the resorption of bone, erythrocyte clearance (spleen, liver), collagen degradation (arteries), clearance of surfactant (lung) as well as metabolic features (Davies, 2013). Moreover, they can both promote or inhibit inflammatory processes through release of cytokines and therefore play an important role in tissue remodelling (Wynn, 2010, 2016). Thus, macrophages are important for the physiological functionality of the tissues in addition to their significant role in infection and tissue damage (Zani, 2015). The heterogeneity of macrophages, which is in part associated with their developmental paths, is the subject of this research project.

## **1.2 Origin of tissue resident macrophages**

Classically, macrophages are described as a member of the mononuclear phagocyte system (MPS) (Klein, 2007; Okabe, 2018) that derives from circulating monocytes, originating from bone marrow (BM) progenitors. Recently, the origins and distribution of macrophages within tissues during the process of development have been an area of

extensive research. Using microarray, proteomic analysis, fate mapping and gene expression patterns, researchers were able to reverse many aspects of the perception regarding the origin and the heterogeneity of tissue resident macrophages.

Based on a study by Moore and Metcalf, the yolk sac has been described as the main source of definitive haematopoiesis as early as 1970, where E7.5 mice embryos were cultured for a short period after Yolk sac removal. Interestingly, no hematopoietic cells in fetal liver were observed, concluding that Yolk sac progenitors are the source for early embryonic haematopoiesis (Moore, 1970). By employing the newly developed techniques, scientists were able to show that macrophages appear in the yolk sac (YS) earlier than hemopoietic stem cells (HSC) derived haematopoiesis. These YS derived macrophages can found in the blood islands of the YS as early as embryonic day 8 (E8) (J. Y. Bertrand, 2010), seed fetal liver at E9 (Kieusseian, 2012) and colonize developing embryonic tissues between embryonic day E9.5 and E10.5 (Schulz, 2012). While, definitive HSC appear within the hematogenic endothelium of the aorto-gonado-mesonephros (AGM) region around E10.5 (Boisset, 2010), initiate fetal definitive haematopoiesis from E12.5, and later migrate to the bone marrow and enucleate the definitive haematopoiesis (Kissa, 2010).

Tissue resident macrophages in most tissues such as alveolar macrophages, Kupffer cells, peritoneal macrophages, Langerhans cells, and spleen are derived from the YS (Hashimoto, 2013; Sawyer, 1982; Yamada, 1990; Zhou, 2013). They self-maintain by local proliferation in steady state with negligible monocytic cells recruitment to most organs however the recruitment of monocytes increases in case of inflammation (Hashimoto, 2013; Yona, 2013). The extent of replacement from BM hematopoiesis varies according to specific tissue turnover and age. Indeed, tissues with high turnover rate such as the intestine and dermis are continuously maintained from blood monocytes pool (Bain, 2014; Tamoutounour, 2013). Currently, there is a considerable body of research showing that macrophages in most tissues are of mixed origin i.e., YS and BM derived macrophages (Cavaillon, 2011; Ginhoux, 2016; Perdiguero, 2015). One

exception is microglia, the central nervous system (CNS) resident macrophages; which considered to originate solely from YS progenitors, that colonize the CNS early during the embryonic development before the blood– brain barrier establishment and persist throughout adulthood by self-renewal (Ginhoux, 2010).

### **1.3 Macrophage activation**

Macrophage interaction with other cell types such as lymphocytes, microorganisms and their products, and environmental immune-modulators, can define the macrophage activation phenotype (Mills, 2000; Nau, 2002). It became conventional to use the simplistic M1/M2 terminology, that divides activated macrophages into two subsets with distinct characteristics and functions in immune response. In fact, the terminology stemmed from associating those characteristic phenotypes to the activity of the cytokines produced by CD4 T helper lymphocyte a major class of lymphocytes. Cytokines released by TH1 (T helper 1) promote M1 phenotype, while cytokines produced by TH2 (T helper 2) lymphocyte induce M2 status (Mills, 2000).

On one hand, classically activated macrophages (M1) linked to augmented microbicidal activity, inflammatory and antigen-presentation functions, are characteristic for intracellular microbial infections and are involved in tissue injury during chronic infections (Edwards, 2006; Nathan, 2000). M1 activation is induced by pathogen associated molecular pattern (PAMP) such as Lipopolysaccharides (LPS), muramyl dipeptide, lipoteichoic acid and cytokines such GM-CSF and IFN- $\gamma$  (Lehtonen, 2007; Nau, 2002; Pace, 1983). LPS is the most thoroughly investigated M1 macrophage inducer. Macrophages recognize LPS by Toll-like receptor 4 (TLR4) a member of the PRR family. Binding of LPS to its receptor leads to NF- $\kappa$ B activation. LPS stimulation results in significant nitric oxide production, release of the inflammatory cytokines such as IL-1, IL-8 and TNF, in addition to

increased Major Histocompatibility Complex (MHC) proteins expression, in addition to other molecules involved in antigen processing and presentation (Gilad, 1996).

On the other hand, alternatively activated macrophages (M2-like) show anti-inflammatory properties together with a specific set of antimicrobial functions, and they are associated with parasitic infections, allergies, tissue repair and fibrosis (Albina, 1990; Hesse, 2001). M2 can be subclassified to various subgroups including M2a, M2b and M2c according to their stimuli namely interleukin-4 (IL-4), antigen-antibody complex and Toll-like receptor (TLR) ligands, and IL-10 and glucocorticoids respectively (Stouch, 2014). However, IL-4 the main product of Th2 is among the most appreciated stimuli of alternatively activated macrophages, binding of IL-4 to its receptor on macrophages induces JAK–STAT pathway that leads to activation of STAT6, a transcription factor critical for expression of M2 signature genes such as *Retnla*, *Arg1*, and *Chil3* (Murray, 2011). IL-4 induced M2 macrophages are characterized by increased mannose receptor expression, arginase/ornithine production, and their compromised ability to produce nitric oxide and inflammatory cytokines secretion (Hesse, 2001; Stein, 1992)

## **1.4 Macrophage heterogeneity and tissue microenvironment programming**

Tissue resident macrophages are in constant interaction with the stroma in their tissue of residence; thus, cytokines and metabolites contribute towards shaping of transcriptional and epigenetic programs of tissue macrophages and thereby tissue specific function. Several landmark studies emphasize macrophage programming by their tissue milieu. One example is the study carried out by Lavin and his colleagues, where they examined the gene expression and chromatin landscape of tissue resident macrophages isolated from various tissues namely CNS, spleen, lungs, liver, peritoneum, as well as large and small intestine. It was concluded that by regulating the transcription factors

(TFs), the tissue of residence determines the tissue resident macrophages identity and function (Lavin, 2014). Moreover, adoptive transfer of mature macrophages between organ compartments results in their rapid molecular and phenotypic adaptation to the new microenvironment (Gosselin, 2014; Lavin, 2014). The macrophage lineage-determining factors (LDTFs) such as PU.1, are determined by differentiation signals such as M-CSF and IL34. In addition to that, the tissue microenvironment induces the expression of divergent secondary transcription factors known as tissue-specific transcription factors (TSTFs) that establish tissue-specific enhancers (Gosselin, 2014; Kohyama, 2009; Teitelbaum, 2003). Thus, tissue environment induces TSTFs that work in close coordination with LDTFs (Stanley, 2014; Y. Wang, 2012). Altogether, phenotypes and functional programs of tissue macrophages are determined by the signals they receive in their tissue microenvironments which programs them to fulfil distinct functional demands of different tissues (Gordon, 2013). For instance, Kupffer cells (KCs) guarantee physiological liver function by clearing the blood of microbes, cell debris, and old erythrocytes (Ganz, 2012). Microglia eliminate non-needed neuronal synapses, and those which failed to reach maturity, thereby fine-tune the CNS development and functionality (Ekdahl, 2012). In lymph nodes, subcapsular sinus macrophages activate adaptive immunity by taking the immune complexes and presenting these complexes to follicles B cells (Junt, 2007). Adipose tissue macrophages control lipolysis and regulate heat production in white and brown adipose tissue respectively (Guttenplan, 2018). Moreover, bone resorption by osteoclasts (the macrophages in bone) is vital for bone remodelling and turnover (Raggatt, 2010).

Therefore, the tissue resident macrophages functions are defined by their specific tissue microenvironment and are fundamental for the ordinary tissue physiology. Consequently, defects in their functions were linked to many diseases such as some bone diseases, adult-onset diabetes, in addition to immunocompromising and neurodevelopmental disorders (Wynn, 2013). Therefore, deciphering and manipulation of the

functions of tissue resident macrophage seem to represent a possible therapeutic approach for such illnesses.

## **1.5 Phagocytosis**

Macrophages engulf pathogens and apoptotic cells in a process known as phagocytosis, that was first observed by 'Elie Metchnikoff more than one century ago (Cavaillon, 2011). Since then, it is been considered as the first line of defence against infection and it has a critical role in adaptive immune response induction. Moreover, a large body of evidences connects phagocytosis to tissue turnover, homeostasis and remodelling (Boada-Romero, 2020).

Phagocytosis requires the recognition and binding of the target by receptors expressed on the cell surface. After recognition and internalisation, the engulfed particles accommodated in the phagosome, a membrane-bound vesicle. After detachment from cell plasma membrane, phagosome undergoes strict fusion and fission processes in addition to various biochemical changes including increased acidity that changes it into mature phagosome, a microbicidal compartment (Desjardins, 1994; Pitt, 1992). First of all, phagosome fuses with early endosome giving rise to early phagosome that has distinct markers such as GTPase Rab5. As phagosome proceeds towards late phagosome, its PH changes i.e., becomes more acidic (pH 5.5–6.0) and other markers such as GTPase Rab7 become prominent (Kinchen, 2010). Finally, late phagosome develops into mature phagosome the supreme microbicidal compartment, through interaction with lysosomes which results in even more drop in pH (4.5-5) and activation of hydrolases and oxygen species production (Luzio, 2010).

The end result of phagocytosis is not only killing invading microorganism but also critical for presentation of degraded antigen to T lymphocytes on either MHC1 or MHC2 depending on the antigen nature, the step that is critical for immune response fate; either

induction of adaptive immunity in response to microorganisms or tolerance in case of ingestion of apoptotic bodies (Ravichandran, 2007; Roberts, 2017).

## **1.6 Cell death**

Macrophages play an important role in tissue homeostasis and apoptotic cells clearance by means of a plethora of receptors that recognize translocated phosphatidylserine (PS) and modified sugars. However, their response to the pathogens and environmental insults results in their death by either apoptosis or necrosis. Due to its importance, cell death is a strictly regulated and has a significant impact on organogenesis and maintaining tissue homeostasis during development and adult life; it is also important for defining the outcome of intracellular bacterial infections beside its involvement in various pathologies (Behar, 2011; FADEEL, 2005; GLÜCKSMANN, 1951; Seimon, 2009).

Apoptosis and necrosis are two different types of cell death. Apoptosis involves DNA segmentation and plasma membrane blebbing where intact organelles in addition to nucleic acid segments are accommodated in a plasma membrane bound vesicle; eventually known as apoptotic bodies that released outside the cell. While apoptosis is a normal process that does not lead to tissue damage or induce inflammation, it is vital for organs development and adult tissues turnover. Necrosis is non-physiological type of cell death that was characterized by organelles deformation and non-reversible cell swelling ending up with cell rupture and release of cell content, the event that effects surrounding cells and eventually leads to exudative inflammation (Cohen, 1993; Steller, 1995).

One well-studied inducer of cell death is Fas ligand (fasL or CD95L). CD95/CD95L mediated cell death is a defence mechanism through which the immune system eliminates virus infected cells. It is also central in the process of developing immune tolerance by eliminating autoreactive T cells in the thymus and B cells in spleen as well as eliminating

unneded T and B lymphocytes and hereby supressing unwanted immune response (Krammer, 1998). CD95 cell death receptor belongs to the family of tumour necrosis factor receptor (TNF-R), that has a cytoplasmic death domain through which the apoptotic signal is transduced (Kischkel, 1995). The signalling pathway triggered by binding of its ligand CD95L (fas ligand) on cytotoxic T lymphocytes, CD95L can also be released in form of vesicles or by proteolytic shedding (Martínez-Lorenzo, 1999; Tanaka, 1995). Engagement of CD95/CD95 L leads to CD95 oligomerization and recruitment of Fas-associated death domain protein (FADD) an adaptor protein that reacts homological by means of its death domain with CD95 death domain at one end, and with caspase 8 by means of its death-effector domain (DED) at the other, the event that leads to its proteolytic cleavage and release of Caspase8 into cytoplasm (Muzio, 1996) and eventually Caspase 3 activation by either mitochondrial dependant or independent pathway (Scaffidi, 1998).

Another inducer of cell death, is ultra violet (UV) irradiation, an ionizing radiation involved in skin aging, inflammation, arresting of immune response and skin cancer development (Fisher, 1996; Kraemer, 1997; Kripke, 1990). As an ionizing agent UV irradiation induces stress response namely DNA damage response and ER stress response and activates cascade of signalling pathways that eventually results in Caspase 8 activation and cell death by Apoptosis (Zitvogel, 2010). UV induced cell death is well investigated in keratinocytes and it is established that P53 is central player in the UV induced Cell death. However, more evidences prove that UV irradiation can activate Fas (CD95) and induce cell death in similar way as FasL (Aragane, 1998; Rehemtulla, 1997).

## **1.7 Immunometabolism and metabolic reprogramming**

The field of immunometabolism has more recently evolved and connects immune cell functions to their metabolic phenotype. The link between metabolic pathways and their intermediates to cellular response found to be prominent in cancer, thereafter a large body of work in this area has been conducted to explore the association of various

metabolic pathways in T cells, differentiation and activation states and targeting them for cancer and autoimmune diseases therapy (Buck, 2015; O'Sullivan, 2015; Ramsay, 2015). Later on, several studies have explored and established the involvement of macrophages both bone marrow derived and tissue resident macrophages, not only in combating infection, but also in diverse tissue functions introducing further complexity that impacts the metabolic dynamics of the cells.

Metabolic pathways such as glycolysis, the Tricarboxylic acid cycle (TCA cycle), and lipid metabolism are more than merely energy providers. They also affect activation status of macrophages and thereby affect the outcome of infections and other pathologies, such as type 2 diabetes and atherosclerosis (Semenkovich, 2006). For instance, the delivery of surplus amount of nutrients leads to elevated mitochondrial metabolism and elevated reactive oxygen species (ROS) production and oxidative stress, mitochondrial and ER and thereby inflammation. In fact, the incidence of metabolic syndrome seems to be a factor that helps to foresee the onset of diabetes (Wannamethee, 2005). Increased glucose uptake and metabolic switch towards glycolysis has been established as a proinflammatory feature in T lymphocytes and macrophages. For instance, activation of glycolysis is a hallmark for proinflammatory Th17 phenotype development (Buck, 2015). Similarly, elevated glycolytic activity is also considered as M1 (proinflammatory) macrophage feature and is crucial for releasing proinflammatory cytokines (Newsholme, 1986; Tannahill, 2013). Moreover, glycolysis found to elevate during phagocytosis (OREN, 1963).

Elevated glycolytic metabolism is characteristic of M1 macrophages, which permits the rapid production of ATP to cope with fast-replicating microbes. While M2 macrophages is linked to augmented  $\beta$ -oxidation, that considered to be the energy efficient metabolic pathway and thus more suitable for defence against slow-growing and endemic parasites (Figure 1.1). LPS and IL4 are among the most appreciated stimuli that provide macrophage polarisation to classical proinflammatory (M1-like) and alternative (M2-like) anti-inflammatory and pro-fibrotic subsets. The first is, the most known TLR agonist, that

is in addition to induction of LPS-inducible genes expression it activates Akt and leads to enhanced glucose oxidation and production of phospholipids and thereby facilitating inflammatory cytokines secretion (Hardie, 2007). While the second is proved to be responsible for metabolic switch to  $\beta$ -oxidation in (M2) via induction of PPAR- $\gamma$  and PPAR- $\delta$ , and PGC1 $\beta$  (Vats, 2006).

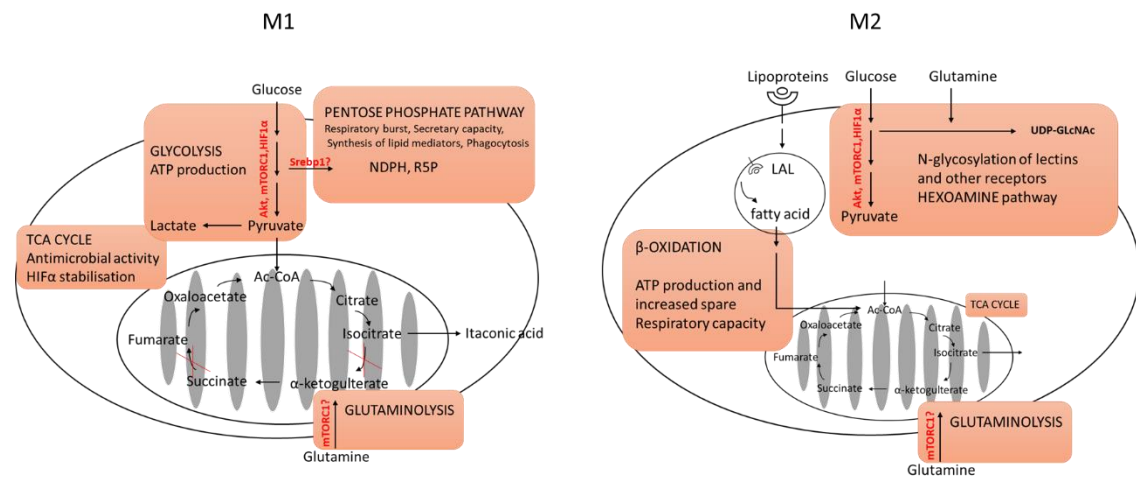


**Figure 1.1:** Illustration summarizes the main metabolic changes in M1 and M2 macrophages. adapted from (Covarrubias, 2015)

Glycolysis also known as anaerobic respiration, partially harvests the ATP out of glucose and converts it into pyruvate. In the absence of oxygen pyruvate is converted to lactate that leads to acidification. However, in presence of oxygen mitochondria oxidise pyruvate through TCA into carbon dioxide. The Seahorse XFe96 instrument measures the two major cellular metabolic pathways, mitochondrial respiration and glycolysis, simultaneously and in real-time, by measuring changes in O<sub>2</sub> concentration (oxygen consumption or OCR), and pH (extracellular acidification rate, or ECAR) in the extracellular environment surrounding living cells cultured in a microplate, that result from changes in these two energy pathways.

## 1.8 The inflammasomes

The term 'inflammasome' was coined by Martinon, Burns and Tschopp in 2002, to describe intracellular multi-component protein complex that recruits and activates inflammatory caspases (Martinon, 2002). Its assembly can be triggered by pathogens and damage-associated molecular patterns (DAMP) (Muruve, 2008). Inflammasome machinery consists of intracellular sensors for example NOD-like receptors (NLRs) and DNA sensors, the adaptor molecule apoptosis-associated Speck-like protein containing a CARD (ASC), or Pycard, and procaspase-1 (P-Y Ting, n.d.). The inflammasome is classified into several groups according to the sensory molecules involved. While NLR family including NLRP1, NLRP3 and NLRC4 has NLR sensors, Absent In Melanoma 2 (AIM2) has a DNA sensor.

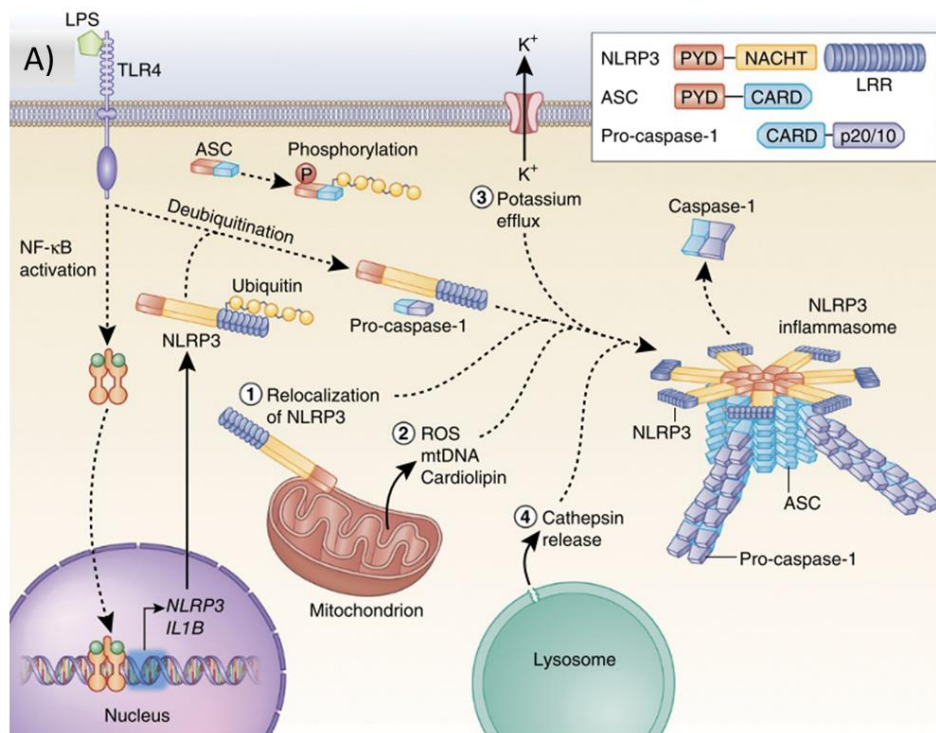
Inflammasome activation results in secretion of IL1 $\beta$  and IL18, both play central role in eliciting local and generalized inflammatory response to micro-organisms and other immunologic challenges. In addition, both are pivotal for the modulation of adaptive immune response (Chen, 2011; C.A. Dinarello, 1995; Charles A. Dinarello, 1998). IL1 $\beta$  secretion is considered as the hallmark of inflammasome activation. It is found to be involved in tissue injury, abnormal airway morphogenesis and bronchopulmonary dysplasia (BPD) in the developing mice embryos (Liao, 2015; Stouch, 2016). Moreover, Inflammasome components expression and activation found to be abnormal in numerous types of cancers, alcoholic liver disease and autoinflammatory disorders (Agostini, 2004; Le Daré, 2021; H. Wang, 2018).

### 1.8.1 The NLRP3 inflammasome

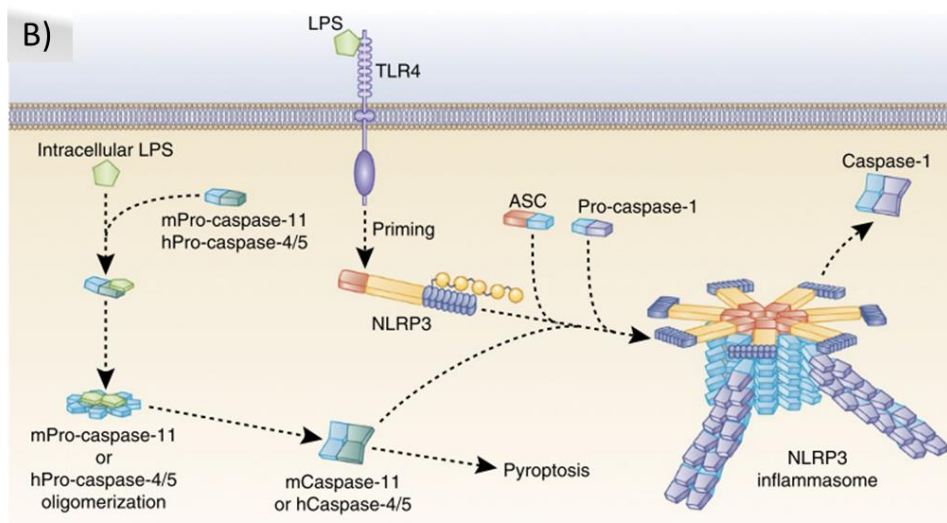
The NLRP3 inflammasome is the most studied family of inflammasomes that can be triggered by pathogen as well as particulate matters, it is also found to be involved in bacterial and viral infections, cancer and chronic inflammatory diseases (Allen, 2009a; DUEWELL, 2010a). It can be activated by either canonical or non-canonical pathway (Figure 3.2). In most systems, two consecutive signals are required for canonical NLRP3

inflammasome activation. Signal one, is provided by cytokines such as tumour necrosis factor (TNF), IL1 $\beta$  or PAMPs such as LPS (Luigi Franchi, Tatjana Eigenbrod, 2009; Xing, 2017). Cytokines or LPS, signal through NF-kb which leads to the transcriptional upregulation of the inflammasome component NLRP3, Caspase1 and IL1  $\beta$  (Bauernfeind, 2009). Whereas signal two leads to the inflammasome machinery assembly, and is provided by diverse set of DAMPs, for example particulates, crystals such as silica, uric acid, and cholesterol, ATP, and nigericin, or PAMPs such as, fungi, bacterial toxins, and RNA viruses(Allen, 2009b; Franchi, 2009; Gross, 2009; Jo, 2016). Inflammasome assembly starts with NLRP3 oligomerization via homotypic interaction between its NACHT domains, the event that leads to ASC recruitment and ASC filament formation. ASC assembly enables caspase 1 autonomous cleavage and activation which acts on pro IL1  $\beta$  and cleaves it into its mature form (Lu, 2014; Schmidt, 2016).

Activation of NLRP3 through non-canonical pathway requires cytosolic LPS. Outer membrane vesicles (OMVs) are secretory vesicles of gram negative bacteria which range from 20 to 250 nm in diameter, LPS abundant and capable of activating signalling via NOD and NF-kB (Ellis and Kuehn 2010; Gankema et al. 1980; Bonham and Kagan 2014). Consequently, cytosolic LPS recognition by caspase 4 and 5 in human and Caspase 11 in mice triggers their auto-proteolytic cleavage and activation which in turn cleaves Gasdermin D (GSDMD) and leads to its insertion in cell membrane and triggering of pyroptosis and consequent K<sup>+</sup> efflux that leads to NLRP3 activation IL1  $\beta$  secretion (Kayagaki, 2015; Lee, 2018; Shi, 2014, 2015).



Debbie Maizels/Nature Publishing Group



Debbie Maizels/Nature Publishing Group

**Figure 1.2: Mechanisms of NLRP3 inflammasome activation.** A) Canonical and B) non-canonical pathway. Permission to reuse was provided from Springer Nature under license number (5158450053132) (Guo, 2015).

## **1.9 ER-hoxb8**

Hoxb8 is a protein that formerly known as Hox-2.4. It is encoded by hoxb8 gene a member of Homeobox family, a group of genes highly conserved in nature. Hoxb8 protein is a sequence-specific transcription factor, with ability to arrest myeloid differentiation and allow the progenitors to divide indefinitely. Homeobox proteins are involved in embryonic development, haematopoiesis and leukemic transformation in adults (Gene, 1993; Kongsuwan, 1989; Pear, 1998; Perkins, 1993).

Estrogen-regulated Hoxb8 (ER-Hoxb8) has been utilized to generate stable bone marrow derived hematopoietic progenitors with myeloid and lymphoid potential that can be used to study and manipulate biological functions of leukocytes (Redecke, 2013; G. G. Wang, 2006). Hoxb8 cells generated from bone marrow have been validated as tool for studying neutrophils functionality their response to infections both in vitro and in vivo (Orosz, 2021; Saul, 2019; Sochalska, 2020). In combination with cas9 genetic modulation tool, BM ER-hoxb8 has also been used for studying macrophage migration and response to intracellular infection (Accarias, 2020; Cabron, 2018; Roberts, 2019). Moreover, BM ER-hoxb8 progenitors have been exploited to study osteoclasts and their role in osteoarthritis (Di Ceglie, 2016; Zach, 2015).

We decided to adopt the system to generate YS derived macrophage cell line allowing us to study their biology, functional characterization in direct comparison with BM ER-hoxb8 under identical conditions. Thereby, we exclude the microenvironment programming and investigate origin specific differences.

## **1.10 Research Rational**

Macrophages are widely spread cell type; they present in almost every tissue. Beside their role in immune defence against microbial invasions they serve tissue specific functions and are key for tissue homeostasis. Therefore, their cellular identity is continuously

imprinted by tissue microenvironment. Upon adoptive transfer of mature macrophages between organ, transferred cells adopt molecular signature and phenotypic properties similar to their host tissue counterparts. Despite the strong impact of the local milieu on macrophage identity, great deal of heterogeneity can be observed among macrophages within the same tissue. This heterogeneity might be explained in part by diverse developmental origins of macrophage populations, that extends to various organs in which a dual origin of tissue macrophages has been identified, such as heart, lung, kidney and other organs. However, the impact of ontogeny on the cellular identity of macrophages remains unclear. A precise knowledge of the macrophage programs and their regulation might contribute to better understanding of inflammatory processes and, ultimately, offers tools to modulate their functions to improve tissue remodelling.

Therefore, we aimed to address the influence of developmental origin of macrophages on their cellular identity, with this aim in mind we sought to compare macrophages from the two ontogenic origins i.e., yolk sac versus bone marrow haematopoiesis, independently of tissues environmental cues. In order to achieve this goal, we immortalized their precursors *ex vivo* using conditional *Hoxb8* and studied their functions under defined conditions *in vitro*.

## 2. Materials and methods

### 2.1 Table of materials and software

REAGENT or RESOURCE	SOURCE
<b>Antibodies</b>	
<b>Western blot antibodies</b>	
NLRP3 ( D4D8T )	Cell Signaling (15101T)
ASC/TMS1 ( D2W8U )	Cell Signaling (67824T)
Caspase1 ( E271C )	Cell Signaling (24232T)
Beta Actin	Abcam (ab8227)
<b>Flow cytometry antibodies</b>	
APC anti-mouse CD16/32 Antibody	Biolegend (101326)
APC/Cyanine7 anti-mouse CD45 Antibody	Biolegend (103116)
Brilliant Violet 421™ anti-mouse F4/80 Antibody	Biolegend (123132)
PE anti-mouse CD115 (CSF-1R) Antibody	Biolegend (135506)

Alexa Fluor® 647 anti-mouse CX3CR1 Antibody	Biolegend (149004)
PE Rat Anti-CD11b	BD (553311)
APC/Cyanine7 anti-mouse/human CD11b	Biolegend (101226)
BV 605 anti-mouse Ly-6G	Biolegend (127639)
Purified Rat Anti-Mouse CD16/CD32 (Mouse BD Fc Block™)	BD (553141)
<b>Immunofluorescence antibodies</b>	
anti-KI67	Abcam (ab15580)
CX3CR1 Recombinant Rabbit Monoclonal Antibody (1H14L7)	Thermo Fisher (702321)
Anti-F4/80 antibody [Cl:A3-1]	Abcam (ab6640)
<b>Bacterial and Virus Strains</b>	
<i>pCL-Eco</i>	Generation protocol is described in 2.2.2.1
<i>pMSCVneo-ER-Hoxb8</i>	
<i>ER-Hoxb8 MSCV</i>	
<b>Reagents, Chemicals and Recombinant Proteins</b>	

RPMI-Medium	Sigma (R 8758)
FBS Superior	BIO-SELL (S 0615)
Penicilin-streptomycin (P/S)	Sigma (P 4333)
Estradiol	Sigma (E2257)
Beta-Mercaptoethanol	Sigma (M3148)
Recombinant Mouse Macrophage Colony Stimulating Factor (rm M-CSF)	Immuno Tools (12343115)
Recombinant Mouse Interferon Gamma (rm IFN-gamma)	Immuno Tools (12343536)
Recombinant Mouse Interleukin-4 (rm IL-4)	Immuno Tools (12340043)
Dimethyl sulfoxide (DMSO)	Carl Roth (A994.1)
Dulbecco's Phosphate Buffered Saline	Sigma-Aldrich (P5493)
Tween® 20	Merck (P1379)
Trypsin/EDTA solution	Biochrom GmbH (L2153)
Trypan Blue solution	Sigma (T8154)
Giemsa solution	Sigma-Aldrich (GS500)
May-Grünwald solution 0.2 %	Sigma-Aldrich (63590)

NucBlue nucleus stain	Thermo Fisher (R37605)
Paraformaldehyde (PFA)	Carl Roth (0335.3)
Lipopolysaccharides from Escherichia coli O26:B6 (LPS)	Sigma (L8274)
Oligomycin	Sigma (O4876)
2,4-Dinitro-phenol	Sigma (34334)
Sodium pyruvate	Sigma (P8574)
Rotenone	Sigma (R8875)
Antimycin A	Sigma (A8674)
Glucose	Sigma (G6152)
XF assay medium	Agilent (102365-100)
Seahorse XFe96 FluxPak	Agilent (102416-100)
HISTOPAQUE-1083	Sigma-Aldrich (10831)
Ibidi mounting medium for fluorescence microscopy	Ibidi (50001)
Recombinant murine (rm) IL-3	Sigma-Aldrich (I4144)
Recombinant murine (rm) IL-6	Sigma-Aldrich (I9646)
Collagenase D	Roche (11088866001)

Deoxyribonuclease I	Sigma-Aldrich (D7291)
Polybrene Transfection Reagent	Sigma-Aldrich (TR-1003)
<b>Critical Commercial Assays</b>	
Mouse IL-1 beta/IL-1F2 DuoSet ELISA	R&D Systems (DY401-05)
Anti-Ly-6G MicroBeads UltraPure + LS Columns	Miltenyibiotec (130120337)
SsoAdvanced Universal SYBR Green Supermix	BIO-RAD (64296124)
RNeasy Micro Kit	Qiagen (74004)
RNeasy Mini Kit	Qiagen (74104)
High-capacity cDNA reverse transcription kit	Applied Biosystems (10400745)
DuoSet Ancillary Reagent Kit 2 (5 plates)	Applied Biosystems (DY008)
Recombinant Mouse Interleukin-4 (rmIL-4)	Immuno Tools (12340043)
Bio-Plex Pro Mouse Cytokine MIG	BIO-RAD LABORATORIES (171G6005M)
Bio-Plex Pro Mouse Cytokine MIP-2	BIO-RAD LABORATORIES (171G6006M)
MO CYTO IL-18 SET	BIO-RAD LABORATORIES (171G6009M)

Bio-Plex Pro Mouse Cytokine 2 Standards	BIO-RAD LABORATORIES (71I60001)
pHrodo™ Green Zymosan Bioparticles™ Conjugate for Phagocytosis	Thermo Fisher (P35365)
Quant-iT PicoGreen dsDNA Assay Kit	Thermo Fisher (P7589)
Pierce™ BCA Protein Assay Kit	Thermo Fisher (23225)

### Experimental Models: Cell Lines

HEK-293T	293T ATCC® CRL-3216™
NIH-3T3	NIH/3T3 ATCC® CRL-1658™
RAW 264.7 murine Cell Line	Merk (91062702)
SCF producing CHO-MGF cell line	

### Experimental Models: Organisms/Strains

C57BL/6J mouse line	JAX (000664)
B6N.129S2-Casp1tm1Flv/J mouse line	JAX (016621)

### Oligonucleotides

Mm_Actb	Qiagen (QT00095242)
Mm_Runx1_1_SG QuantiTect Primer Assay	Qiagen (QT00100380)

Mm_Kit_1_SG QuantiTect Primer Assay	Qiagen (QT00145215)
CX3CR1	Qiagen (QT00259126)
Mm-Csf1r_1_SG QuantiTect Primer Assay	Qiagen (QT01055816)
Mm_Lyz2_1_SG QuantiTect Primer Assay	Qiagen (QT01555701)
EmR F4/80 QuantiTect Primer Assay	Qiagen (QT00099617)

---

### Software and Algorithms

Microsoft Office 2016	Microsoft
Seahorse Wave Software	Agilent
GraphPad Prism version 7.00 for Windows	GraphPad Software, La Jolla California USA
FlowJo™ Software for Windows	Treestar, Ashland, Oregon, USA
ZEN Digital Imaging for Light Microscopy, RRID:SCR_013672	Zeiss
Mendeley reference management software	Elsevier
Other	The RNA-seq raw data have been deposited in NCBI GEO under the accession code GSE176409. The mass spectrometry

---

proteomics data have been deposited to the ProteomeXchange Consortium via the PRIDE partner repository with the dataset identifier PXD026922.

## **2.2 Experimental model and subject details**

### **2.2.1 Mice**

C57BL/6J CD45.2 (*Ptprc<sup>b</sup>*) congenic mice were purchased from Jackson Laboratories. *Casp1/Casp11* double knockout mice were previously described (Kuida et al., 1995), and were kindly provided by Veit Hornung, Gene Center Munich, Ludwig-Maximilian-University, Germany. All animal procedures were performed in adherence to our project

license (55.2-2532.Vet\_02-16-183) issued by the German regional council at the Regierungspräsidium Oberbayern, Munich, Germany.

## 2.2.2 Cell lines

### 2.2.2.1 Generation of yolk sac and bone marrow derived ER-Hoxb8 progenitors

For the immortalization of BM hematopoietic progenitors, we followed the published protocol (Redecke, 2013)(Redecke, 2013), here we are describing for the first time the generation of Yolk sac Hoxb8-SCF. The *pCL-Eco* and *pMSCVneo-ER Hoxb8* plasmids were kindly provided by H. Häcker (Department of Pathology, University of Utah), the protocol was established with the help of Professor Barbara Walzog, Department of Physiology at LMU.

HEK-293T cells (ATCC 293T ATCC® CRL-3216™) were transfected with both ecotropic packaging vector *pCL-Eco* and retroviral backbone *pMSCVneo-ER-Hoxb8* using Lipofectamin (Invitrogen 11668-019). Forty-eight hours following the transfection the virus-containing supernatant was collected. NIH-3T3 cells were used for the virus titration, the CFU per milliliter was determined, the virus was aliquoted at a multiplicity of infection (MOI) of 10 and kept at -80°C till it is needed.

Bone marrow hoxb8 hematopoietic progenitors generation was performed as described previously (Redecke, 2013). In brief, 8- to 10- week-old wild type and *casp1/11 ko* mice were sacrificed by cervical dislocation, femurs tibias and humerus bones were collected and the bone marrow was isolated. Then the progenitors were enriched on HISTOPAQUE-1083 (Sigma-Aldrich) gradient. The progenitors were cultivated in stem cell medium composed of RPMI 1640 containing 15% FCS, 1% penicillin/streptomycin, in addition to, 10 ng/ml recombinant murine (rm) IL-3 (Sigma-Aldrich), 20 ng/ml rmIL-6

(Sigma-Aldrich), in addition to 2% SCF-containing supernatant (produced by Chinese hamster ovary cells), 72 hours later Hoxb8 retroviral transfection was carried out.

In order to immortalize macrophage progenitors from the embryonic yolk sac, yolk sac membranes from mouse embryos were isolated at embryonic day (E) 9.5. Pregnant C57BL/6J females were sacrificed by cervical dislocation. Embryos were removed from the uterus and washed with cold phosphate buffered saline (PBS)(Invitrogen). The YS membrane was collected and digested in enzymatic mixture composed of 1 mg/ml Collagenase D (Roche 11088866001), 100 U/ml Desoxyribonuclease I (Sigma-Aldrich D7291) and 1% FCS (BIO-SELL S0615), at 37 °C for 15 minutes. Yolk sac membranes were mechanically dissociated and sieved using a 100µm cell strainer (BD).

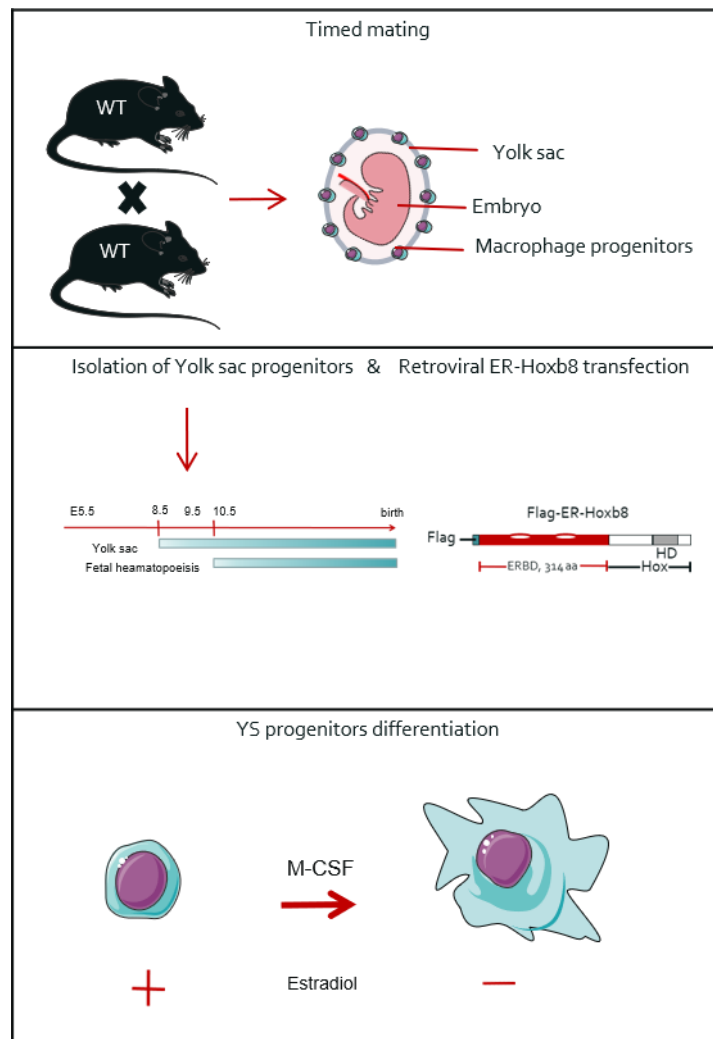


**Figure 2.1:** Schematic diagram illustrates the process of generation and differentiation Yolk Sac derived Hoxb8 progenitors

## 2.3 Methodology

### 2.3.1 Generation of SCF supernatant

The Chinese hamster ovary cells, genetically engineered to produce Stem Cell Factor (CHO-SCF) were cultivated in 30ml RPMI 1640 (Sigma R8758) supplemented with 10%

FCS (BIO-SELL S0615) in addition to 1% penicillin/streptomycin (Sigma P4333) in a T175 cell culture flask. 1-2 days after confluency, medium was collected and passed through a 0.4 µm sterile filter prior freezing at -20°C for future use.

### **2.3.2 Thawing and culturing HoxB8 progenitor cells**

Cells were thawed quickly using 10ml of cold proliferation Medium, transferred to 15ml Falcon tube and pelleted at 300g for 5 mins, supernatant was decanted and the pellet was suspended in 12 ml proliferation medium and transferred to T75 cell culture flask and incubated at 37 / 5% co2 for 2 to 5 days and checked every day till they are confluent then they were split at density of 500 thousand cell/T75 flask.

### **2.3.3 Determination of cell counts**

In order to count the number of the cultured cells, 20 µl of the cell suspension were mixed (ratio 1:1) with trypan blue staining solution (Sigma Aldrich) that stains dead cells with blue leaving viable cells clear. After incubating for approximately 3 minutes at room temperature, 20 µl of the mixture was transferred to a Neubauer cell counting chamber (Laboroptik). The number of living cells in 1 milliliter of cells suspension was calculated according to the following equation:

$$\text{Number of cells per ml} = \text{mean} * \text{dilutionfactor}(2) * \text{area}(10^4)$$

### **2.3.4 Growth curve**

In order to compare the growth and doubling time between BM and YS ER-Hoxb8 progenitors, one hundred thousand cells of each cell line were seeded in 3 ml of proliferation medium per each well of 6 well plate at 12pm, cells were counted every day in the same time for 6 days, doubling time was calculated using Doubling Time calculator tool (Roth, 2006) according to the following equation:

$$\text{DoublingTime} = \frac{\text{duration} * \log(2)}{\log(\text{finalConcentration}) - \log(\text{InitialConcentration})}$$

### **2.3.5 Differentiation of ER-Hoxb8 progenitors to Macrophages**

5x10<sup>5</sup> YS and BM ER-Hoxb8 progenitor cells were seeded per 10 cm tissue culture dish in 5ml of differentiation medium (RPMI 1640 with 10% FCS (BIO-SELL), 1% penicillin/streptomycin (Sigma), 30 µM 2-Mercapto-Ethanol (Sigma) and 6% SCF-containing supernatant and 10 ng/ml M-CSF (ImmunoTools)) at 37°C/5% CO<sub>2</sub>. Cell culture medium was changed every second day till desired experiments were performed. Bright field images during the process of differentiation were collected with Zeiss Axiovert 200, Axio-cam HRC microscope.

### **2.3.6 Detachment of differentiated adherent cells**

Differentiated macrophages were washed twice with cold (4°C) PBS (Sigma-Aldrich) and incubated at 37°C in 2 ml Accutase (Sigma) for 5-10 minutes with slight agitation till full cell detachment was achieved. If detachment was incomplete, cells were gently detached using a cell scraper. Subsequently, detached cells were washed using cell culture medium and kept on ice for further processing.

### **2.3.7 Flow cytometry**

To determine the expression of CD16/32, CD45, CD11b, CSF1r and F4/80 on BM and YS cells during their differentiation towards macrophages, cells were detached/transferred into 15ml falcon tube and pelleted at 400 g for 5 minutes, after decanting the supernatant, cells were resuspended in cold PBS (Sigma-Aldrich), transferred to non-tissue treated round-bottom 96-well plates in order to be stained for FACS analysis. The mixtures of desired antibodies were prepared with 1% BSA/PBS and incubated together with the cells for 20 minutes at 4°C. Flow cytometry evaluation was achieved using BD

Biosciences LSR Fortessa flow cytometer and data were analyzed using FlowJo 10 (Tree-star, Ashland, Oregon, USA).

### **2.3.8 Giemsa May-Grünwald stain**

In order to assess *hoxb8* macrophage morphology, *hoxb8* progenitors were seeded and differentiated in 1 well glass slide (Nunc® Lab-Tek® II Chamber Slide™ system). On day 5, slides were placed in May-Grünwald-Giemsa (Sigma-Aldrich 63590) staining solution for 5 minutes, then washed in Phosphate Buffer pH 7.2, for 90 seconds, followed by Giemsa staining solution (Sigma-Aldrich) (diluted 1:20 in deionized water) for 15-20 minutes. Slides were rinsed in deionized water, air-dried and analysed with Zeiss Imager.M2 microscope.

### **2.3.9 Immunofluorescence staining**

For immunofluorescence evaluation of various markers, BM and YS ER-Hoxb8 progenitors were plated and differentiated on 8 well chamber slides (Nunc® Lab-Tek® Chamber Slide™ system). On day 5, differentiation medium was decanted and slides were washed two times using PBS, fixed with 4% PFA (Carl Roth) for 10 minutes and washed again. Blocking was performed with 10% donkey serum for 30 mins. Slides were stained with primary antibodies namely anti-Ki67 (ab15580), anti-CX3CR1 (702321) and anti-F4/80 (ab6640) followed by secondary antibodies generated in respective host for 1 hour each. Nuclei were counterstained with Hoechst (Invitrogen H3569). Slides were mounted using Ibbidi mounting medium for fluorescence microscopy (Ibbidi 50001) and visualized using a ZEISS LSM 880 microscope.

### **2.3.10 Phagocytosis assay**

YS and BM ER-Hoxb8 progenitor cells were plated and differentiated on 8 well chamber slides. On day 5 differentiation medium was decanted and slides were washed with sterile PBS. Subsequently, 100 µl of pHrodo™ Green Zymosan Bioparticles™ Conjugate for

Phagocytosis (Thermofisher) were added per well and incubated for 60 minutes at 37°C. Slide was washed with PBS, fixed using 4% PFA for 10 minutes and washed again before staining for F-actin with Invitrogen™ Texas Red™-X Phalloidin (Invitrogen T7471). Nuclei were counterstained with Hoechst (Invitrogen H3569). Slides were visualized using ZEISS LSM 880 microscope.

### **2.3.11 Gene expression analyses**

RNeasy Micro Kit (Qiagen 74004) was used for RNA isolation. Subsequently High-Capacity cDNA Reverse Transcription Kit (Applied Biosystems 10400745) with RNase Inhibitor (Thermofisher Scientific E00381) was used to transcribe the isolated RNA to cDNA. Quantification of cDNA was performed with desired primers (see Key Resource Table) by real-time polymerase chain reaction with SsoAdvanced Universal SYBR Green Super-mix (BIO-RAD 64296124) using StepOnePlus Real-Time PCR System.

### **2.3.12 Lysate collection for transcriptome and proteome analyses**

Hoxb8 progenitors' cells were differentiated for 5 days, tissue culture plates were then washed twice with PBS. For stimulation experiments cells were incubated for 5 hours in 5 ml of differentiation medium supplemented with 100 ng/ml LPS (Sigma L8274), or 100 ng/ml IL4 (ImmunoTools 12340043) as indicated. After stimulation, cells were washed, pelleted and resuspended in 500 µl TRIzol (Sigma T9424) (for transcriptome analyses) or 500 µl of urea/thiourea buffer (for protein analyses) in low protein binding 1,5 ml Eppendorf tubes.

### **2.3.13 RNA sequencing and data analysis**

Library preparation and RNA sequencing was carried out with IMG, Martinsried, Germany. And the procedure is summarized below.

### **2.3.13.1 RNA quantification and purity**

Purity and concentration of all RNA samples were measured using the NanoDrop ND-1000 spectral photometer (Thermo Fisher Scientific). Further, the 2100 Bioanalyzer (Agilent Technologies) together with RNA Nano/HS LabChip Kits (Agilent Technologies) were used to determine RNA integrity.

### **2.3.13.2 Library preparation**

Library preparation was achieved with the Illumina TruSeq® Stranded mRNA technology, according to the manufacturer's protocol. The protocol started with an RNA fragmentation step using divalent cations. Samples were then introduced into a reverse transcription to generate first strand cDNA. In the second strand cDNA synthesis dTTP was replaced by dUTP, to evade DNA replication and thus guarantee strand specificity. Following that, the adenylation of the 3'-ends and sequencing adapters ligation were accomplished. Those comprise sequencing primer- and flow cell-binding sites, as well as guides for multiplexed sequencing of pooled libraries. Adapter-ligated fragments were amplified during a limited-cycle PCR reaction. After the limited cycle PCR at the end of the library preparation, DNA 1000/HS LabChip kits were used together with 2100 Bioanalyzer (Agilent Technologies) to quality control the prepared samples. Additionally, quantification of libraries was performed using the very sensitive fluorescent dye-based Qubit® ds DNA HS Assay Kit (Thermo Fisher Scientific). Briefly, the ds DNA concentration (ng/μl) of each sample was determined against known concentration standard. The DNA concentration was determined by creating a linear trend line and applying the mathematical equation of the linear regression. Sequencing library was generated by pooling the single libraries and equal DNA amount from each sample was added. Following quantification, the dilution and NaOH denaturation of the final sequencing library were performed to ensure the presence of single stranded DNA fragments for cluster generation.

### **2.3.13.3 Cluster generation and sequencing**

Cartridge loading was conducted following the manufacture's recommendations for NovaSeq 6000 according to the standard workflow using a SP flowcell. Template amplification and clustering was performed onboard of the NovaSeq 6000 applying the exclusion amplification (ExAmp) chemistry. For cluster generation and subsequent sequencing of all samples, one single-read 75 cycle run was performed, on a SP flowcell. Cluster generation and sequencing were operated under the control of the NovaSeq Control Software (NVCS) v1.6.0. After cluster generation, adapter sequences ligated to each fragment hybridize with sequencing primers and sequencing is carried out. Sequencing was performed with reads of a length of 75 bp (single-read).

### **2.3.13.4 Data analysis**

RNA sequencing reads were aligned to the mouse genome (ENSEMBL release GRCm38.94) and counted per-gene using STAR (version 2.6.1d). Transcript-per-million (TPM) estimates were obtained using RSEM (version 1.3.0). Differential expression analysis was performed in R/bioconductor with DESeq (1.26.0). Data analysis was carried out together with Tobias Straub, Bioinformatics Core Facility, LMU Biomedical Center, Martinsried, Germany.

## **2.3.14 Protein profiling by mass spectrometry**

MS analysis of indicated samples was carried out at the Interfaculty Center for Genetics and Functional Genomics at the University of Greifswald, Germany. Elke Hammer and Josefine Plocke generated the raw data, and greatly supported bioinformatic analysis, data presentation and its interpretation.

Sample preparation and mass spectrometric analyses by liquid chromatography coupled tandem mass spectrometry (LC-MS/MS) on a LTQ-Orbitrap Velos instrument was carried out as described earlier (Bhardwaj, 2017). For all conditions four bioreplicates from independent experiments were analysed. In short: Protein was extracted by multiple freeze-thaw cycles, and collected by 1-hour centrifugation (room temperature, 19.000g) after nucleic acid fragmentation with a sonication probe. Three µg protein of each sample was reduced (DTT) and alkylated (iodoacetamid) before digestion with trypsin at a protein to enzyme ratio 25:1 (37°C, 16 h). Peptides' mixtures were desalted on C18 material (µZipTip, Merck Millipore). Peptides were separated by LC (nano-Acquity UPLC system, Waters) before data-dependent acquisition of MS data. MS spectra were acquired in the Orbitrap whereas fragment spectra (MS2) of the 20 most abundant ions were recorded in a linear ion trap (LTQ).

Mass spectrometric raw data was searched against a mouse SwissProt database (16/09/2016). Identification and comparative quantification of proteins in YS and BM macrophages was carried out in Progenesis QI (Nonlinear Dynamics) via a Mascot search algorithm (v2.3, Matrix Science). For protein quantitation Hi3-non-conflicting peptides (score >20) were considered.

For data analysis of cells stimulated with LPS in comparison with untreated cells peptide/protein identification at FDR of 1% was carried out with the Andromeda algorithm implemented in MaxQuant v1.5.3.8., MaxQuant LFQ algorithm for label-free quantification was used to normalize for the differences in peptide loading (Cox, 2014). Resulting protein intensities (Label Free Quantification values (LFQ)) were exported and statistically analysed.

### **2.3.15 UV and FasL induced cell death assays**

Hoxb8 progenitors were differentiated for 5 days, cells were detached by cell scraping and seeded at a density of 20 thousand cells in 3 ml of differentiation medium in each well of 12 well plates. Macrophages were treated with different doses of SuperFasLigand

(Enzo Life Sciences ALX-522-020-C005) or UV irradiation on a UV Stratalinker 1800 (Stratagene), respectively. At the indicated time points, cell culture supernatants were collected and macrophages were detached by Accutase (Sigma A6964) treatment. The corresponding cell culture supernatants and detached macrophages were combined and washed with annexin V binding buffer (BD Biosciences 556454). Afterwards, macrophages were stained with annexin V-FITC (BD Biosciences 556547) and 2 µg/ml propidium iodide (Sigma-Aldrich 25535-16-4) in 100 µl annexin V binding buffer for 15 min on ice. Subsequently, stained macrophages were washed with annexin V binding buffer and subjected to flow cytometry on an LSR II cytometer (BD Biosciences). Annexin V-FITC-positive, propidium iodide-negative macrophages were considered as apoptotic, while annexin V-FITC and propidium iodide-double-positive macrophages were considered as necrotic. Induction of cell death experiments were performed in collaboration with Kerstin Lauber lab, Clinic and Polyclinic for Radiotherapy and Radiation Oncology, LMU hospital.

### **2.3.16 Extracellular flux XF96 Seahorse measurement**

Differentiated Hoxb8 macrophages were detached by cell scraping and seeded at a density of approximately  $10^5$  cells per well (in 200 µL differentiation medium) in a Seahorse 96-well plate. The extracellular flux XF96 Seahorse measurement was performed as described previously (Keuper, 2014; Yi, 2017).

On the day of measurement, medium was removed and cells were incubated with and without the following stimuli: 100 ng/ml LPS (Sigma L8274) or 100 ng/ml IL4 (Immuno Tools 12340043). After 4 hours incubation time, medium was replaced with 180 µl/well XF assay medium (Agilent 102365-100) supplemented with 11 mM glucose (Sigma G6152) (pH 7.5) and incubated for 60 minutes in an air incubator. The XF96 plate (Seahorse Bioscience, Agilent Technologies) was then moved to Seahorse extracellular flux analyser (Agilent Technologies) with the temperature being adjusted to (37 °C) and left to reach equilibrium. Each assay cycle contained 1 minute of mixing, 2 minutes of

waiting, and 3 minutes of acquiring. Oxygen consumption rates (OCR) and extracellular acidification rates (ECAR) were analysed and dissected into different functional modules as described in detail previously (Keuper, 2014). In short: following 4 basal assay cycles, oligomycin (1 µg/ml) (Sigma O4876) was injected to achieve ATP synthase inhibition to determine OCR linked to ATP production. After 3 cycles, 2,4-Dinitrophenol (DNP; 100 µM) (Sigma 34334) was injected to provoke maximal respiration, indicating maximal substrate oxidation rates (3 cycles). Next, pyruvate (5 mM) (Sigma P8574) was injected to remove rate-limitation by glycolysis (3 cycles). In order to estimate the non-mitochondrial OCR, Rotenone (Sigma R8875) in addition to antimycin A (AA) (Sigma A8674) were added and measured for 4 cycles. The mean of 4 OCR measurement after injection of R/AA was deducted from all other OCR measurements. To determine the glycolysis derived extracellular acidification rates (ECARs), 2-deoxy-glucose (2DG, 100 mM) was injected. The mean of 4 ECAR measurements after 2DG injection was deducted from all ECAR values to obtain ECAR that results from glycolysis. Mitochondrial efficiency was determined by calculating coupling efficiency CE (the fraction of basal mitochondrial respiration that is linked to ATP synthesis) and by calculating cellular respiratory control ratio cRCR (maximal respiration divided by proton leak). After the measurement, the wells of XF96 plate were lysed and Quant-iT PicoGreen dsDNA Assay Kit (Thermo Fisher) was used to determine the dsDNA amount per well. All rates were normalized to 130 ng dsDNA (= mean DNA content/well of all measurements). Extracellular flux XF96 Seahorse measurement was performed in collaboration with Martin Jastroch Lab Helmholtz Center Munich and Stockholm University.

### **2.3.17 Multiplex immunoassays**

Cytokines` concentration in cell supernatants of Hoxb8 macrophages was quantified at Professor Lauber lab. To determine Cytokines` concentration hoxb8 cells were differentiated in 6 well plates for 5 days with  $5 \times 10^4$  cell per well. Medium was changed on day 3 and 4. On day 5, medium was replaced with either 2 ml of differentiation medium only,

or differentiation medium with stimuli as follows with 100 ng/ml LPS (Sigma L8274) or 100 ng/ml IL4 (Immuno Tools 12340043). Three wells per condition were used and supernatants were pooled. The Bio-Plex Pro Mouse Cytokine Assay (BIO-RAD LABORATORIES 171G6005M, 171G6006M and 171G6009M) was used on a Luminex 200 system according to the manufacturer's protocol (Bio-Rad Laboratories, Munich, Germany).

### **2.3.18 Cholesterol monohydrate crystals preparation**

Cholesterol monohydrate crystals were prepared and kindly provided by Mahajan, Ujjwal Mukund, The Medical Clinic and Polyclinic II, LMU hospital. Briefly, ultrapure cholesterol (100 mg, Sigma Aldrich) was dissolved in 95% pure ethanol. The solution was mixed with distilled water (1:9) and incubated for at least 10 minutes at room temperature for stabilization of cholesterol monohydrate crystals. Following incubation, suspension was incubated at 55°C to remove ethanol by evaporation. Subsequently, cholesterol crystals were re-suspended in PBS. The suspension was then subjected to ultra-sonication for 15 min at 30% power. Cholesterol monohydrate size was quantified and regulated by hydrodynamic diameter measured using Zetasizer (Malvern Analytical) and kept at 4°C for future use.

### **2.3.19 Monosodium urate crystals preparation**

For the production of MSU crystals, a solution of 10mM uric acid with 154mM NaCl was prepared and pH was adjusted to 7.2 using NaOH. the solution then agitated left for overnight at 37C. On the next day the supernatant was decanted and crystals were harvested. Followed by three cycles of washing using cold sterile PBS and filtrated using filter paper. Subsequently, the crystals were left under the hood for 1-day until complete dryness was reached at room temperature. Afterward, crystals were suspended in PBS at a concentration of 125 mg/ml, sterilized using autoclave and kept at 4°C for future use.

### **2.3.20 IL1 $\beta$ quantification using ELISA**

Differentiated Hoxb8 cells were washed and incubated in 5 ml of differentiation medium supplemented with 200 ng/ml LPS (Sigma L8274) for 3 hours. Then, 250  $\mu$ g/ml MSU, 375  $\mu$ g/ml cholesterol crystals or 2  $\mu$ g/ml Ecoli OMVs were added and incubated for indicated time periods. Supernatant was collected and IL1 $\beta$  was measured using Mouse IL-1 beta/IL-1F2 DuoSet ELISA, (R&D Systems DY401-05) according to the manufacturer's instruction. Tecan GENios was used for OD evaluation, concentrations were calculated with standard curve (detection limit 15.6 pg/ml).

### **2.3.21 Western blotting**

Cell were harvested in 500  $\mu$ l of Radioimmunoprecipitation assay buffer (RIPA buffer) (Sigma-Aldrich R0278) supplemented with Halt™ Protease Inhibitor Cocktail (100X) (Thermo Scientific PIER87786) and collected in 1.5 ml Eppendorf tubes. After incubation for 30 minutes on ice, lysates were centrifuged for 20 minutes at 14000g. Supernatant was collected and protein amount was estimated using Pierce™ BCA Protein Assay Kit (Thermofisher 23225) according to manufacturer's instructions. 10  $\mu$ g amount of total protein was loaded per lane on a 10%/4 to 12% NuPAGE Bis-Tris gel (Thermofisher NP0301BOX and NP0322PK2). After electrophoresis, proteins were transferred to nitrocellulose membrane. 5% non-fat milk for 1 hour at room temperature was enough for membranes blocking. Subsequently, the membrane was washed and incubated with desired primary antibodies at 4°C overnight. Following washing the membranes for 3 times, secondary antibodies were incubated for 1 hour at room temperature. For final evaluation, membrane was washed again and incubated with ECL western blot substrate (Thermofisher 32209), before transfer to an Amersham ImageQuant 800 Western blot imaging system. Membranes were incubated in Restore™ Plus Western Blot Stripping Buffer (thermoscientific 10016433) for 5 minutes, followed by a washing step and the blocked with 5% non-fat milk for 1 hour at room temperature, before incubation with indicated primary antibodies.

### **2.3.22 Quantification and statistical analysis**

All experiments were performed with at least two independent clones per cell line. Extracellular flux assays were evaluated by 2-way ANOVA, followed by Sidak post-hoc test. Comparisons between other groups were calculated by using either 2-way ANOVA, unpaired, two-tailed t-tests (\*\*\*)  $p < 0,001$ , (\*\*)  $p < 0,01$ , (\*)  $p < 0,05$ . Error bar indicate mean  $\pm$  standard deviation. All graphs and calculations were generated with GraphPad Prism 7 software.

### 3. Results

#### 3.1 Characterization of E9.5 YS progenitors

We first sought to investigate cells populations in 9.5 YS tissues. In previous studies, investigators described YS erythromyeloid progenitors as KIT<sup>+</sup> Cx3cr1<sup>-</sup> population (Hoeffel, 2015; Perdiguero, 2015; Stremmel, 2018). Flowcytometry analysis of single cell suspensions from E9.5 YS showed YS erythromyeloid progenitors' population (KIT<sup>+</sup> Cx3cr1<sup>-</sup>) while pre-macrophages were (KIT<sup>-</sup> Cx3cr1<sup>+</sup>) (Figure 3.1). Those populations were also identifiable at RNA level as indicated by RT-PCR (Figure 3.2).

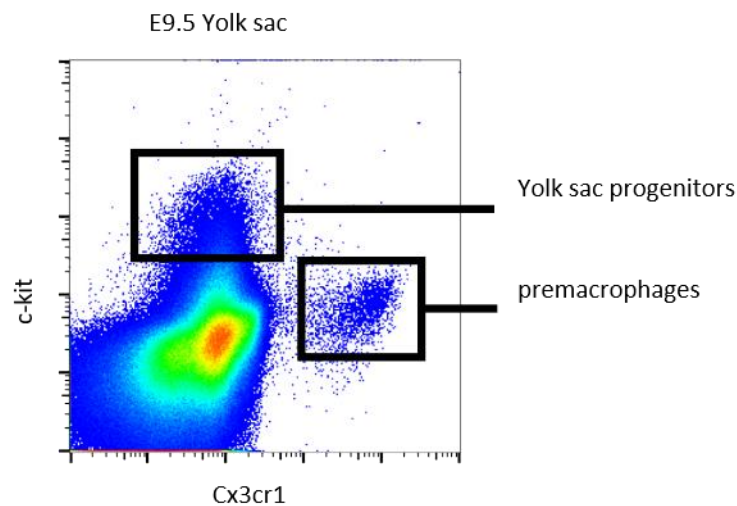


**Figure 3.1: Flow cytometry analysis of expression patterns of early E9.5 hematopoietic cells in the YS membrane.** After enzymatic digestion, cells were stained for c-kit and Cx3cr1 and evaluated using BD Biosciences LSR Fortessa flow cytometer. Data were analyzed using FlowJo 10. YS progenitors are Cx3cr1<sup>-</sup> C-kit<sup>+</sup> population. Cells were gated on live cells. n=.

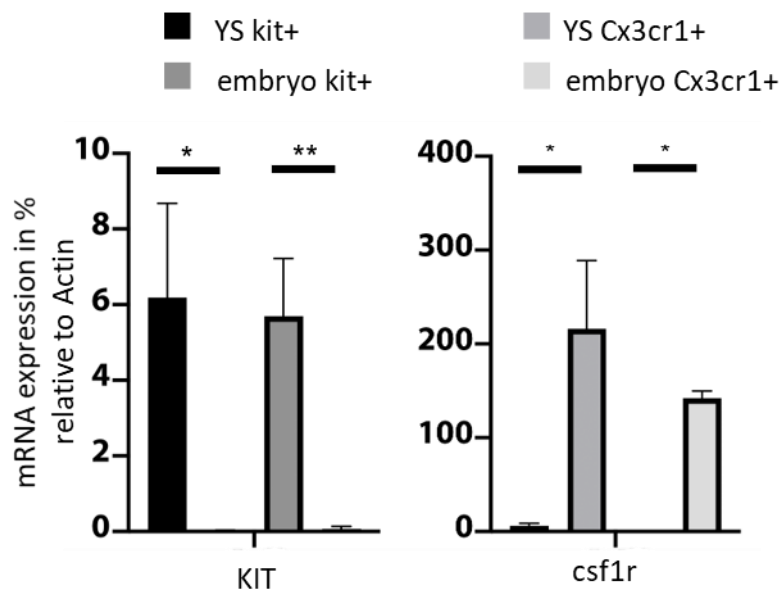


**Figure 3.2: Gene expression comparison of YS progenitors from E9.5 yolk sac membrane to same age embryo.** mRNA expression analysis of sorted *kit+* YS and embryonic *KIT+* progenitors and *CX3CR1+* pre-macrophages from YS and embryo. Data are presented as mean $\pm$ SD; n=3; \*p<0.05; \*\* p<0.01.

### 3.2 Immortalization of YS and BM hematopoietic progenitors using conditional Hoxb8

In this study we investigated the differences between macrophages originating from YS and BM in-vitro under defined conditions, in order to overcome the effects of tissues microenvironment. We employed Hoxb8 system to immortalize hematopoietic progenitors isolated from E 9.5 YS and BM of 8-12 weeks old mice. Cells were transduced with an estrogen-regulated Hoxb8 (ER-Hoxb8) allowing their maintenance and expansion at the progenitor level (Redecke, 2013). Within 5days of estrogen removal and supplementing macrophage colony-stimulating factor (M-CSF), both cell lines differentiated to mature macrophages (Figure 2.1).

### **3.3 Characterization of YS and BM *hoxb8* progenitors**

We then confirmed *Kit* expression in immortalized *Hoxb8* cell lines from both YS and BM origins, in addition, markers of early progenitor states, namely *Kit* and *Runx1*, were downregulated in BM and YS *Hoxb8* macrophages upon maturation while, markers of macrophage differentiation, such as *Lyz2*, *Csf1r* and *Cx3cr1*, were upregulated in both populations (Figures 3.3).

In summary, the *Hoxb8* system successfully conserves the progenitor stage of cells isolated from the YS as well as the BM.

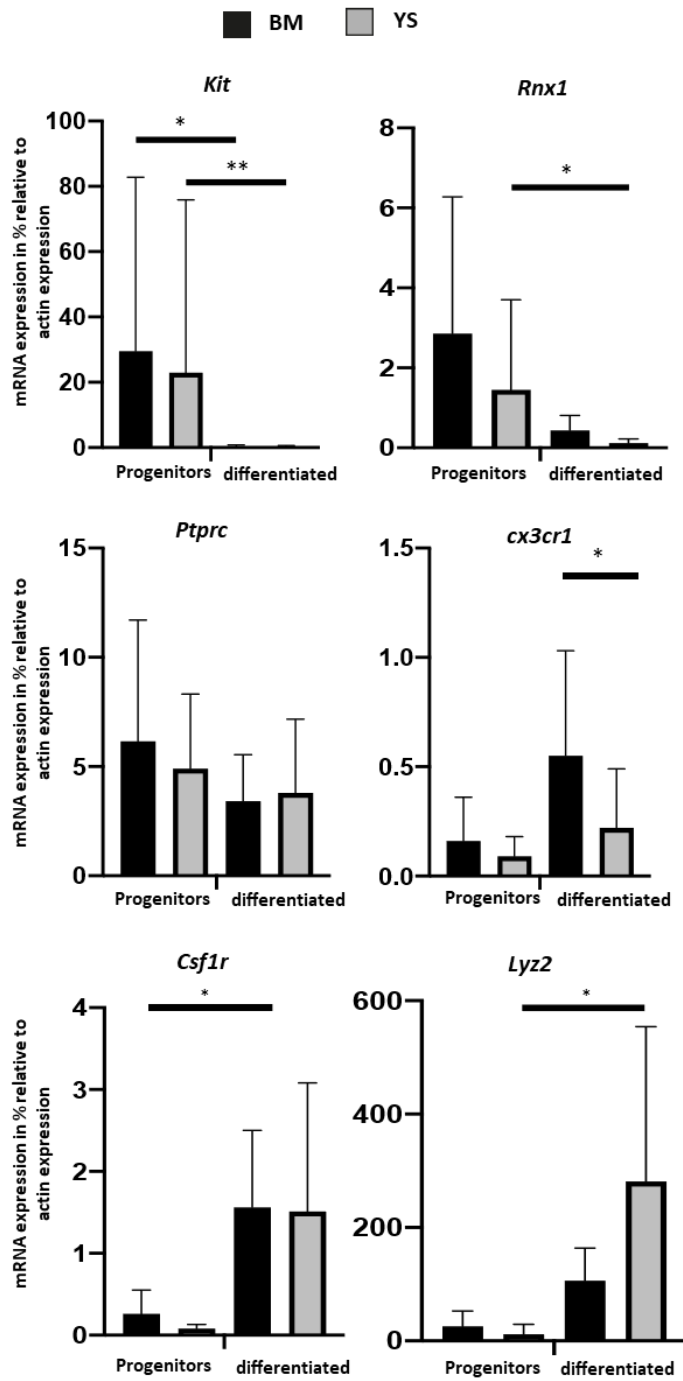


**Figure 3.3: Gene expression analysis.** mRNA expression analyses of Hoxb8 progenitors and differentiated Hoxb8 macrophages for indicated genes in percent (%) relative to *actin* expression. Data are presented as mean±SD; n=3; \*p<0.05; \*\* p<0.01.

Further, we compared cell growth between YS and BM Hoxb8 cell lines. Cell proliferation was similar in both populations with doubling time of approximately 16 hours (Figure 3.4).

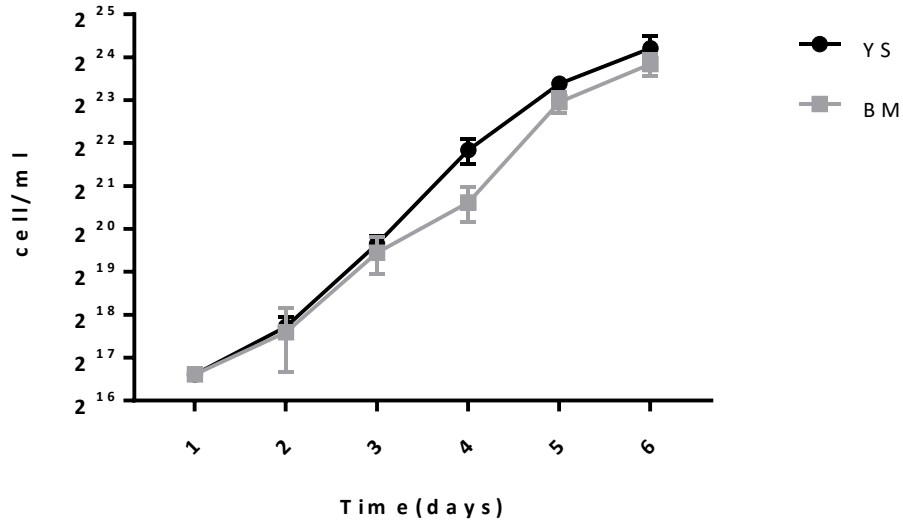


**Figure 3.4:** Growth curve for YS and BM Hoxb8 progenitors. Cells were counted every 24 hours over a period of 6 days. Data are presented as mean $\pm$ SD; n=3, no significant difference. Data was analyzed using 2way ANOVA.

### 3.4 YS and BM Hoxb8 cell lines differentiation, morphology and phagocytic capacity

To compare the rate of differentiation YS and BM hoxb8 cells into macrophages, we removed estradiol from the culture medium and added M-CSF. Consequent to estrogen withdrawal and M-CSF supply, YS- and BM-derived Hoxb8 progenitors differentiated in similar fashion reaching mature macrophage morphology around day 5 and showing the typical macrophage morphology (Figure 3.5).

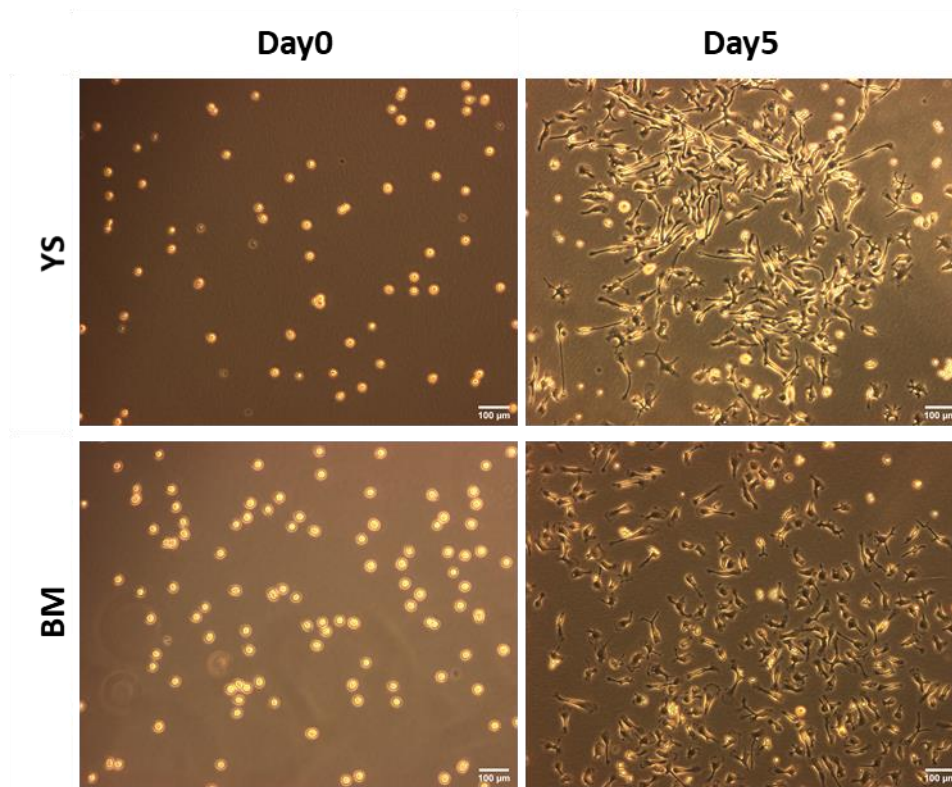


**Figure 3.5: Bright field images of Hoxb8 cell lines during the process of macrophage differentiation.** Hoxb8 cells were incubated with M-CSF after estradiol withdrawal. Their differentiation was observed over 5 days period and representative images were taken to compare their differentiation. Scale bars represent 10  $\mu\text{m}$ .

Giemsa May-Grünwald stain is one of Romanowsky stains that used as reference stain in hematology and cytopathology to differentiate cells. May-Grünwald-Giemsa-stained macrophages from both origins i.e., BM and YS showed the typical macrophage morphology (Figure 3.6).

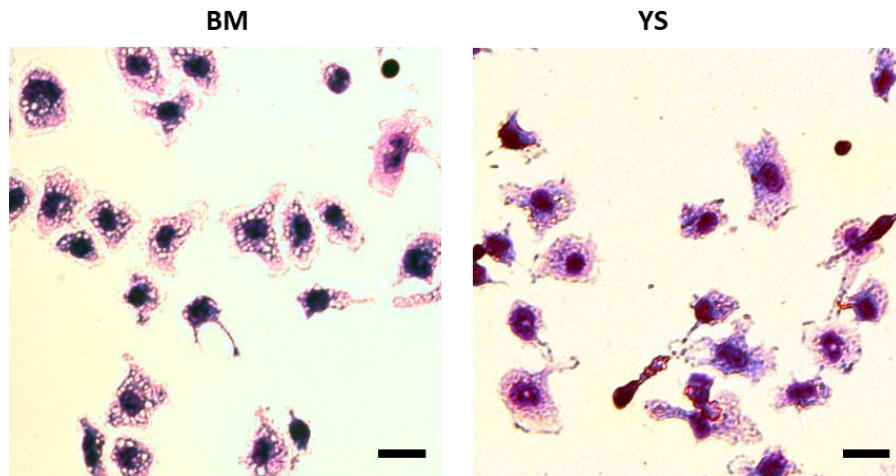


**Figure 3.6: macrophage morphology in May-Grünwald-Giesma stained smears.** After 5 days of differentiation BM and YS Hoxb8 macrophages show typical macrophage morphology. Representative images (n=6). Scale bars represent 20  $\mu$ m.

In our attempt to test the purity of the differentiated hoxb8 cells, we performed flowcytometry analysis of differentiated cells on day 5 of incubation with M-CSF, macrophages represented the most prominent cell populations in YS- as well as BM-derived Hoxb8 cells. A small population of floating and loosely adhering cells represented undifferentiated progenitor cells as well as a minor proportion of neutrophils characterized by LY6G expression. However, medium exchange and simple washing allowed removal of these cells before macrophage harvest (Figures 3.7).

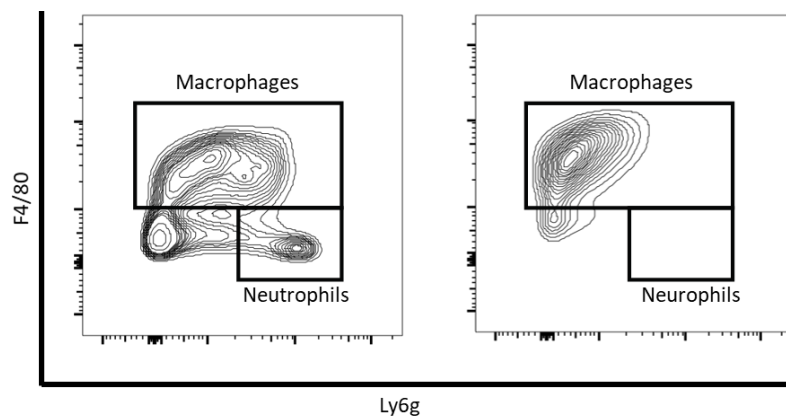


**Figure 3.7: Flow cytometry analysis of floating or adherent differentiated *Hoxb8* BM cells.** Cells labeled with indicated antibodies (representative plot, n=3).

Analogue expression patterns for KI67 as well as leukocyte (CD45), myeloid (CD11b) and macrophage (F4/80, CSF1R) markers were confirmed at protein level by immunofluorescence and flowcytometry (Figures 3.8 and 3.9).

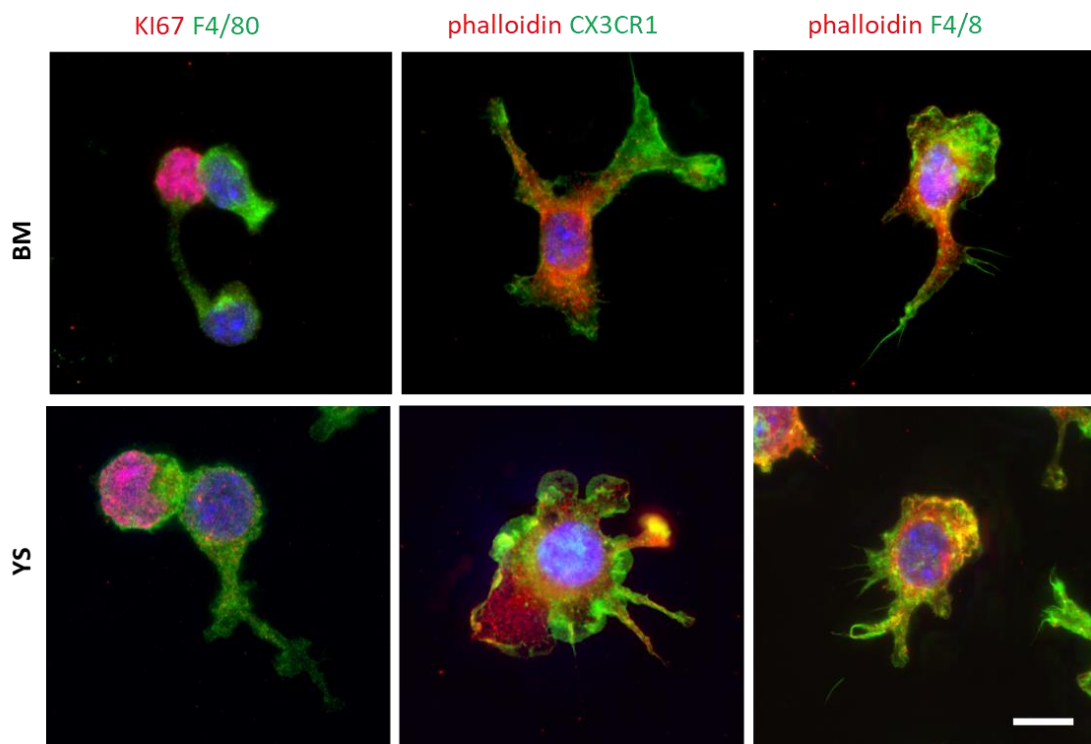


**Figure 3.8: Representative epifluorescence microscopy images of *Hoxb8* macrophages.** Immunofluorescence staining with anti-KI67, anti-CX3CR1 and anti-F4/80. (Nucleus, Hoechst, blue). Scale bar: 20  $\mu$ m.

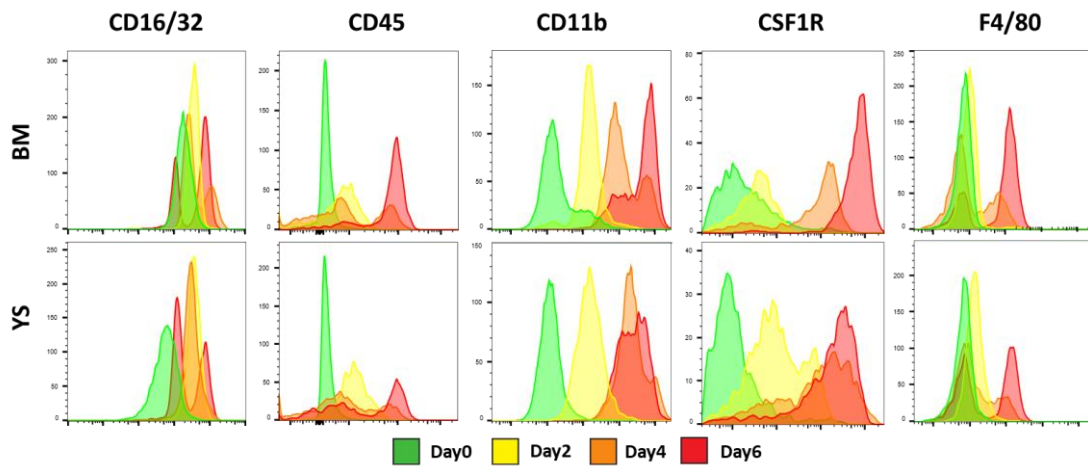


**Figure 3.9: Flow cytometry analyses of Hoxb8 progenitors in the process of differentiation towards macrophages.** (d0 to d6) labelled with indicated antibodies (a representative experiment of n=3).

Differentiated YS and BM Hoxb8 macrophages exhibited efficient phagocytotic capacity when incubated with Zymosan bioparticles, as phagosomes and lysosomes fuse and the pH become more acidic, pHrodo dye conjugated to engulfed Zymosan bioparticles emits green fluorescence indicating successful phagocytosis. In immunofluorescence analyses, both cell types showed comparable amounts of engulfed particles after 60 minutes incubation (Figure3.10).

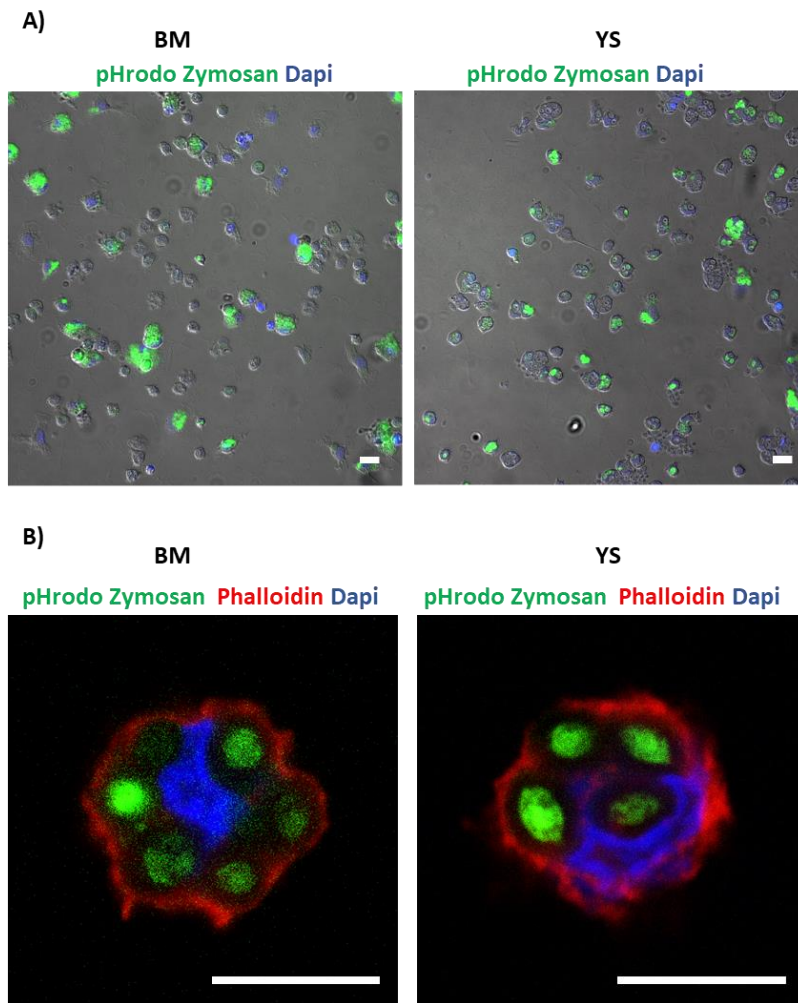


**Figure 3.10: Phagocytosis assay.** BM and YS *hoxb8* macrophages successfully phagocytose pHrodo Zymosan bioparticles (GFP, green) after 1 hour of incubation A) Images taken with epifluorescence microscopy (Nucleus *Hoechst*, blue), B) confocal images (phalloidin in red, Nucleus, *Hoechst*, blue). Representative images (n=3). Scale bar: 20  $\mu$ m.

### 3.5 BM and YS *Hoxb8* macrophages response to cell death stimuli

YS-derived macrophages are long-lived in the brain and other tissues. In contrast, BM-derived macrophages longevity is controversial, they are continuously recruited to systems that are in continuous communication with their surrounding environment and their recruitment rises in case of infection and inflammation to serve defense function. We

therefore asked, whether YS and BM Hoxb8 macrophage might respond differentially to defined inducers of cell death; namely, Fas ligand (SuperFasL) and ultraviolet (UV) rays. Macrophages were labelled with (AnxV) as measurement of apoptosis and (AnxV and PI) as indicator of secondary necrosis and the percentage of AnxV+ and AnxV+ PI+ cells over period of 34 hours were quantified on an LSR II flow cytometer. On one hand, YS and BM macrophages showed dose dependant susceptibility to UV, as majority die with secondary necrosis (AnxV+ PI+ cells (%)). On the other hand, Both YS and BM macrophages showed resistance to SuperFasL, interestingly the percentages of cells that showed apoptosis and/or secondary necrosis were minimal regardless the SuperFasL concertation.

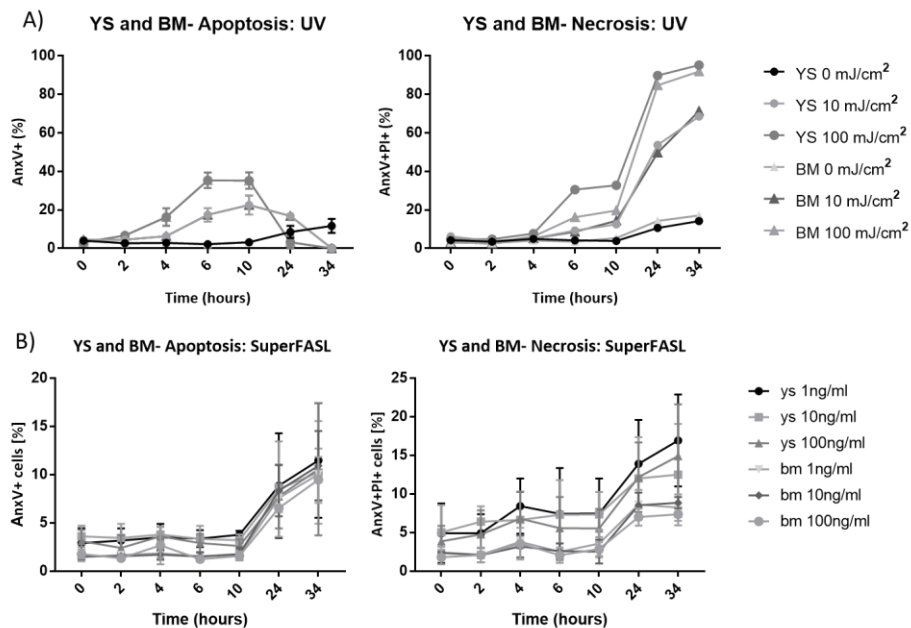


**Figure 3.11: YS and BM macrophages response to cell death stimuli.** Quantification of UV- and SuperFasL-dependent apoptosis and necrosis in differentiated Hoxb8 macrophages (A and B respectively) after incubating with annexin V-FITC and propidium iodide. n=3. Unpaired, two-tailed t-test.

### 3.6 Comparison of Transcriptome of BM and YS Hoxb8 macrophages

We next conducted a transcriptome analysis to compare RNA expression of BM and YS Hoxb8 macrophages under identical environmental conditions. Principal Component Analysis (PCA) of progenitors and differentiated BM and YS under steady state and LPS and IL4 stimulation allows an explorative analysis with reduced dimensions. Using this statistical approach, we assessed data sets and their variance with a reduced number of variables. We identified clusters of 1) YS and BM progenitors, 2) mature macrophages in the presence and absence of IL-4, 3) LPS-stimulated differentiated macrophages when applying the indicated principal components 1 and 2 (Figure 3.11).

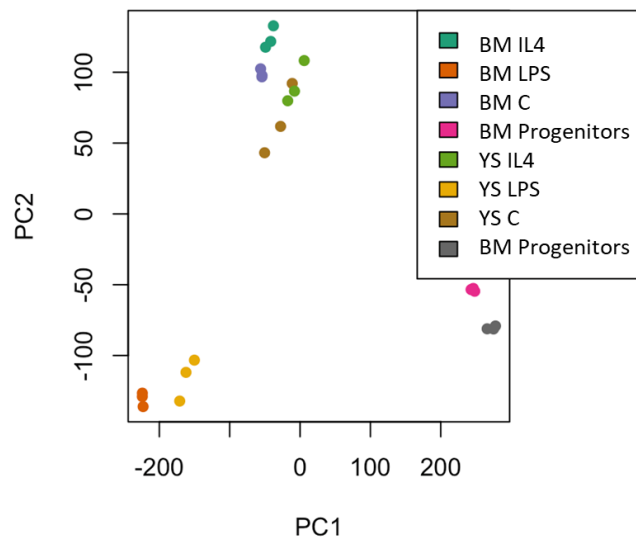


**Figure 3.12: Principal Component Analysis (PCA) of progenitors and differentiated BM and YS under steady state and LPS and IL4 stimulation.** BM hoxb8 progenitors and YS hoxb8 progenitors. BM C and YS C: are differentiated YS and BM hoxb8 cells without stimulation. BM LPS and YS LPS: are differentiated YS and BM hoxb8 cells stimulated with 100 ng/ml LPS for 5 hours. BM IL4 and YS IL4: are differentiated YS and BM hoxb8 cells stimulated with 100 ng/ml IL4 for 5 hours.

A large proportion of genes overlapped as expected (Figure 3.12). Nonetheless, we identified several genes that were differentially expressed between YS and BM

macrophages. on one hand, RNA abundance of Ripk3 and Pycard were increased in BM Hoxb8 macrophages (Figures 3.12). Similarly, C-X-C motif chemokine ligand (Cxcl) 10 and Cxcl11 in addition to inducible nitric oxide synthase (Nos2) were upregulated in BM Hoxb8 macrophages. Further, in BM Hoxb8 macrophages we identified an increased abundance of apoptosis-associated genes such as Tgm2, which promotes leukocyte apoptosis (Sándor, 2016). Additional, Fam129a encodes for the apoptosis-regulating protein Niban was among upregulated genes in BM macrophages (Ji, 2012; Tang, 2019).

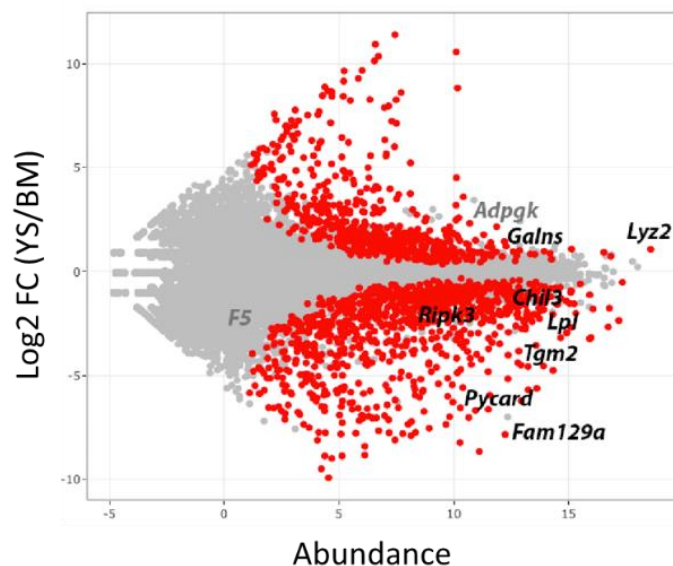


**Figure 3.13: MA-plot of macrophage gene expression.** The plot indicates fold changes (log2) of differentiated YS and BM hoxb8 cells without stimulation plotted against abundance (log2). Genes are marked in grey (not significant) or red (significant differences), genes of interest labelled.

On the other hand, YS-derived Hoxb8 macrophages expressed higher RNA levels of clusterin (apolipoprotein J), which has been associated with apoptotic cell clearance and matrix reorganization (Cunin, 2016; Shim, 2011). Similarly, the transcription factor Mafk, which is known to promote anti-inflammatory polarization and cholesterol efflux, was upregulated in YS-derived Hoxb8 macrophages (H, 2017). Triggering receptor expressed

on myeloid cells 2 (Trem2) and Sal-like protein (SALL) 1 and 3, were upregulated in YS macrophages (figure 3.13). Similarly, Microtubule-associated tumor suppressor candidate 2 (Mtus2) is among the most upregulated genes in YS Hoxb8 macrophages, and has recently been identified as a binary protein interaction partner of macrophage colony-stimulating factor (M-CSF) in a large screening approach (Luck, 2020).

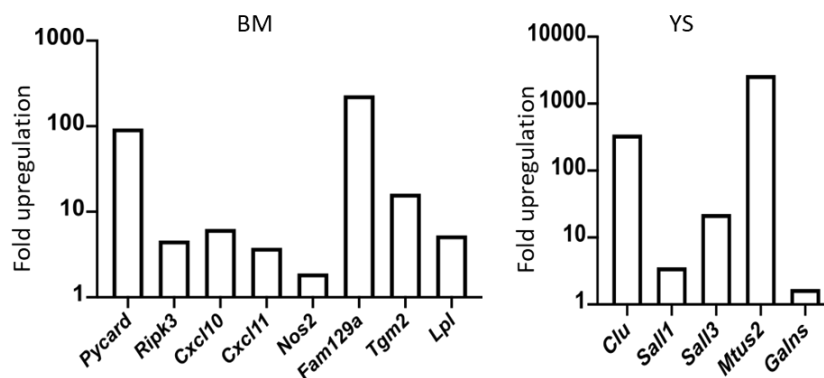


**Figure 3.14: Fold upregulation of selected genes in BM and YS-derived macrophages.** The graph shows selected genes that were found to be significantly upregulated in differentiated BM hoxb8 macrophages in comparison to differentiated YS hoxb8 macrophages and vice versa.

We further investigated RNA expression levels after stimulation with either IL4 or LPS under standardized in vitro conditions. Cell type specific differences between YS and BM macrophages in top regulated genes were in part independent of cytokine stimulation (Figure 3.14 and 3.15), supporting the role of cell-intrinsic macrophage programs.

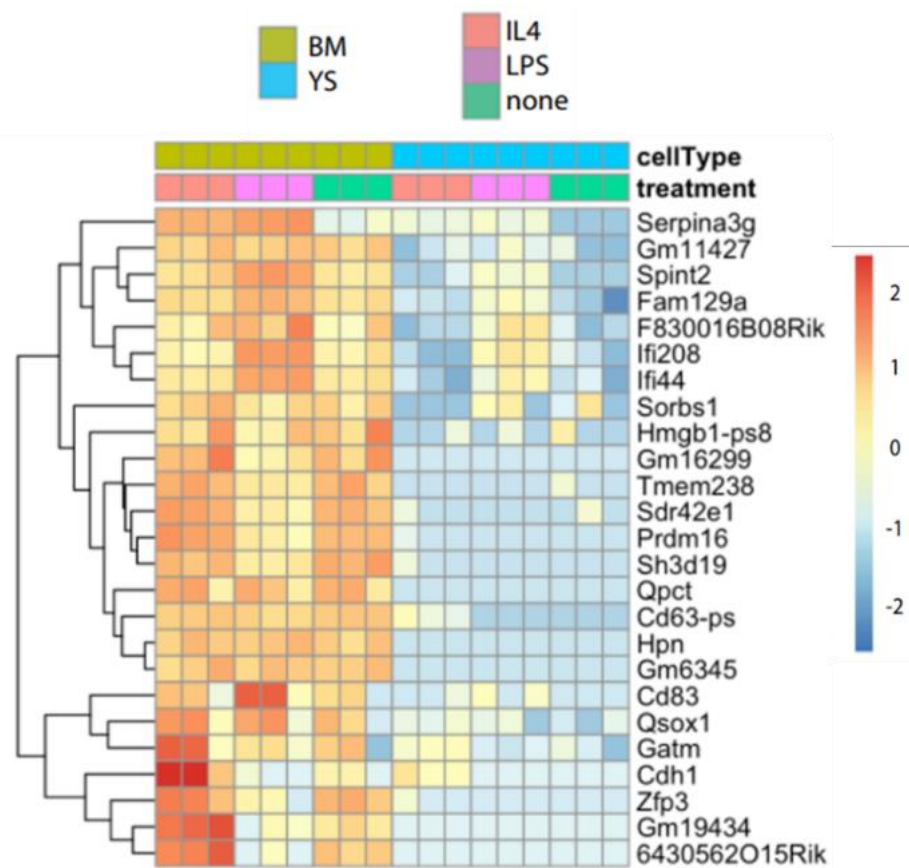


**Figure 3.15: Heatmap showing the top 25 upregulated genes in BM compared to YS macrophages.** RNA transcripts of differentiated YS and BM *hoxb8* cells without stimulation and stimulated with either LPS or IL4 (100 ng/ml each for 5 hours).

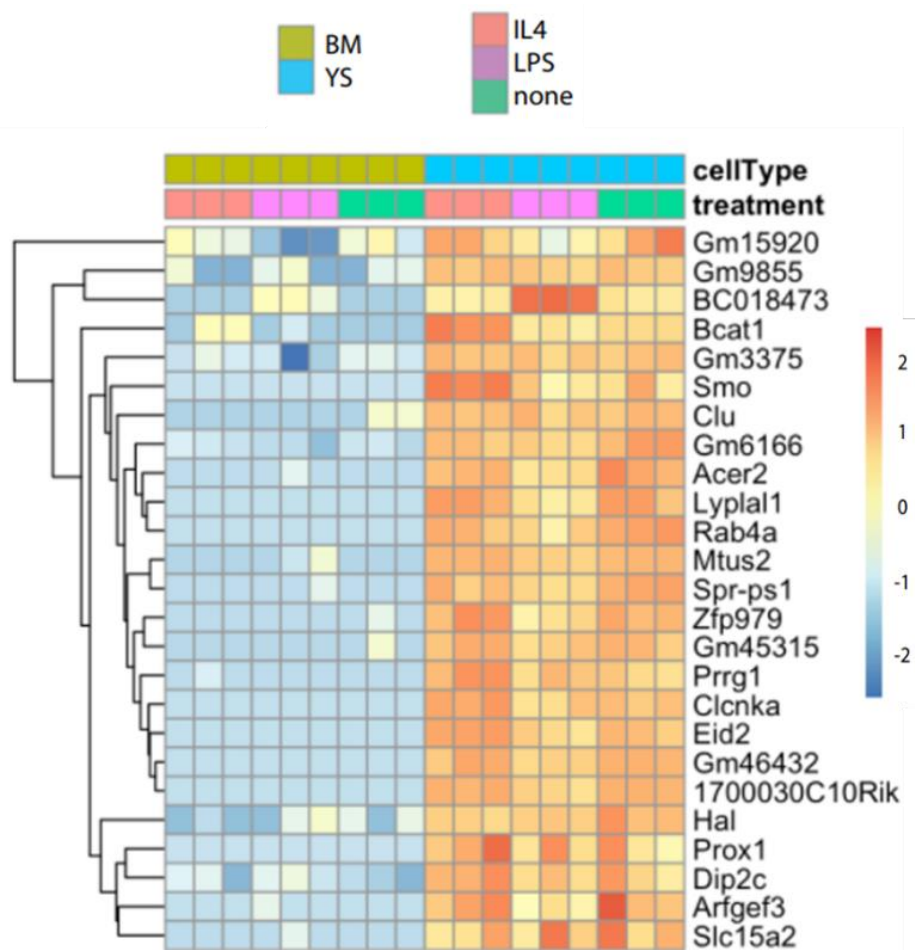


**figure 3.16** Heatmap showing the top 25 downregulated genes in BM compared to YS macrophages. RNA transcripts of differentiated YS and BM *hoxb8* cells without stimulation and stimulated with either LPS or IL4 (100 ng/ml each for 5 hours).

### 3.7 Proteome analysis of BM and YS *Hoxb8* macrophages

We next conducted an in-depth proteome analysis by quantitative mass spectrometry to further compare both YS and BM macrophages under identical environmental conditions. Besides a large proportion of overlapping proteins as expected, we identified proteins with differential abundance between both cell populations (Figure 3.16).

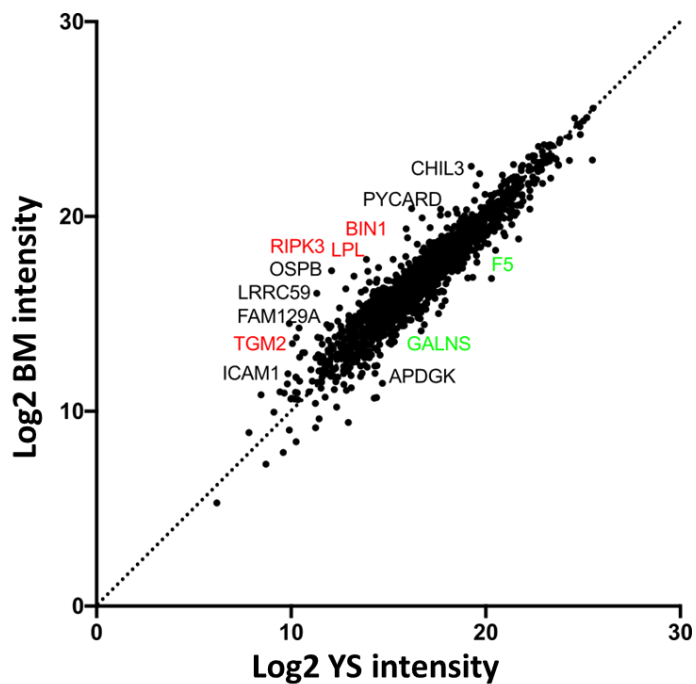


**Figure 3.17: Proteome analysis of day 5 differentiated Hoxb8 macrophages.** Protein intensities (log<sub>2</sub>) of BM versus YS macrophages are indicated. Selected, differentially abundant proteins are annotated and colored in red (BM) or green (YS).

BM Hoxb8 macrophages expressed high levels of the inflammasome activator ASC (PYCARD) and proteins of the TNF signaling pathway such as receptor-interacting serine/threonine-protein kinase 3 (RIPK3). Further in line with the transcriptome analysis, we determined high abundance of the apoptosis-associated enzyme TGM2. Likewise, Intercellular adhesion molecule 1 (ICAM1), an important adhesion molecule involved in leukocyte migration, showed increased abundance in BM macrophages. Lastly, lipoprotein lipase (LPL), Myc box-dependent-interacting protein 1 (BIN1), Oxysterol-binding protein 1 (OSBP), the leucine-rich repeat-containing protein 59 (LRRC59) and protein niban (FAM129A) displayed high abundance in BM Hoxb8 macrophages (Figure 3.16).

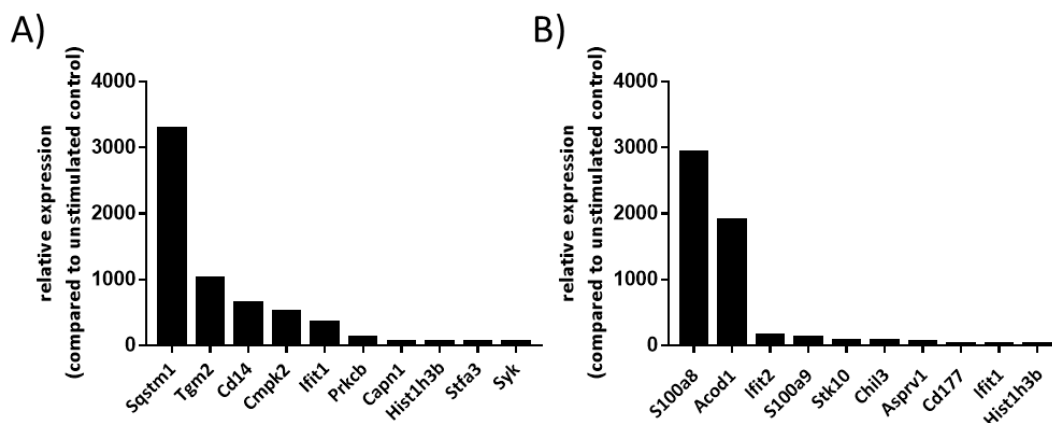


**Figure 3.18: Top 10 upregulated proteins in BM and YS macrophages after LPS stimulation.** Top upregulated proteins of LPS stimulated BM (A) and YS (B) after LPS stimulation (100 ng/ml for 5 hours) in comparison to unstimulated BM and YS macrophages respectively.

YS Hoxb8 macrophages showed increased abundance of coagulation factor 5, the lysosomal protein galactosamine (N-Acetyl)-6-sulfatase (GALNS) and ADP-dependent glucokinase (ADPGK), a protein of the glycolysis pathway (Figure 3.16). Interestingly, Chitinase-like protein 3 precursor (CHIL3) – a protein which has been associated with alternatively activated macrophages – was slightly elevated in BM-derived Hoxb8 macrophages, whereas after lipopolysaccharide (LPS) stimulation CHIL3 was identified among the top ten upregulated proteins in YS-derived macrophages (Figure 3.17). BM-derived Hoxb8 macrophages showed an increased abundance of sequestosome-1 (SQSTM1), which has been associated with autophagy, after stimulation. In addition, TGM2 and CD14 expression significantly increased after LPS in BM-derived macrophages.

### 3.8 Comparison of YS and BM derived macrophage energy metabolism

The decision to carry out extracellular flux measurement was guided by the differences in oxidative phosphorylation indicated in the gene set enrichment analysis GSEA (see appendix). Extracellular flux allows interrogation of this aspect on the functional level

by measuring changes in O<sub>2</sub> concentration (oxygen consumption or OCR), and pH (extracellular acidification rate, or (ECAR), that result from changes in mitochondrial respiration and glycolysis pathways. We carried the measurement in steady state as well as under LPS and IL4 stimulation.

OCR from the medium surrounding cells reflects important metabolic activity such as non-mitochondrial respiration, mitochondrial respiration, ATP-linked, Proton Leakage (PL) maximum oxidation maximum oxidation after adding pyruvate. Under steady state, BM derived macrophages showed higher maximum substrate oxidation capacity (figure) and lower proton leak respiration (PL) in comparison to YS derived macrophages (figure 3.19).

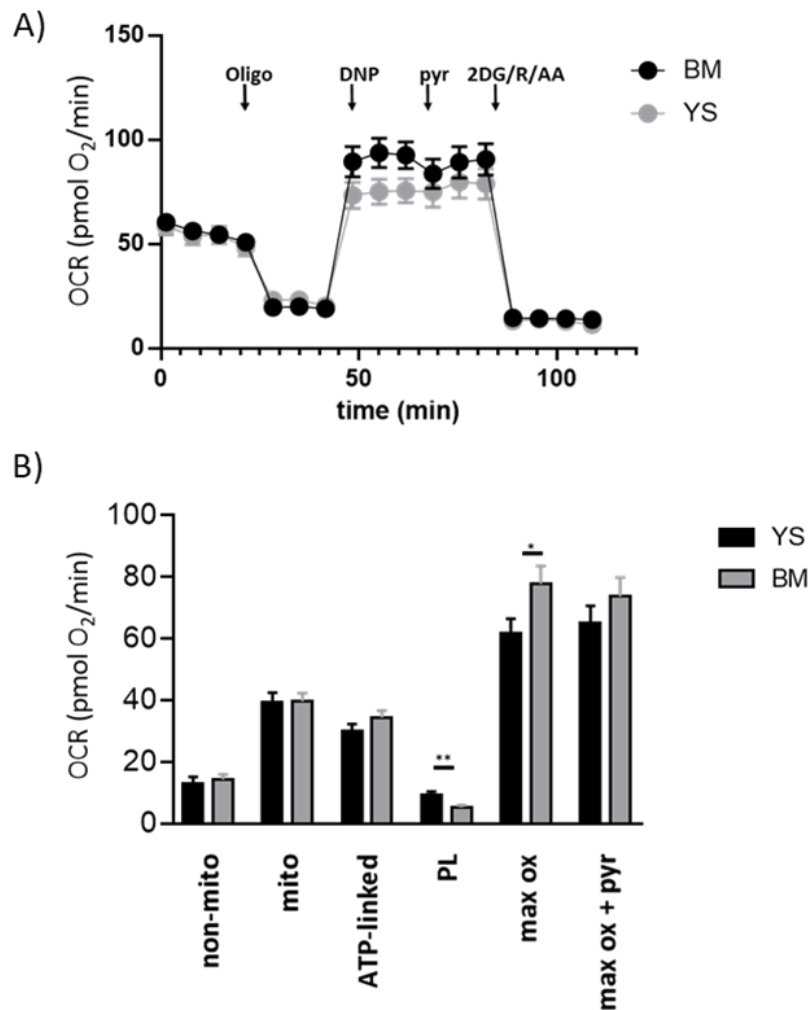


**Figure 3.19: Oxygen Consumption Rate (OCR).** A) Time laps Oxygen consumption rates (OCR) traces of unstimulated BM and YS macrophages using respiratory inhibitors to probe bioenergetic modules. Oligomycin, DNP, Rotenon and AA, known inhibitors of the mitochondria and the electron chain reaction were automatically and consecutively injected to the wells of XF96 plate in order to estimate mitochondrial respiration and glycolysis. Moreover, Pyruvate was injected to feed TCA cycle and 2DG was injected to shut down glycolysis. B) Oxygen Consumption Rate OCR dissected into non-mitochondrial respiration, mitochondrial respiration, ATP-linked, Proton Leakage (PL) maximum oxidation maximum oxidation after adding pyruvate. In steady state, BM derived macrophages show higher maximum substrate oxidation capacity and lower proton leak respiration (PL) in comparison to YS derived macrophages. Data represent the mean of 26-29 wells measured on three independent experimental days and are normalized to 130 ng ds DNA/well. Statistic: T-Test, \*  $p < 0.05$ ; \*\*  $p < 0.01$ ; \*\*\*  $p < 0.001$ .

Coupling efficiency (CE) corresponds to the fraction of basal mitochondrial respiration dedicated to ATP production while, Cellular respiratory control ratio (cRCR) measures the ratio of Maximum substrate oxidation capacity to proton leak respiration, as from our experiment, BM show higher efficiency to produce ATP as retrieved from (CE) and (cRCR) in steady state, interestingly, LPS and IL4 stimulation seem to improve efficiency of ATP production in YS (figure 3.20).

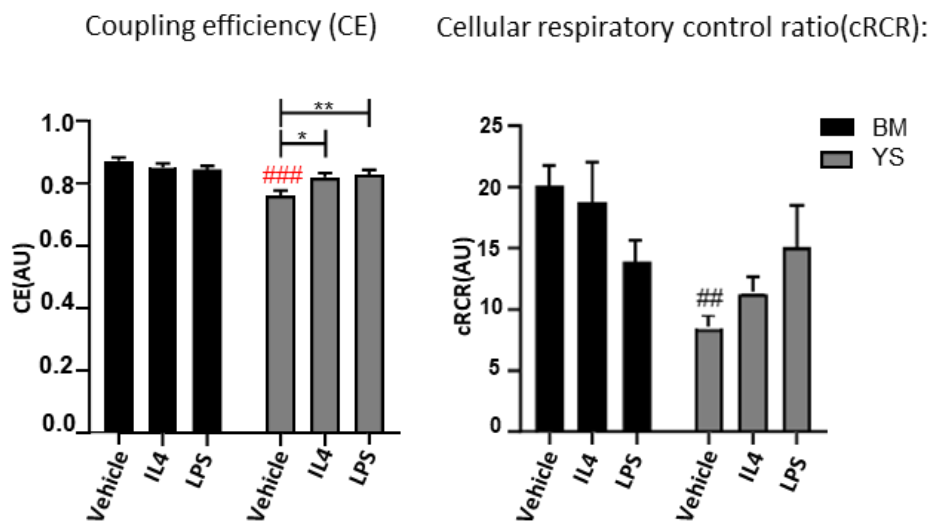


**Figure 3.20: Mitochondrial efficiency.** Coupling efficiency (CE) is the respiratory fraction driving ATP synthesis at resting state, cellular respiratory control ratio (cRCR) is determined using proton leak and uncoupler-induced respiration. Data represent the mean of 26-29 wells measured on three independent experimental days and are normalized to 130 ng ds DNA/well. 2-way ANOVA, followed by Sidak post-hoc test. Stimulation: \*  $p < 0.05$ ; \*\*  $p < 0.01$ ; \*\*\*  $p < 0.001$ ; cell line: #  $p < 0.05$ ; ##  $p < 0.01$ ; ###  $p < 0.001$ .

Time lapse ECAR traces for BM and YS, can be dissected into different functional modules such as non-glycolytic acidification, glycolysis (acidification) and induced glycolysis, while LPS stimulation has significantly increased glycolysis in YS, BM derived macrophages show higher glycolytic activity than their YS counterparts under all conditions (Figure 3.21).

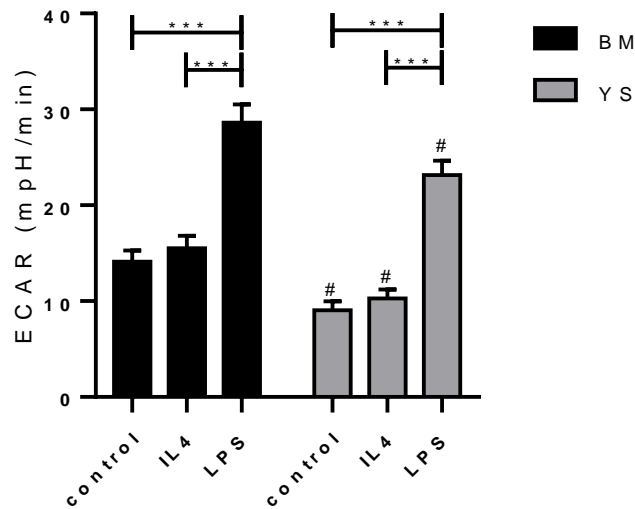


**Figure 3.21: ECAR linked to glycolytic activity of unstimulated and stimulated macrophages.** Data represent the mean of 26-29 wells measured on three independent experimental days and are normalized to 130 ng ds DNA/well. 2-way ANOVA, followed by Sidak post-hoc test. Stimulation: \* p<0.05; \*\* p<0.01; \*\*\*p<0.001; cell line: # p<0.05; ## p<0.01; ### p<0.001.

There was no significant difference in ATP turnover/demand between BM and YS, neither at steady state nor under stimulation with LPS or IL4 (figure 3.22). moreover, ATP production was Partitioned into OXPHOS and glycolysis, BM derived macrophages showed higher glycolytic contribution to ATP homeostasis however LPS found to increase YS macrophages dependence on glycolysis for ATP production (figure 3.23).

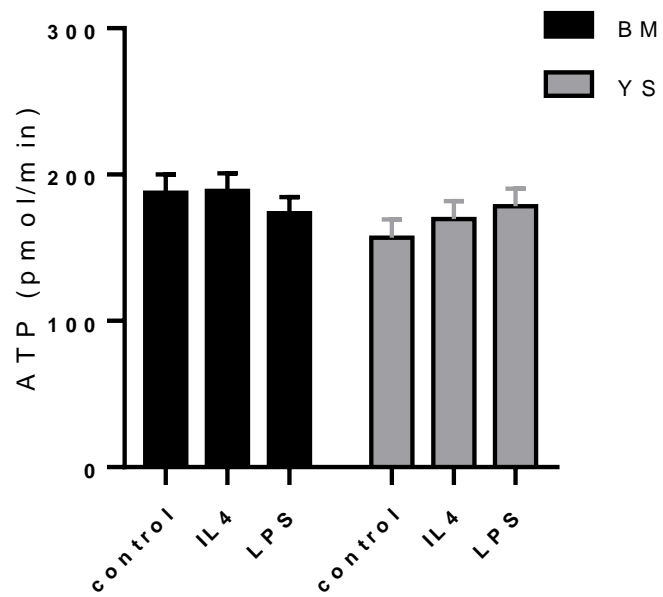


**Figure 3.22: Comparison of total ATP Demand/turnover between BM and YS macrophages.** Neither LPS nor IL4 significantly changes ATP demand/turnover in BM and YS macrophages. Data represent the mean of 26-29 wells measured on three independent experimental days and are normalized to 130 ng ds DNA/well. 2-way ANOVA, followed by Sidak post-hoc test.

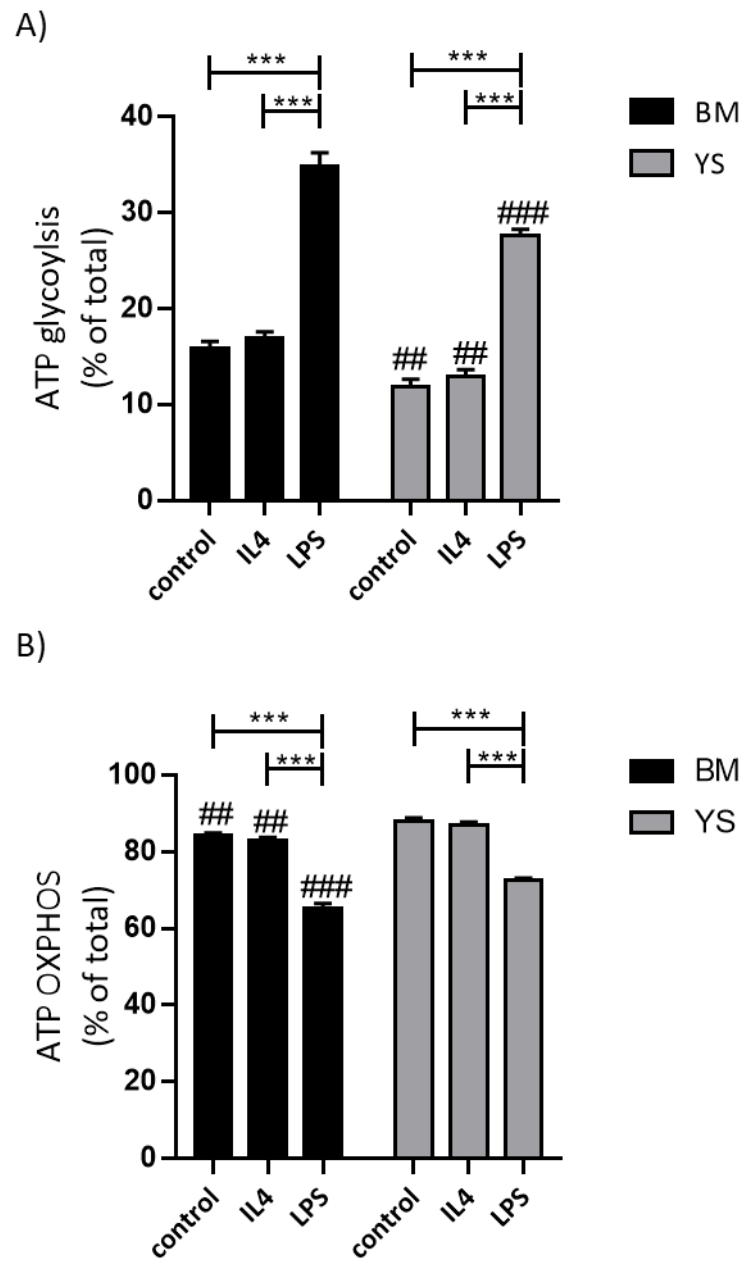


**Figure 3.23: Partitioning of ATP production.** From glycolysis A) and oxidative phosphorylation B) under steady state as well as LPS and IL4 stimulation. BM macrophages showed further dependence on glycolysis for ATP production, while LPS switches ATP production to glycolysis in YS macrophages. Data represent the mean of 26-29 wells measured on three independent experimental days and are normalized to 130 ng ds DNA/well. 2-way ANOVA, followed by Sidak post-hoc test. Stimulation: \*  $p < 0.05$ ; \*\*  $p < 0.01$ ; \*\*\*  $p < 0.001$ ; cell line: #  $p < 0.05$ ; ##  $p < 0.01$ ; ###  $p < 0.001$ .

Plotting OCR against ECAR revealed higher overall metabolic activity in BM versus YS-derived Hoxb8 macrophages, in addition LPS triggered metabolic switch from oxidative phosphorylation to glycolysis ('Warburg-like effect'), an effect happened to be more pronounced in BM-derived macrophages. IL4 stimulation did not induce metabolic switch (Figure 3.24).

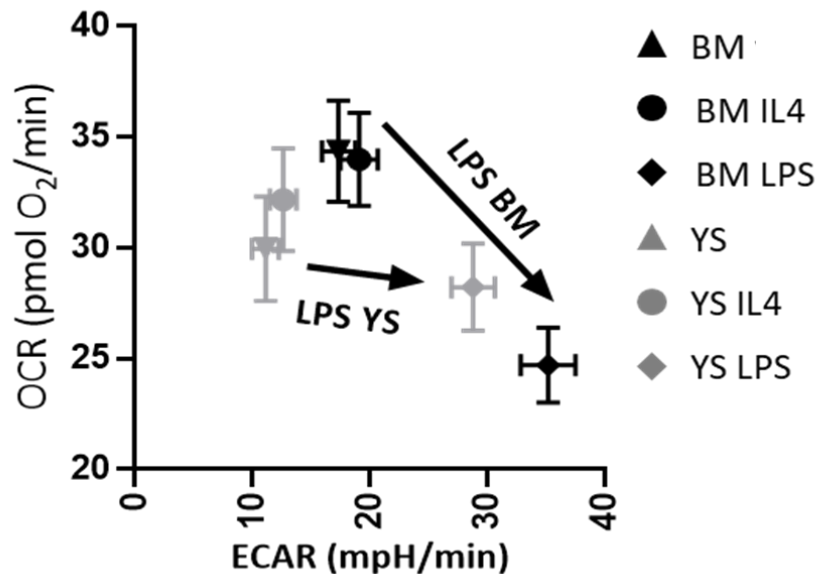


**Figure 3.24: BM and YS macrophages metabolic switch following LPS and IL4 stimulation.** Glycolytic ECAR plotted against ATP-linked OCR revealing the metabolic switch induced by LPS in BM Hoxb8 macrophages while IL4 does not seem to affect the metabolic status of BM and YS macrophages.

In summary, BM-derived Hoxb8 macrophages higher mitochondrial efficiency in the steady state and higher glycolytic activity under all conditions. Moreover, YS cells show higher dependence on oxidative phosphorylation for ATP production while BM cells depend on glycolysis.

### 3.9 Cytokine secretion and Inflammasome activation

First, we studied the response of Hoxb8 macrophages to LPS and IL4 in a multiplex cytokine analysis. Interestingly, cytokine release was similar between YS and BM macrophages (Figure 3.25).

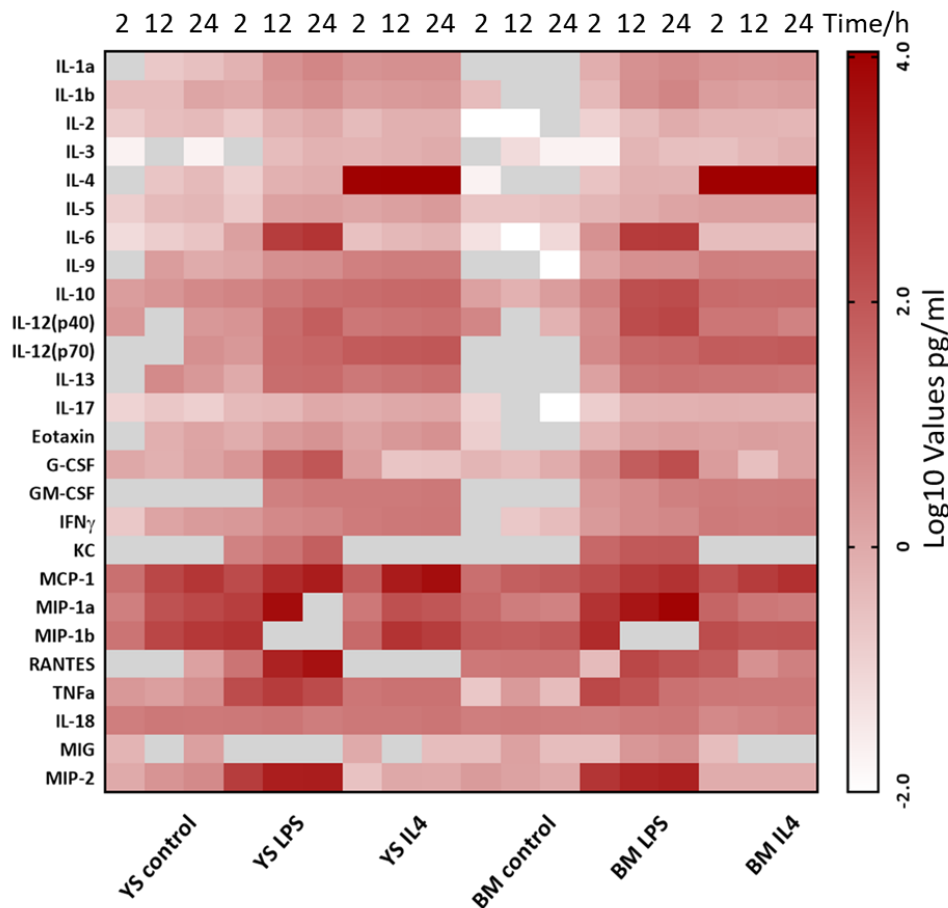


**Figure 3.25: Cytokine expression analysis by Multiplex ELISA.** Quantification of cytokines in cell culture supernatant of stimulated Hoxb8 macrophage. BM and YS macrophages were treated for 2,12 and 24 hours with 100 ng/ml LPS or IL-4. Non-polarized cells served as controls. Data are shown as heatmap; Results are representative for three independent experiments. untreated (control) and LPS or IL4 stimulated samples. n=3. Pearson's correlation.

The increased abundance of PYCARD, an important adaptor protein associated with inflammasome activation, on both RNA and protein level, drove us to further investigate

both canonical and non-canonical activation of the NLRP3 inflammasome pathway in YS and BM macrophages.

In order to investigate canonical activation of the NLRP3 inflammasome pathway, we primed Hoxb8 macrophages with LPS and stimulated them with crystals (Düwell, 2010b). Using ELISA, we carried IL1 $\beta$  quantification as measure of inflammasome activation. Monosodium urate (MSU), Cholesterol (CH) and Bilirubin (BIL) crystals, classical activators of the canonical inflammasome pathway induced the release of IL1 $\beta$  from LPS-primed BM macrophages. As expected, IL1 $\beta$  secretion was absent in caspase 1/11-deficient BM macrophages. Notably, IL1 $\beta$  secretion from LPS-primed and crystal-stimulated YS Hoxb8 macrophages was low, indicating low-level of inflammasome activation (Figure 3.26).

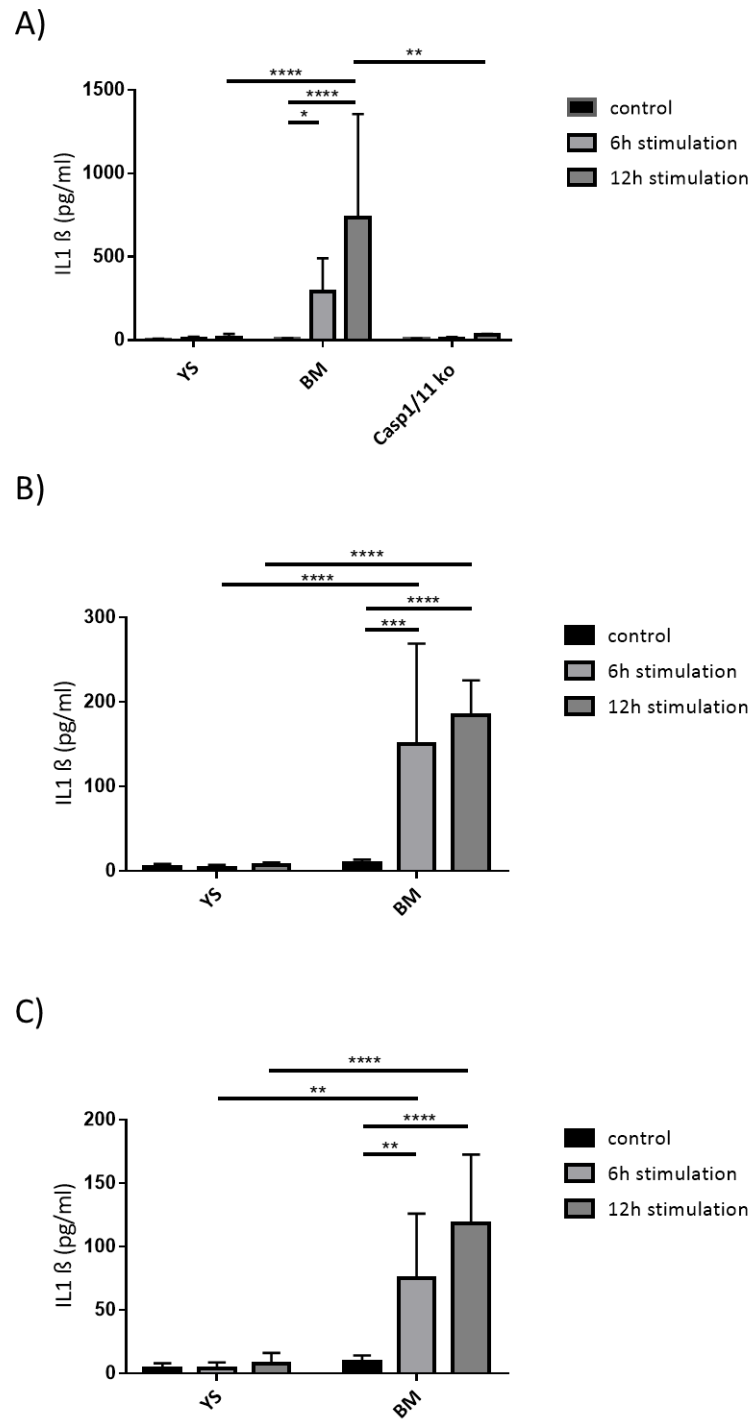


**Figure 3.26: Measurement of IL-1 $\beta$  in cell culture supernatants after stimulation with LPS followed by MSU, CH and BIL crystals. Y5 and BM macrophage were left without stimulation (control) or treated with**

200 ng/ml LPS for 3 hours followed by either A) 250 ug/ml MSU crystals, B) Cholesterol crystals, C) Bilirubin crystals. Stimulation was carried out for 6 and 12 hours. Data are presented as mean±SD; Two-way ANOVA test.; n=6-8 per group; \* p<0.05; \*\* p<0.01; \*\*\*p<0.001.

Furthermore, we confirmed our findings using western blot and determined a pronounced inflammasome response upon MSU crystal stimulation in BM Hoxb8 macrophages represented by high expression levels of PYCARD and CASP1, in contrary to YS macrophages (Figure 3.27).

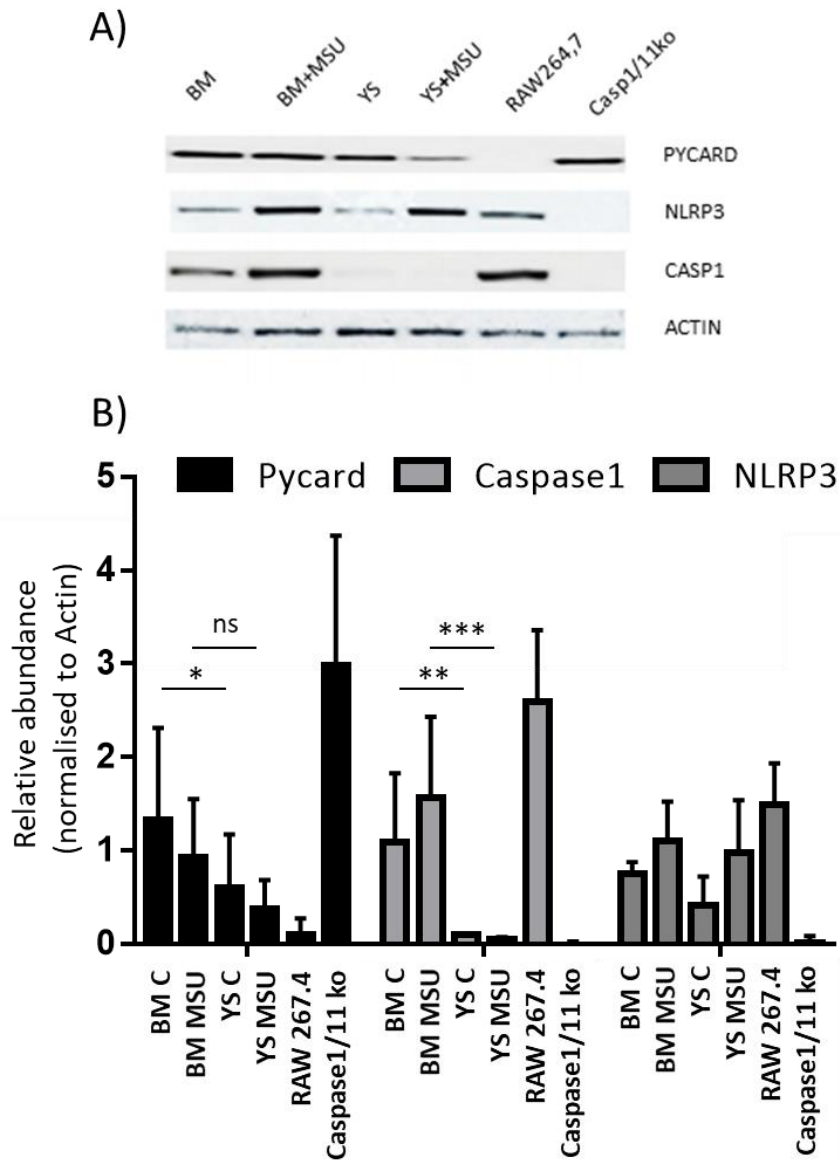


**Figure 3.27: Quantification of NLRP3 inflammasome proteins in BM and YS macrophage cells lysate after stimulation with LPS followed by MSU crystals.** Western blotting of non-stimulated YS and BM macrophage or treated with 200 ng/ml LPS for 3 hours followed by 250 ug/ml MSU crystals for 24 hours, A) Western blots representative of 5 independent experiments. B) Quantitative comparison of Proteins level of NLRP3 inflammasome components using Western blot normalized to Actin. Data are presented as mean±SD; n=3; \*p<0.05 \*\* p<0.01; \*\*\*p<0.001.

To address non-canonical inflammasome activation, we harnessed *Escherichia coli* outer membrane vesicles (*E. coli* OMVs). OMVs are typically produced by Gram-negative bacteria and mediate cytosolic LPS localization leading to robust caspase-11 activation (Vanaja, 2016). Stimulation with *E. coli* derived OMVs elicited a pronounced IL1 $\beta$  response in BM derived macrophages which was abrogated in their YS-derived counterparts (Figure 3.28).

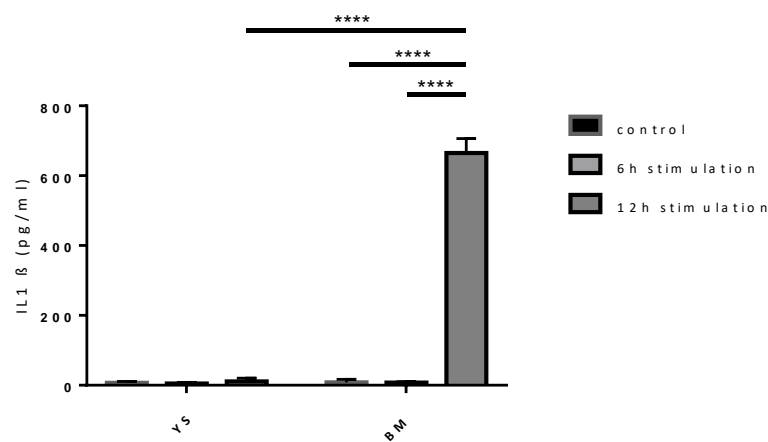


**Figure 3.28: Measurement of IL-1 $\beta$  in cell culture supernatants after stimulation with *E. coli* OMVs.** YS and BM macrophages were treated with 2 $\mu$ g/ml *Escherichia coli* outer membrane vesicles (OMVs) for 6 and 12 h. Data are presented as mean $\pm$ SD; (n=3). \* p<0.05; \*\* p<0.01; \*\*\*p<0.001; \*\*\*\*p<0.0001. Two-way ANOVA test.

Altogether, BM-derived but not YS-derived Hoxb8 macrophages exhibited robust NLRP3 inflammasome activation via both canonical and non-canonical pathways, suggesting a fundamental difference between macrophages originating from YS and BM.

## 4. Discussion

### 4.1 Methods

Conditional expression of Hoxb8 in hematopoietic progenitors allows to preserve their proliferative, immature status and to prohibit terminal differentiation into immune effector cells (Redecke, 2013; G. G. Wang, 2006). Upon estrogen withdrawal the ectopically expressed gene encoding Hox is inactivated allowing synchronous differentiation of Hoxb8 progenitors under guidance of specific cytokines. In the presence of GM-CSF or M-CSF, they differentiate into dendritic cells and macrophages and granulocytes respectively. Hoxb8 dendritic cells show potent immune functions both in vivo and in vitro, and were protective against tumor when injected prior the encounter of experimentally induced tumor. Hoxb8 macrophages show phagocytic activity and produced NO in levels comparable to primary bone marrow macrophages (Redecke, 2013). However, to the best of our knowledge, YS derived hoxb8 cell lines have not been reported to date.

In previous studies, differences in lineage commitment and efficiency have been described for the SCF Hoxb8 system when differentiating myeloid cells in vitro. The efficiency can be modified by preselection of hematopoietic cells subjected to Hoxb8 transfection. For example, depleting Mac1+, B220+, Thy1.2+ cells from whole bone marrow before Hoxb8 transfection has been described to promote lineage decision towards neutrophils (98%-99%). ER-Hoxb8 progenitors immortalized in presence of GM-CSF only were described to have more than 99% macrophage commitment (G. G. Wang, 2006). Our protocol is a modified version of both and comprised of isolation of BM mononuclear progenitors without negative selection in addition to hoxb8 transfection in presence of SCF. Besides, our modified differentiation protocol that includes changing the medium and supply M-CSF every other day purifies the population and removes all other

non-adherent progenitors and or granulocytes. By applying our protocol, we achieved macrophage populations of high purity as confirmed by flow cytometry, Giemsa stain and RNA seq and proteomic analysis.

Erythro-myeloid progenitors (EMP) that appear in the yolk sac of mouse embryos by E8.25 have been defined as first 'definitive' progenitors (Bertrand, 2005; Palis, 1999). EMPs seed fetal liver already by E9, in Yolk sac EMPs peak between E9.5 and E10.5 (Kieusseian, 2012). We have chosen E9.5 embryonic age, as EMP production is at its peak and the progenitor cells are about to exit the YS to travel to the embryo proper and seed the different tissues (Boisset, 2010; Stremmel, 2018).

Flow cytometry is a well-established method for studying cell death through determination of the percentage of AnxV<sup>+</sup> and AnxV<sup>+</sup> PI<sup>+</sup> after labelling them with (AnxV) as measurement of apoptosis and (AnxV and PI) as indicator of secondary necrosis. We employed the method to measure BM and YS macrophages response to FasL and UV radiation. However, determination of the percentage and the type of cell death following stimulation and or infection may reveal more in-depth differences in YS and BM cell death response during microbial and immunological challenge. Furthermore, this may reveal more differences related to the nature of the two cell types as YS macrophages represent tissue macrophages that are long-lived while BM macrophages represent monocyte derived macrophages that are recruited to tissues in case of infection to provide defence functions and die shortly after the performing their purpose. For instance, investigation of cell death after stimulation with MSU crystals or other inflammasome stimuli will be valuable to decipher differences in pyroptosis, the inflammasome specific form of cell death.

We investigated NLRP3 both canonical and not canonical. However, neither other NLRs inflammasomes such as NLRP1 and NLRC4 inflammasomes nor AIM2 inflammasomes were studied. In the light of these limitations, we cannot conclude whether activation of other inflammasomes is impaired in YS macrophages. Besides, no in vivo investigation was performed to further investigate our in vitro findings due to the in vivo system

complexity and the lack of scientific tools, as distinguishing cells from different origin in the tissues is not an easy task due to the microenvironment reprogramming. However, mice models of myeloid cells depletion such as CD169-DTR, macrophages depletion such as CD11b-DTR and gene deficiency models such as Csf1r-KO seem to represent valuable tools for further investigating these findings in inflammation settings.

## 4.2 Results

Macrophages play a fundamental role in both inflammation and tissue homeostasis, defending the body against infection besides carrying out vital tissue-specific functions. Nevertheless, they are also involved in the pathology of several illnesses such as malignancies and diverse inflammatory conditions. Currently, it is known that macrophages of different developmental origin i.e., YS and BM co-exist and function in conjunction with each other in the steady state. In case of microbial challenge or inflammation the diversity is enhanced further as blood monocytes are recruited to tissues and differentiate into macrophages (Ginhoux, 2016). Moreover, tissue resident macrophages are long-lived; potentially they are maintained throughout life independently of BM progenitors.

The co-existence of macrophages of different ontogeny, i.e., YS and BM, in most tissues necessitates the investigation of its impact on macrophage function. As the phenotype and functions of macrophages are largely modulated by the tissue of residence, the heterogeneity among macrophage populations in a defined tissue persists be implicated to their ontogeny (DR, 2014; Stergachis, 2013). Nonetheless, how macrophage origin and environment integrate to define gene expression networks and functions remains indeterminate. Understanding the influence of macrophages developmental origin and the microenvironment of the tissue of residence on macrophages is essential for designing therapeutic approaches to modulate macrophage functions at specific tissues and at specific pathology settings.

In this study, we aimed to differentiate the cell-intrinsic programs and functions of YS and BM macrophages under defined conditions independently of the organ environment. Scientists have been hampered in addressing this question due to adaptation and re-programming of macrophages within tissues. To overcome these limitations, we established stable YS and BM Hoxb8 progenitor cells, which can be cultured and differentiated to mature macrophages as needed.

EMPs are described to be Kit+, CD41+, CD16/32+ (FCγII/III receptors), Cx3cr1- and CD45<sup>low</sup> and Runx1 dependent (J. Bertrand, 2005; McGrath, 2015; Perdiguero, 2015; Stremmel, 2018). Our YS ER-hoxb8 progenitors are KIT+ Cx3cr1-CD16/32+ in addition to their expression of Runx1. Hence, Hoxb8 system conserves the progenitor status of YS progenitors, and allows us to differentiate them into macrophages and compare them to their bone marrow counterparts under defined conditions without the influence of tissue micro-environment.

Through a broad variety of experimental approaches, including immunofluorescence analysis, flow cytometry, proteomics, transcriptomics, chemokine analyses and functional assays, we were able to draw the following conclusions: macrophage progenitors expand and differentiate within 5 days into mature macrophages independently of their cellular origin. These macrophages express a very similar panel of basic macrophage markers and they are equally capable of phagocytosis. Moreover, they show a similar resistance to FasL and susceptibility to UV induced cell death. Nevertheless, various differences in their cell-intrinsic programs were recognized ensuing further analysis.

As from our transcriptomics and proteomics analysis, a large proportion of genes and proteins overlapped as expected. However numerous differentially expressed genes between macrophages of YS and BM origin were detected that link them to their developmental origin. On one hand, Fam129a encodes for the apoptosis-regulating protein Niban (Ji, 2012; Tang, 2019), which has recently been identified in human atherosclerotic plaques in a macrophage subpopulation with strong implications to be of BM origin (Winkels, 2018), was upregulated in BM hoxb8 macrophages. On the other hand,

clusterin (apolipoprotein J) RNA was more abundant in YS *hoxb8* macrophages. At the protein level, Clusterin has been shown to act as a binding partner of TREM2, which is significantly expressed in brain microglia that are exclusively of YS origin; which facilitates their uptake of amyloid-beta (Ginhoux, 2010; Turnbull, 2006; Yeh, 2016). In line with this, we identified the upregulation of Sal-like protein (SALL) 1 and 3, which have been globally linked to microglia development in both mouse and human (Bian, 2020; Mass, 2016).

By paying a closer look at our proteome and RNA sequencing data, Pycard (central protein in inflammasome pathway) and RIPK3, which is another protein playing a role in NLRP3 inflammasome activation, found to be downregulated in YS derived macrophages compared to their BM counterparts as well as reduced levels of SQSTM1. In addition, TGM2 and CD14 expression significantly increased after LPS stimulation in BM-derived macrophages in comparison to LPS stimulated YS macrophages. CD14, in association with TLR4, is involved in the inflammatory response to LPS stimulation, which is a process commonly associated with M1-like macrophages (Düewell, 2010b; Wright, 1990). All these findings drove us to inspect the inflammasome as an important part of the innate immunity, as well as the adaptive immune response modulation. In particular, we examined whether the observable differences at RNA and protein levels extend to functional properties. In order to do so, we stimulated our cells with canonical NLRP3 stimuli such as MSU, CH and Bil and non-canonical NLRP3 inflammasome stimulus such as *E. coli* OMV and measured IL1 $\beta$  secretion, which is considered as the hallmark for activation of inflammasome. Interestingly, IL1 $\beta$  secretion is reduced in YS derived macrophages in comparison to BM derived macrophages under stimulation with canonical and non-canonical NLRP3 stimuli, to a level (below the detection limit of our sensitive ELISA assay) comparable to non-stimulated and casp1/11 knock out macrophages that were used as control. These findings are consistent with the results from Lakhdari and colleagues (2019) where they compared F4/80<sup>HI</sup> YS macrophages to CD11b<sup>HI</sup> fetal liver derived macrophages at both mRNA and protein level. Indeed, when stimulation was

performed with LPS, IL1 $\beta$  expression was found to be restricted to CD11bHI fetal liver macrophages, but not detected in F4/80HI cells (Lakhdari, 2019). Moreover, authors demonstrated upregulation of other inflammatory response genes after LPS stimulation in CD11bHI I fetal liver macrophages, but not in F4/80HI yolk sac derived macrophages. Additionally, we employed immunoblotting technique to check the expression level of NLRP3, ASC (pycard) and Casp1 levels in YS and BM macrophages after MSU stimulation. Interestingly, their levels were higher in BM macrophages in comparison to YS macrophages. Although NLRP3 level increased after MSU stimulation in both YS and BM, which indicates the triggering of NF-kB signalling pathway activation (Shimada, 2011), it did not result in IL1b secretion in YS macrophages, which may be explained by the respectively lower pycard and casp1 levels.

Proinflammatory and non-inflammatory properties of BM and YS respectively are further confirmed with extracellular flux measurement. In fact, BM cells showed higher glycolytic levels in steady state and glycolysis increased further upon LPS stimulation that links them even more to inflammasome activation (Tannahill, 2013). Moreover, our YS macrophages resemble microglia; established YS derived tissue macrophages and alveolar macrophages in their utilization of the Oxidative Phosphorylation pathway, a pathway broadly linked to anti-inflammatory and tissue-regenerative phenotypes (Gimeno-Bayón, 2014; Kelly, 2015; OREN, 1963). YS macrophages show an increased dependence on oxidative phosphorylation for ATP production in contrary to their BM counterparts, which seem to bear a resemblance to M1 macrophages in their dependence on glycolysis for securing their energy supply. Additionally, the transcription factor Mafb, known to promote anti-inflammatory polarization and cholesterol efflux, was upregulated in YS-derived Hoxb8 macrophages (H, 2017). Finally, clusterin (apolipoprotein J), which has been associated with apoptotic cell clearance and matrix reorganisation, common properties of M2-like macrophages found to be upregulated in YS-derived Hoxb8 (Cunin, 2016; Shim, 2011).

Non inflammatory signature of YS could have various biological implications. For instance, as the mother's immune system represents a critical challenge to the fetus in the uterus. The development of immunologic tolerance and balance of the counter reactions of maternal immune response and fetal immune response against each other's antigens represents an important aspect for the completion of the pregnancy. Thus, colonization of the various organs of the growing embryos with non-inflammatory YS derived macrophages increases the survival chances of the embryos. Besides, it might play a role in development of immunologic tolerance towards food antigens and more importantly tolerance against normal bacterial flora. Similarly, presence of such macrophages in the tissues in the settings of chronic inflammation may support in balancing inflammatory versus repair responses that could results in a better outcome.

The reduced inflammatory properties of YS derived macrophages do not only apply to mouse but extend to human as well. In their study on human embryonic hematopoiesis, Bian and his colleagues showed that as macrophages develop towards microglia they lose the expression of the inflammatory transcription factors and at the same time the expression of tissue development and neurodevelopmental genes increases, the property that may pave the road for many therapeutic approaches and applied research in the field of inflammatory diseases (Bian, 2020).

Hence, the precise mechanism of inflammasome regulation in YS macrophages remains to be elucidated. Furthermore, studying how specific tissue macrophage characteristics are established and preserved and whether the ontogeny related functional difference maintained in vivo, regardless the influence of microenvironment; need to be further investigated in order to assist in unravelling the effect of environment, as opposed to cell ontogeny on macrophage cellular identity. Answering such questions may open a window for better understanding of macrophage heterogeneity and function with vital clinical relevance to chronic inflammation and other pathology outcome.

## 5. Conclusions

The findings of this study add to the growing body of research that indicates that the ontogeny of macrophages contributes to their cellular identity and reveals important functional differences in inflammasome activation and metabolism. Further complementary studies such as investigating whether the differences between YS and BM are maintained regardless of the tissue microenvironment and whether BM-derived macrophages replacing embryonic macrophages in case of inflammation can acquire functional and homeostatic properties of prior embryonic macrophages, will be crucial for the field of macrophage biology. Eventually, translating these findings to human macrophage biology may be crucial and may help with the design of suitable therapeutic interventions for inflammatory diseases and cancer where macrophages play a central role in determining clinical outcome.



## References

- Accarias, S., Sanchez, T., Labrousse, A., Ben-Neji, M., Boyance, A., Poincloux, R., ... Le Cabec, V. (2020). "Genetic engineering of Hoxb8-immortalized hematopoietic progenitors – a potent tool to study macrophage tissue migration." *Journal of Cell Science*, 133(5), jcs236703. <https://doi.org/10.1242/jcs.236703>
- Agostini, L., Martinon, F., Burns, K., McDermott, M. F., Hawkins, P. N., & Tschopp, J. (2004). "NALP3 forms an IL-1 $\beta$ -processing inflammasome with increased activity in Muckle-Wells autoinflammatory disorder." *Immunity*, 20(3), 319–325. [https://doi.org/10.1016/S1074-7613\(04\)00046-9](https://doi.org/10.1016/S1074-7613(04)00046-9)
- Albina, J. E., Mills, C. D., Henry, W. L., & Caldwell, M. D. (1990). "Temporal expression of different pathways of 1-arginine metabolism in healing wounds." *The Journal of Immunology*, 144(10).
- Allen, I. C., Scull, M. A., Moore, C. B., Holl, E. K., McElvania-TeKippe, E., Taxman, D. J., ... Ting, J. P. Y. (2009a). "The NLRP3 Inflammasome Mediates In Vivo Innate Immunity to Influenza A Virus through Recognition of Viral RNA." *Immunity*, 30(4), 556–565. <https://doi.org/10.1016/j.immuni.2009.02.005>
- Allen, I. C., Scull, M. A., Moore, C. B., Holl, E. K., McElvania-TeKippe, E., Taxman, D. J., ... Ting, J. P. Y. (2009b). "The NLRP3 Inflammasome Mediates In Vivo Innate Immunity to Influenza A Virus through Recognition of Viral RNA." *Immunity*, 30(4), 556–565. <https://doi.org/10.1016/j.immuni.2009.02.005>
- Aragane, Y., Kulms, D., Metze, D., Wilkes, G., Pöppelmann, B., Luger, T. A., & Schwarz, T. (1998). "Ultraviolet light induces apoptosis via direct activation of CD95 (Fas/APO-1) independently of its ligand CD95L." *Journal of Cell Biology*, 140(1), 171–182. <https://doi.org/10.1083/jcb.140.1.171>
- Bain, C. C., Bravo-Blas, A., Scott, C. L., Gomez Perdiguero, E., Geissmann, F., Henri, S., ... Mowat, A. M. I. (2014). "Constant replenishment from circulating monocytes maintains the macrophage pool in the intestine of adult mice." *Nature Immunology*, 15(10), 929–937. <https://doi.org/10.1038/ni.2967>
- Bauernfeind, F. G., Horvath, G., Stutz, A., Alnemri, E. S., MacDonald, K., Speert, D., ... Latz, E. (2009). "Cutting Edge: NF- $\kappa$ B Activating Pattern Recognition and Cytokine Receptors License NLRP3 Inflammasome Activation by Regulating NLRP3 Expression." *The Journal of Immunology*, 183(2), 787–791. <https://doi.org/10.4049/jimmunol.0901363>
- Behar, S. M., Martin, C. J., Booty, M. G., Nishimura, T., Zhao, X., Gan, H. X., ... Remold, H. G. (2011, May 9). "Apoptosis is an innate defense function of macrophages against Mycobacterium tuberculosis." *Mucosal Immunology*. Nature Publishing Group. <https://doi.org/10.1038/mi.2011.3>
- Bertrand, J., Giroux, Y. S., Golub, R., Klaine, M., Jalil, A., Boucontet, L., ... Cumano, A. (2005). "Characterization of purified intraembryonic hematopoietic stem cells as a tool to define their site of origin." *PNAS*, 102(1), 134–139. Retrieved from <https://doi.org/10.1073/pnas.0402270102>
- Bertrand, J. Y., Chi, N. C., Santoso, B., Teng, S., Stainier, D. Y. R., & Traver, D. (2010). "Haematopoietic stem cells derive directly from aortic endothelium during development." *Nature*, 464(7285), 108–111. <https://doi.org/10.1038/nature08738>
- Bertrand, J. Y., Giroux, S., Golub, R., Klaine, M., Jalil, A., Boucontet, L., ... Cumano, A. (2005). "Characterization of purified intraembryonic hematopoietic stem cells as a tool to define their site of origin." *Proceedings of the National Academy of Sciences of the United States of America*, 102(1), 134–139. <https://doi.org/10.1073/pnas.0402270102>
- Bhardwaj, A., Yang, Y., Ueberheide, B., & Smith, S. (2017). "Whole proteome analysis of human tankyrase knockout cells reveals targets of tankyrase-mediated degradation." *Nature Communications* 2017

- 8:1, 8(1), 1–13. <https://doi.org/10.1038/s41467-017-02363-w>
- Bian, Z., Gong, Y., Huang, T., Lee, C. Z. W., Bian, L., Bai, Z., ... Liu, B. (2020). “Deciphering human macrophage development at single-cell resolution.” *Nature*, 582(7813), 571–576. <https://doi.org/10.1038/s41586-020-2316-7>
- Boada-Romero, E., Martinez, J., Heckmann, B. L., & Green, D. R. (2020, July 1). “The clearance of dead cells by efferocytosis.” *Nature Reviews Molecular Cell Biology*. *Nature Research*. <https://doi.org/10.1038/s41580-020-0232-1>
- Boisset, J. C., Van Cappellen, W., Andrieu-Soler, C., Galjart, N., Dzierzak, E., & Robin, C. (2010). “In vivo imaging of haematopoietic cells emerging from the mouse aortic endothelium.” *Nature*, 464(7285), 116–120. <https://doi.org/10.1038/nature08764>
- Bonham, K. S., & Kagan, J. C. (2014, May 14). “Endosomes as platforms for NOD-like receptor signaling.” *Cell Host and Microbe*. *Cell Press*. <https://doi.org/10.1016/j.chom.2014.05.001>
- Buck, M. D., O’Sullivan, D., & Pearce, E. L. (2015, August 24). “T cell metabolism drives immunity.” *Journal of Experimental Medicine*. *Rockefeller University Press*. <https://doi.org/10.1084/jem.20151159>
- Cabron, A.-S., El azzouzi, K., Boss, M., Arnold, P., Schwarz, J., Rosas, M., ... Zunke, F. (2018). “Structural and Functional Analyses of the Shedding Protease ADAM17 in HoxB8-Immortalized Macrophages and Dendritic-like Cells.” *The Journal of Immunology*, 201(10), 3106–3118. <https://doi.org/10.4049/jimmunol.1701556>
- Cavaillon, J.-M. (2011). “The historical milestones in the understanding of leukocyte biology initiated by Elie Metchnikoff.” *Journal of Leukocyte Biology*, 90(3), 413–424. <https://doi.org/10.1189/jlb.0211094>
- Chen, M., Wang, H., Chen, W., & Meng, G. (2011). “Regulation of adaptive immunity by the NLRP3 inflammasome.” *International Immunopharmacology*, 11(5), 549–554. <https://doi.org/10.1016/j.intimp.2010.11.025>
- Cohen, J. J. (1993). “Apoptosis.” *Immunology Today*, 14(3), 126–130. [https://doi.org/10.1016/0167-5699\(93\)90214-6](https://doi.org/10.1016/0167-5699(93)90214-6)
- Covarrubias, A. J., Aksoylar, H. I., & Horng, T. (2015, August 1). “Control of macrophage metabolism and activation by mTOR and Akt signaling.” *Seminars in Immunology*. *Academic Press*. <https://doi.org/10.1016/j.smim.2015.08.001>
- Cox, J., Hein, M. Y., Luber, C. A., Paron, I., Nagaraj, N., & Mann, M. (2014). “Accurate Proteome-wide Label-free Quantification by Delayed Normalization and Maximal Peptide Ratio Extraction, Termed MaxLFQ.” *Molecular & Cellular Proteomics : MCP*, 13(9), 2513. <https://doi.org/10.1074/MCP.M113.031591>
- Cunin, P., Beauvillain, C., Miot, C., Augusto, J. F., Preisser, L., Blanchard, S., ... Delneste, Y. (2016). “Clusterin facilitates apoptotic cell clearance and prevents apoptotic cell-induced autoimmune responses.” *Cell Death and Disease*, 7(5). <https://doi.org/10.1038/cddis.2016.113>
- Davies, L., SJ, J., JE, A., & PR, T. (2013). “Tissue-resident macrophages.” *Nature Immunology*, 14(10), 986–995. <https://doi.org/10.1038/NI.2705>
- Desjardins, M., Huber, L. A., Parton, R. G., & Griffiths, G. (1994). “Biogenesis of phagolysosomes proceeds through a sequential series of interactions with the endocytic apparatus.” *Journal of Cell Biology*, 124(5), 677–688. <https://doi.org/10.1083/jcb.124.5.677>
- Di Ceglie, I., Ascone, G., van den Akker, G., Haecker, H., Haecker, G., van der Kraan, P., ... van Lent, P. (2016). “ER-HOXB8 cell line, a new tool for the study of osteoclasts in osteoarthritis.” *Osteoarthritis*

- and Cartilage, 24, S132. <https://doi.org/10.1016/j.joca.2016.01.257>
- Dinareello, C.A. (1995). "Blocking interleukin-1 in sepsis." *Journal of Endotoxin Research*, 2(3), 157–162. <https://doi.org/10.1177/096805199500200303>
- Dinareello, Charles A. (1998). "Interleukin-1 $\beta$ , interleukin-18, and the interleukin-1 $\beta$  converting enzyme." In *Annals of the New York Academy of Sciences* (Vol. 856, pp. 1–11). New York Academy of Sciences. <https://doi.org/10.1111/j.1749-6632.1998.tb08307.x>
- DR, W., & I, A. (2014). "The role of chromatin dynamics in immune cell development." *Immunological Reviews*, 261(1), 9–22. <https://doi.org/10.1111/IMR.12200>
- Duewell, P., Kono, H., Rayner, K. J., Sirois, C. M., Vladimer, G., Bauernfeind, F. G., ... Latz, E. (2010a). "NLRP3 inflammasomes are required for atherogenesis and activated by cholesterol crystals." *Nature*, 464(7293), 1357–1361. <https://doi.org/10.1038/nature08938>
- Duewell, P., Kono, H., Rayner, K. J., Sirois, C. M., Vladimer, G., Bauernfeind, F. G., ... Latz, E. (2010b). "NLRP3 inflammasomes are required for atherogenesis and activated by cholesterol crystals." *Nature*, 464(7293), 1357–1361. <https://doi.org/10.1038/nature08938>
- Edwards, J. P., Zhang, X., Frauwirth, K. A., & Mosser, D. M. (2006). "Biochemical and functional characterization of three activated macrophage populations." *Journal of Leukocyte Biology*, 80(6), 1298–1307. <https://doi.org/10.1189/jlb.0406249>
- Ekdahl, C. T. (2012). "Microglial activation-tuning and pruning adult neurogenesis." *Frontiers in Pharmacology*. <https://doi.org/10.3389/fphar.2012.00041>
- FADEEL, B., & ORRENIUS, S. (2005). "Apoptosis: a basic biological phenomenon with wide-ranging implications in human disease." *Journal of Internal Medicine*, 258(6), 479–517. <https://doi.org/10.1111/j.1365-2796.2005.01570.x>
- Fisher, G. J., Datta, S. C., Talwar, H. S., Wang, Z. Q., Varani, J., Kang, S., & Voorhees, J. J. (1996). "Molecular basis of sun-induced premature skin ageing and retinoid antagonism." *Nature*, 379(6563), 335–339. <https://doi.org/10.1038/379335a0>
- Flannagan, R. S., Jaumouillé, V., & Grinstein, S. (2012). "The Cell Biology of Phagocytosis." *Annual Review of Pathology: Mechanisms of Disease*. <https://doi.org/10.1146/annurev-pathol-011811-132445>
- Franchi, L., Eigenbrod, T., & Núñez, G. (2009). "Cutting Edge: TNF- $\alpha$  Mediates Sensitization to ATP and Silica via the NLRP3 Inflammasome in the Absence of Microbial Stimulation." *The Journal of Immunology*, 183(2), 792–796. <https://doi.org/10.4049/jimmunol.0900173>
- Gankema, H., Wensink, J., Guinee, P. A. M., Jansen, W. H., & Witholt, B. (1980). "Some characteristics of the outer membrane material released by growing enterotoxigenic *Escherichia coli*." *Infection and Immunity*, 29(2), 704–713.
- Ganz, T. (2012). "Macrophages and systemic iron homeostasis." *Journal of Innate Immunity*. <https://doi.org/10.1159/000336423>
- Gene, H. (1993). "Characterization of the *Xenopus*," 24.
- Gilad, E., Zingarelli, B., O'Connor, M., Salzman, A. L., Bertok, L., & Szabo, C. (1996). "Effects of radiodetoxified endotoxin on nitric oxide production in J774 macrophages and in endotoxin shock." *Journal of Endotoxin Research*, 3(6), 513–519. <https://doi.org/10.1177/096805199600300610>
- Gimeno-Bayón, J., López-López, A., Rodríguez, M. J., & Mahy, N. (2014). "Glucose pathways adaptation supports acquisition of activated microglia phenotype." *Journal of Neuroscience Research*, 92(6), 723–731. <https://doi.org/10.1002/jnr.23356>

- Ginhoux, F., Greter, M., Leboeuf, M., Nandi, S., See, P., Gokhan, S., ... Merad, M. (2010). "Fate mapping analysis reveals that adult microglia derive from primitive macrophages." *Science*. <https://doi.org/10.1126/science.1194637>
- Ginhoux, F., & Williams, M. (2016). "Tissue-Resident Macrophage Ontogeny and Homeostasis." *Immunity*. <https://doi.org/10.1016/j.immuni.2016.02.024>
- GLÜCKSMANN, A. (1951). "CELL DEATHS IN NORMAL VERTEBRATE ONTOGENY." *Biological Reviews*, 26(1), 59–86. <https://doi.org/10.1111/j.1469-185X.1951.tb00774.x>
- Gordon, S., & Pluddemann, A. (2013). "Tissue macrophage heterogeneity: Issues and prospects." *Seminars in Immunopathology*, 35(5), 533–540. <https://doi.org/10.1007/s00281-013-0386-4>
- Gosselin, D., Link, V. M., Romanoski, C. E., Fonseca, G. J., Eichenfield, D. Z., Spann, N. J., ... Glass, C. K. (2014). "Environment drives selection and function of enhancers controlling tissue-specific macrophage identities." *Cell*, 159(6), 1327–1340. <https://doi.org/10.1016/j.cell.2014.11.023>
- Gross, O., Poeck, H., Bscheider, M., Dostert, C., Hanneschläger, N., Endres, S., ... Ruland, J. (2009). "Syk kinase signalling couples to the Nlrp3 inflammasome for anti-fungal host defence." *Nature*, 459(7245), 433–436. <https://doi.org/10.1038/nature07965>
- Guo, H., Callaway, J. B., & Ting, J. P. Y. (2015, July 9). "Inflammasomes: Mechanism of action, role in disease, and therapeutics." *Nature Medicine*. Nature Publishing Group. <https://doi.org/10.1038/nm.3893>
- Guttenplan, K. A., & Liddel, S. A. (2018). "Play It Again, SAM: Macrophages Control Peripheral Fat Metabolism." *Trends in Immunology*. <https://doi.org/10.1016/j.it.2017.12.004>
- H, K. (2017). "The transcription factor MafB promotes anti-inflammatory M2 polarization and cholesterol efflux in macrophages." *Scientific Reports*, 7(1). <https://doi.org/10.1038/S41598-017-07381-8>
- Hardie, D. G. (2007). "AMP-activated/SNF1 protein kinases: conserved guardians of cellular energy." *Nature Reviews Molecular Cell Biology*, 8(10), 774–785. <https://doi.org/10.1038/nrm2249>
- Hashimoto, D., Chow, A., Noizat, C., Teo, P., Beasley, M. B., Leboeuf, M., ... Merad, M. (2013). "Tissue-resident macrophages self-maintain locally throughout adult life with minimal contribution from circulating monocytes." *Immunity*. <https://doi.org/10.1016/j.immuni.2013.04.004>
- Hesse, M., Modolell, M., La Flamme, A. C., Schito, M., Fuentes, J. M., Cheever, A. W., ... Wynn, T. A. (2001). "Differential Regulation of Nitric Oxide Synthase-2 and Arginase-1 by Type 1/Type 2 Cytokines In Vivo: Granulomatous Pathology Is Shaped by the Pattern of L-Arginine Metabolism." *The Journal of Immunology*, 167(11), 6533–6544. <https://doi.org/10.4049/jimmunol.167.11.6533>
- Hoeffel, G., & Ginhoux, F. (2015). "Ontogeny of tissue-resident macrophages." *Frontiers in Immunology*. <https://doi.org/10.3389/fimmu.2015.00486>
- Huang, C. F., Chen, L., Li, Y. C., Wu, L., Yu, G. T., Zhang, W. F., & Sun, Z. J. (2017). "NLRP3 inflammasome activation promotes inflammation-induced carcinogenesis in head and neck squamous cell carcinoma." *Journal of Experimental and Clinical Cancer Research*, 36(1), 116. <https://doi.org/10.1186/s13046-017-0589-y>
- Ji, H., Ding, Z., Hawke, D., Xing, D., Jiang, B. H., Mills, G. B., & Lu, Z. (2012). "AKT-dependent phosphorylation of Niban regulates nucleophosmin- and MDM2-mediated p53 stability and cell apoptosis." *EMBO Reports*, 13(6), 554–560. <https://doi.org/10.1038/embor.2012.53>
- Jo, E. K., Kim, J. K., Shin, D. M., & Sasakawa, C. (2016, March 1). "Molecular mechanisms regulating NLRP3 inflammasome activation." *Cellular and Molecular Immunology*. Chinese Soc Immunology. <https://doi.org/10.1038/cmi.2015.95>

- Junt, T., Moseman, E. A., Iannaccone, M., Massberg, S., Lang, P. A., Boes, M., ... Von Andrian, U. H. (2007). "Subcapsular sinus macrophages in lymph nodes clear lymph-borne viruses and present them to antiviral B cells." *Nature*. <https://doi.org/10.1038/nature06287>
- Kayagaki, N., Stowe, I. B., Lee, B. L., O'Rourke, K., Anderson, K., Warming, S., ... Dixit, V. M. (2015). "Caspase-11 cleaves gasdermin D for non-canonical inflammasome signalling." *Nature*, 526(7575), 666–671. <https://doi.org/10.1038/nature15541>
- Kelly, B., & O'Neill, L. A. J. (2015, July 4). "Metabolic reprogramming in macrophages and dendritic cells in innate immunity." *Cell Research*. Nature Publishing Group. <https://doi.org/10.1038/cr.2015.68>
- Keuper, M., Jastroch, M., Yi, C.-X., Fischer-Posovszky, P., Wabitsch, M., Tschöp, M. H., & Hofmann, S. M. (2014). "Spare mitochondrial respiratory capacity permits human adipocytes to maintain ATP homeostasis under hypoglycemic conditions." *The FASEB Journal*, 28(2), 761–770. <https://doi.org/10.1096/FJ.13-238725>
- Kieusseian, A., de la Grange, P. B., Burlen-Defranoux, O., Godin, I., & Cumano, A. (2012). "Immature hematopoietic stem cells undergo maturation in the fetal liver." *Development (Cambridge)*, 139(19), 3521–3530. <https://doi.org/10.1242/dev.079210>
- Kinchen, J. M., & Ravichandran, K. S. (2010). "Identification of two evolutionarily conserved genes regulating processing of engulfed apoptotic cells." *Nature*, 464(7289), 778–782. <https://doi.org/10.1038/nature08853>
- Kischkel, F. C., Hellbardt, S., Behrmann, I., Germer, M., Pawlita, M., Krammer, P. H., & Peter, M. E. (1995). "Cytotoxicity-dependent APO-1 (Fas/CD95)-associated proteins form a death-inducing signaling complex (DISC) with the receptor." *The EMBO Journal*, 14(22), 5579–5588. <https://doi.org/10.1002/j.1460-2075.1995.tb00245.x>
- Kissa, K., & Herbomel, P. (2010). "Blood stem cells emerge from aortic endothelium by a novel type of cell transition." *Nature*, 464(7285), 112–115. <https://doi.org/10.1038/nature08761>
- Klein, I., Cornejo, J. C., Polakos, N. K., John, B., Wuensch, S. A., Topham, D. J., ... Crispe, I. N. (2007). "Phagocytes\_\_Kupffer\_cell\_heterogeneity\_\_functional\_properties\_of\_bone\_marrowderived\_and\_\_sessile\_hepatic\_macrophages." *Blood*. <https://doi.org/10.1182/blood-2007-02-073841>
- Kohyama, M., Ise, W., Edelson, B. T., Wilker, P. R., Hildner, K., Mejia, C., ... Murphy, K. M. (2009). "Role for Spi-C in the development of red pulp macrophages and splenic iron homeostasis." *Nature*, 457(7227), 318–321. <https://doi.org/10.1038/nature07472>
- Kongsuwan, K., Allen, J., & Adams, J. M. (1989). "Expression of HOX-2.4 homeobox gene directed by proviral insertion in a myeloid leukemia." *Nucleic Acids Research*, 17(5), 1881–1892. <https://doi.org/10.1093/nar/17.5.1881>
- Kraemer, K. H. (1997). "Sunlight and skin cancer: Another link revealed." *Proceedings of the National Academy of Sciences of the United States of America*, 94(1), 11–14. <https://doi.org/10.1073/pnas.94.1.11>
- Krammer, P. H. (1998, January 1). "CD95(APO-1/Fas)-mediated apoptosis: Live and let die." *Advances in Immunology*. Academic Press Inc. [https://doi.org/10.1016/s0065-2776\(08\)60402-2](https://doi.org/10.1016/s0065-2776(08)60402-2)
- Kripke, M. L. (1990). "Photoimmunology." *Photochemistry and Photobiology*. Photochem Photobiol. <https://doi.org/10.1111/j.1751-1097.1990.tb08703.x>
- Lakhdari, O., Yamamura, A., Hernandez, G. E., Anderson, K. K., Lund, S. J., Oppong-Nonterah, G. O., ... Prince, L. S. (2019). "Differential Immune Activation in Fetal Macrophage Populations." *Scientific Reports*, 9(1), 1–13. <https://doi.org/10.1038/s41598-019-44181-8>

- Lavin, Y., Winter, D., Blecher-Gonen, R., David, E., Keren-Shaul, H., Merad, M., ... Amit, I. (2014). "Tissue-resident macrophage enhancer landscapes are shaped by the local microenvironment." *Cell*, 159(6), 1312–1326. <https://doi.org/10.1016/j.cell.2014.11.018>
- Le Daré, B., Ferron, P.-J., & Gicquel, T. (2021). "The Purinergic P2X7 Receptor-NLRP3 Inflammasome Pathway: A New Target in Alcoholic Liver Disease?" *International Journal of Molecular Sciences*, 22(4), 1–13. <https://doi.org/10.3390/ijms22042139>
- Lee, B. L., Stowe, I. B., Gupta, A., Kornfeld, O. S., Roose-Girma, M., Anderson, K., ... Kayagaki, N. (2018). "Caspase-11 auto-proteolysis is crucial for noncanonical inflammasome activation." *Journal of Experimental Medicine*, 215(9), 2279–2288. <https://doi.org/10.1084/jem.20180589>
- Lehtonen, A., Ahlfors, H., Veckman, V., Miettinen, M., Lahesmaa, R., & Julkunen, I. (2007). "Gene expression profiling during differentiation of human monocytes to macrophages or dendritic cells." *Journal of Leukocyte Biology*, 82(3), 710–720. <https://doi.org/10.1189/jlb.0307194>
- Liao, J., Kapadia, V. S., Brown, L. S., Cheong, N., Longoria, C., Mija, D., ... Savani, R. C. (2015). "ARTICLE The NLRP3 inflammasome is critically involved in the development of bronchopulmonary dysplasia." <https://doi.org/10.1038/ncomms9977>
- Lu, A., Magupalli, V., Ruan, J., Yin, Q., Maninjay, K., Vos, M., ... Egelman, E. H. (2014). "Unified Polymerization Mechanism for the Assembly of ASC-dependent Inflammasomes." *Cell*, 156(6), 1193–1206. <https://doi.org/10.1016/j.cell.2014.02.008>
- Luck, K., Kim, D.-K., Lambourne, L., Spirohn, K., Begg, B. E., Bian, W., ... Calderwood, M. A. (2020). "A reference map of the human binary protein interactome." *Nature* 2020 580:7803, 580(7803), 402–408. <https://doi.org/10.1038/s41586-020-2188-x>
- Luigi Franchi, Tatjana Eigenbrod, and G. N. (2009). "TNF- $\alpha$  Mediate Sensitization to ATP and Silica via the NLRP3 Inflammasome in the Absence of Microbial Stimulation." *J Immunol.*, 183(2), 792–796. Retrieved from <https://www.ncbi.nlm.nih.gov/pmc/articles/PMC2754237/>
- Luzio, J. P., Gray, S. R., & Bright, N. A. (2010). "Endosome-lysosome fusion." In *Biochemical Society Transactions* (Vol. 38, pp. 1413–1416). *Biochem Soc Trans.* <https://doi.org/10.1042/BST0381413>
- Martínez-Lorenzo, M. J., Anel, A., Gamen, S., Monleón, I., Lasierra, P., Larrad, L., ... Naval, J. (1999). "Activated Human T Cells Release Bioactive Fas Ligand and APO2 Ligand in Microvesicles." *The Journal of Immunology*, 163(3).
- Martinon, F., Burns, K., & Tschopp, J. (2002). "The Inflammasome: A molecular platform triggering activation of inflammatory caspases and processing of proIL- $\beta$ ." *Molecular Cell*, 10(2), 417–426. [https://doi.org/10.1016/S1097-2765\(02\)00599-3](https://doi.org/10.1016/S1097-2765(02)00599-3)
- Mass, E., Ballesteros, I., Farlik, M., Halbritter, F., Günther, P., Crozet, L., ... Geissmann, F. (2016). "Specification of tissue-resident macrophages during organogenesis." *Science*, 353(6304). <https://doi.org/10.1126/SCIENCE.AAF4238>
- McGrath, K. E., Frame, J. M., Fegan, K. H., Bowen, J. R., Conway, S. J., Catherman, S. C., ... Palis, J. (2015). "Distinct Sources of Hematopoietic Progenitors Emerge before HSCs and Provide Functional Blood Cells in the Mammalian Embryo." *Cell Reports*. <https://doi.org/10.1016/j.celrep.2015.05.036>
- Mills, C. D., Kincaid, K., Alt, J. M., Heilman, M. J., & Hill, A. M. (2000). "M-1/M-2 Macrophages and the Th1/Th2 Paradigm." *The Journal of Immunology*, 164(12), 6166–6173. <https://doi.org/10.4049/jimmunol.164.12.6166>
- Modolell, M., Corraliza, I. M., Link, F., Soler, G., & Eichmann, K. (1995). "Reciprocal regulation of the nitric oxide synthase/arginase balance in mouse bone marrow-derived macrophages by TH 1 and TH 2 cytokines." *European Journal of Immunology*, 25(4), 1101–1104.

<https://doi.org/10.1002/eji.1830250436>

- Moore, M. A. S., & Metcalf, D. (1970). "Ontogeny of the Haemopoietic System: Yolk Sac Origin of In Vivo and In Vitro Colony Forming Cells in the Developing Mouse Embryo." *British Journal of Haematology*, 18(3), 279–296. <https://doi.org/10.1111/j.1365-2141.1970.tb01443.x>
- Murray, P. J., & Wynn, T. A. (2011, November). "Protective and pathogenic functions of macrophage subsets." *Nature Reviews Immunology*. NIH Public Access. <https://doi.org/10.1038/nri3073>
- Muruve, D. A., Pétrilli, V., Zaiss, A. K., White, L. R., Clark, S. A., Ross, P. J., ... Tschopp, J. (2008). "The inflammasome recognizes cytosolic microbial and host DNA and triggers an innate immune response." *Nature*, 452(7183), 103–107. <https://doi.org/10.1038/nature06664>
- Muzio, M., Chinnaiyan, A. M., Kischkel, F. C., O'Rourke, K., Shevchenko, A., Ni, J., ... Dixit, V. M. (1996). "FLICE, a novel FADD-homologous ICE/CED-3-like protease, is recruited to the CD95 (Fas/APO-1) death-inducing signaling complex." *Cell*, 85(6), 817–827. [https://doi.org/10.1016/S0092-8674\(00\)81266-0](https://doi.org/10.1016/S0092-8674(00)81266-0)
- Nathan, C., & Shiloh, M. U. (2000). "Reactive oxygen and nitrogen intermediates in the relationship between mammalian hosts and microbial pathogens." *Proceedings of the National Academy of Sciences of the United States of America*, 97(16), 8841–8848. <https://doi.org/10.1073/pnas.97.16.8841>
- Nau, G. J., Richmond, J. F. L., Schlesinger, A., Jennings, E. G., Lander, E. S., & Young, R. A. (2002). "Human macrophage activation programs induced by bacterial pathogens." *Proceedings of the National Academy of Sciences of the United States of America*, 99(3), 1503. <https://doi.org/10.1073/PNAS.022649799>
- Newsholme, P., Curi, R., Gordon, S., & Newsholme, E. A. (1986). "Metabolism of glucose, glutamine, long-chain fatty acids and ketone bodies by murine macrophages." *Biochemical Journal*, 239(1), 121–125. <https://doi.org/10.1042/bj2390121>
- O'Sullivan, D., & Pearce, E. L. (2015, February 1). "Targeting T cell metabolism for therapy." *Trends in Immunology*. Elsevier Ltd. <https://doi.org/10.1016/j.it.2014.12.004>
- Okabe, Y. (2018). "Molecular control of the identity of tissue-resident macrophages." *International Immunology*, (May). <https://doi.org/10.1093/intimm/dxy019>
- OREN, R., FARNHAM, A. E., SAITO, K., MILOFSKY, E., & KARNOVSKY, M. L. (1963). "Metabolic patterns in three types of phagocytizing cells." *The Journal of Cell Biology*, 17(3), 487–501. <https://doi.org/10.1083/jcb.17.3.487>
- Orosz, A., Walzog, B., & Mócsai, A. (2021). "In Vivo Functions of Mouse Neutrophils Derived from HoxB8-Transduced Conditionally Immortalized Myeloid Progenitors." *The Journal of Immunology*, 206(2), 432–445. <https://doi.org/10.4049/jimmunol.2000807>
- P-Y Ting, J., Lovering, R. C., Alnemri, E. S., Bertin, J., Boss, J. M., Davis, B. K., ... Ward, P. A. (n.d.). "The NLR Gene Family: A Standard Nomenclature." <https://doi.org/10.1016/j.immuni.2008.02.005>
- Pace, J. L., Russell, S. W., Schreiber, R. D., Altman, A., & Katz, D. H. (1983). "Macrophage activation: Priming activity from a T-cell hybridoma is attributable to interferon- $\gamma$ ." *Proceedings of the National Academy of Sciences of the United States of America*, 80(12 I), 3782–3786. <https://doi.org/10.1073/pnas.80.12.3782>
- Palis, J., Robertson, S., Kennedy, M., Wall, C., & Keller, G. (1999). "Development of erythroid and myeloid progenitors in the yolk sac and embryo proper of the mouse." *Development*, 126(22), 5073–5084.
- Pear, W. S., Miller, J. P., Xu, L., Pui, J. C., Soffer, B., Quackenbush, R. C., ... Baltimore, D. (1998). "Efficient

- and Rapid Induction of a Chronic Myelogenous Leukemia-Like Myeloproliferative Disease in Mice Receiving P210 bcr/abl-Transduced Bone Marrow." *Blood*, 92, 3780–3792.
- Perdiguerro, E. G., & Geissmann, F. (2015). "The development and maintenance of resident macrophages." *Nature Immunology*, 17(1), 2–8. <https://doi.org/10.1038/ni.3341>
- Perkins, A. C., & Cory, S. (1993). "Conditional immortalization of mouse myelomonocytic, megakaryocytic and mast cell progenitors by the Hox-2.4 homeobox gene." *The EMBO Journal*, 12(10), 3835–3846. <https://doi.org/10.1002/j.1460-2075.1993.tb06062.x>
- Pitt, A., Mayorga, L. S., Stahl, P. D., & Schwartz, A. L. (1992). "Alterations in the protein composition of maturing phagosomes." *Journal of Clinical Investigation*, 90(5), 1978–1983. <https://doi.org/10.1172/JCI116077>
- Raggatt, L. J., & Partridge, N. C. (2010). "Cellular and molecular mechanisms of bone remodeling." *Journal of Biological Chemistry*. <https://doi.org/10.1074/jbc.R109.041087>
- Ramsay, G., & Cantrell, D. (2015). "Environmental and metabolic sensors that control T cell biology." *Frontiers in Immunology*. Frontiers Media S.A. <https://doi.org/10.3389/fimmu.2015.00099>
- Ravichandran, K. S., & Lorenz, U. (2007, November 21). "Engulfment of apoptotic cells: Signals for a good meal." *Nature Reviews Immunology*. Nature Publishing Group. <https://doi.org/10.1038/nri2214>
- Redecke, V., Wu, R., Zhou, J., Finkelstein, D., Chaturvedi, V., High, A. A., & Häcker, H. (2013). "Hematopoietic progenitor cell lines with myeloid and lymphoid potential." *Nature Methods*. <https://doi.org/10.1038/nmeth.2510>
- Rehemtulla, A., Hamilton, C. A., Chinnaiyan, A. M., & Dixit, V. M. (1997). "Ultraviolet radiation-induced apoptosis is mediated by activation of CD-95 (Fas/APO-1)." *Journal of Biological Chemistry*, 272(41), 25783–25786. <https://doi.org/10.1074/jbc.272.41.25783>
- Roberts, A. W., Lee, B. L., Deguine, J., John, S., Shlomchik, M. J., & Barton, G. M. (2017). "Tissue-Resident Macrophages Are Locally Programmed for Silent Clearance of Apoptotic Cells." *Immunity*, 47(5), 913-927.e6. <https://doi.org/10.1016/j.immuni.2017.10.006>
- Roberts, A. W., Popov, L. M., Mitchell, G., Ching, K. L., Licht, D. J., Golovkine, G., ... Cox, J. S. (2019). "Cas9+ conditionally-immortalized macrophages as a tool for bacterial pathogenesis and beyond." *ELife*, 8. <https://doi.org/10.7554/eLife.45957.001>
- Sándor, K., Daniel, B., Kiss, B., Kovács, F., & Szondy, Z. (2016). "Transcriptional control of transglutaminase 2 expression in mouse apoptotic thymocytes." *Biochimica et Biophysica Acta - Gene Regulatory Mechanisms*, 1859(8), 964–974. <https://doi.org/10.1016/j.bbagr.2016.05.011>
- Saul, S., Castelbou, C., Fickentscher, C., & Demaurex, N. (2019). "Signaling and functional competency of neutrophils derived from bone-marrow cells expressing the ER-HOXB8 oncoprotein." *Journal of Leukocyte Biology*, 106(5), 1101–1115. <https://doi.org/10.1002/JLB.2A0818-314R>
- Sawyer, R. T., Strausbauch, P. H., & Volkman, A. (1982). "Resident macrophage proliferation in mice depleted of blood monocytes by strontium-89 (Journal Article) | OSTI.GOV." *Laboratory Investigation*, 46(2), 165–170. Retrieved from <https://www.osti.gov/biblio/5294795-resident-macrophage-proliferation-mice-depleted-blood-monocytes-strontium>
- Scaffidi, C., Fulda, S., Srinivasan, A., Friesen, C., Li, F., Tomaselli, K. J., ... Peter, M. E. (1998). "Two CD95 (APO-1/Fas) signaling pathways." *EMBO Journal*, 17(6), 1675–1687. <https://doi.org/10.1093/emboj/17.6.1675>
- Schmidt, F. I., Lu, A., Chen, J. W., Ruan, J., Tang, C., Wu, H., & Ploegh, H. L. (2016). "A single domain antibody fragment that recognizes the adaptor ASC defines the role of ASC domains in

- inflammasome assembly." *Journal of Experimental Medicine*, 213(5), 771–790. <https://doi.org/10.1084/jem.20151790>
- Schulz, C., Perdiguero, E. G., Chorro, L., Szabo-Rogers, H., Cagnard, N., Kierdorf, K., ... Geissmann, F. (2012). "A lineage of myeloid cells independent of myb and hematopoietic stem cells." *Science*. <https://doi.org/10.1126/science.1219179>
- Seimon, T., & Tabas, I. (2009). "Mechanisms and consequences of macrophage apoptosis in atherosclerosis." *Journal of Lipid Research*, 50(Suppl), S382. <https://doi.org/10.1194/JLR.R800032-JLR200>
- Semenkovich, C. F. (2006, July 3). "Insulin resistance and atherosclerosis." *Journal of Clinical Investigation*. *J Clin Invest*. <https://doi.org/10.1172/JCI29024>
- Shi, J., Zhao, Y., Wang, K., Shi, X., Wang, Y., Huang, H., ... Shao, F. (2015). "Cleavage of GSDMD by inflammatory caspases determines pyroptotic cell death." *Nature*, 526(7575), 660–665. <https://doi.org/10.1038/nature15514>
- Shi, J., Zhao, Y., Wang, Y., Gao, W., Ding, J., Li, P., ... Shao, F. (2014). "Inflammatory caspases are innate immune receptors for intracellular LPS." *Nature*, 514(7521), 187–192. <https://doi.org/10.1038/nature13683>
- Shim, Y.-J., Kang, B.-H., Jeon, H.-S., Park, I.-S., Lee, K.-U., Lee, I.-K., ... Min, B.-H. (2011). "Clusterin induces matrix metalloproteinase-9 expression via ERK1/2 and PI3K/Akt/NF- $\kappa$ B pathways in monocytes/macrophages." *Journal of Leukocyte Biology*, 90(4), 761–769. <https://doi.org/10.1189/jlb.0311110>
- Shimada, K., Crother, T. R., Karlin, J., Chen, S., Chiba, N., Ramanujan, V. K., ... Ardit, M. (2011). "Caspase-1 Dependent IL-1 $\beta$  Secretion Is Critical for Host Defense in a Mouse Model of Chlamydia pneumoniae Lung Infection." *PLoS ONE*, 6(6), e21477. <https://doi.org/10.1371/journal.pone.0021477>
- Sochalska, M., Stańczyk, M. B., Użarowska, M., Zubrzycka, N., Kirschnek, S., Grabiec, A. M., ... Potempa, J. (2020). "Application of the in vitro HOXB8 model system to characterize the contributions of neutrophil-lps interaction to periodontal disease." *Pathogens*, 9(7), 1–13. <https://doi.org/10.3390/pathogens9070530>
- Stanley, E. R., & Chitu, V. (2014). "CSF-1 receptor signaling in myeloid cells." *Cold Spring Harbor Perspectives in Biology*, 6(6), 1–22. <https://doi.org/10.1101/cshperspect.a021857>
- Stein, M., Keshav, S., Harris, N., & Gordon, S. (1992). "Interleukin 4 potently enhances murine macrophage mannose receptor activity: A marker of alternative immunologic macrophage activation." *Journal of Experimental Medicine*, 176(1), 287–292. <https://doi.org/10.1084/jem.176.1.287>
- Steller, H. (1995). "Mechanisms and genes of cellular suicide." *Science*, 267(5203), 1445–1449. <https://doi.org/10.1126/science.7878463>
- Stergachis, A. B., Neph, S., Reynolds, A., Humbert, R., Miller, B., Paige, S. L., ... Stamatoyannopoulos, J. A. (2013). "Developmental Fate and Cellular Maturity Encoded in Human Regulatory DNA Landscapes." *Cell*, 154(4), 888–903. <https://doi.org/10.1016/J.CELL.2013.07.020>
- Stouch, A. N., McCoy, A. M., Greer, R. M., Lakhdari, O., Yull, F. E., Blackwell, T. S., ... Prince, L. S. (2016). "IL-1 $\beta$  and Inflammasome Activity Link Inflammation to Abnormal Fetal Airway Development." *The Journal of Immunology*, 196(8), 3411–3420. <https://doi.org/10.4049/jimmunol.1500906>
- Stouch, A. N., Zaynagetdinov, R., Barham, W. J., Stinnett, A. M., Slaughter, J. C., Yull, F. E., ... Prince, L. S. (2014). "I $\kappa$ B Kinase Activity Drives Fetal Lung Macrophage Maturation along a Non-M1/M2 Paradigm ." *The Journal of Immunology*, 193(3), 1184–1193.

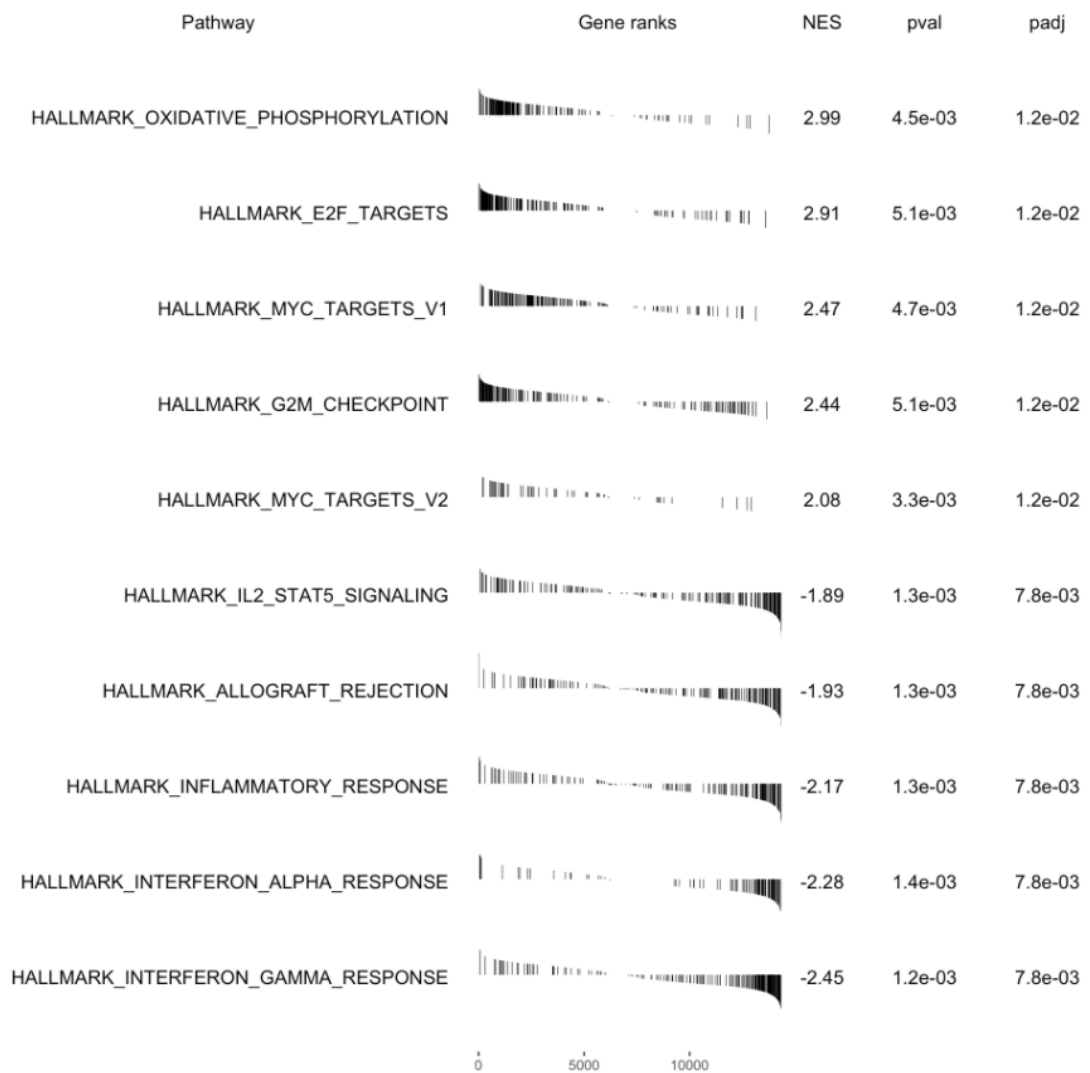
<https://doi.org/10.4049/jimmunol.1302516>

- Stremmel, C., Schuchert, R., Wagner, F., Thaler, R., Weinberger, T., Pick, R., ... Schulz, C. (2018). "Yolk sac macrophage progenitors traffic to the embryo during defined stages of development." *Nature Communications*, 9(1). <https://doi.org/10.1038/s41467-017-02492-2>
- Tamoutounour, S., Guilliams, M., MontananaSanchis, F., Liu, H., Terhorst, D., Malosse, C., ... Henri, S. (2013). "Origins and functional specialization of macrophages and of conventional and monocyte-derived dendritic cells in mouse skin." *Immunity*, 39(5), 925–938. <https://doi.org/10.1016/j.immuni.2013.10.004>
- Tanaka, M., Suda, T., Takahashi, T., & Nagata, S. (1995). "Expression of the functional soluble form of human Fas ligand in activated lymphocytes." *EMBO Journal*, 14(6), 1129–1135. <https://doi.org/10.1002/j.1460-2075.1995.tb07096.x>
- Tang, S., Wang, J., Liu, J., Huang, Y., Zhou, Y., Yang, S., ... Zhang, H. (2019). "Niban protein regulates apoptosis in HK-2 cells via caspase-dependent pathway." *Renal Failure*, 41(1), 455–466. <https://doi.org/10.1080/0886022X.2019.1619582>
- Tannahill, G. M., Curtis, A. M., Adamik, J., Palsson-Mcdermott, E. M., McGettrick, A. F., Goel, G., ... O'Neill, L. A. J. (2013). "Succinate is an inflammatory signal that induces IL-1 $\beta$  through HIF-1 $\alpha$ ." *Nature*, 496(7444), 238–242. <https://doi.org/10.1038/nature11986>
- Teitelbaum, S. L., & Ross, F. P. (2003, August 1). "Genetic regulation of osteoclast development and function." *Nature Reviews Genetics*. Nature Publishing Group. <https://doi.org/10.1038/nrg1122>
- Thompson, M. R., Kaminski, J. J., Kurt-Jones, E. A., Fitzgerald, K. A., Kaminski@umassmed, J., Edu, J. J. K., ... Edu, E. A. K. (2011). "Pattern Recognition Receptors and the Innate Immune Response to Viral Infection." *Viruses*, 3, 920–940. <https://doi.org/10.3390/v3060920>
- Turnbull, I. R., Gilfillan, S., Cella, M., Aoshi, T., Miller, M., Piccio, L., ... Colonna, M. (2006). "Cutting Edge: TREM-2 Attenuates Macrophage Activation." *The Journal of Immunology*, 177(6), 3520–3524. <https://doi.org/10.4049/jimmunol.177.6.3520>
- Vanaja, S. K., Russo, A. J., Behl, B., Banerjee, I., Yankova, M., Deshmukh, S. D., & Rathinam, V. A. K. (2016). "Bacterial Outer Membrane Vesicles Mediate Cytosolic Localization of LPS and Caspase-11 Activation." *Cell*, 165(5), 1106–1119. <https://doi.org/10.1016/j.cell.2016.04.015>
- Vats, D., Mukundan, L., Odegaard, J. I., Zhang, L., Smith, K. L., Morel, C. R., ... Chawla, A. (2006). "Oxidative metabolism and PGC-1 $\beta$  attenuate macrophage-mediated inflammation." *Cell Metabolism*, 4(1), 13–24. <https://doi.org/10.1016/j.cmet.2006.05.011>
- Wang, G. G., Calvo, K. R., Pasillas, M. P., Sykes, D. B., Häcker, H., & Kamps, M. P. (2006). "Quantitative production of macrophages or neutrophils ex vivo using conditional Hoxb8." *Nature Methods*. <https://doi.org/10.1038/nmeth865>
- Wang, H., Luo, Q., Feng, X., Zhang, R., Li, J., & Chen, F. (2018). "NLRP3 promotes tumor growth and metastasis in human oral squamous cell carcinoma." *BMC Cancer*, 18(1), 500. <https://doi.org/10.1186/s12885-018-4403-9>
- Wang, Y., Szretter, K. J., Vermi, W., Gilfillan, S., Rossini, C., Cella, M., ... Colonna, M. (2012). "IL-34 is a tissue-restricted ligand of CSF1R required for the development of Langerhans cells and microglia." *Nature Immunology*, 13(8), 753–760. <https://doi.org/10.1038/ni.2360>
- Wannamethee, S. G., Shaper, A. G., Lennon, L., & Morris, R. W. (2005). "Metabolic Syndrome vs Framingham Risk Score for Prediction of Coronary Heart Disease, Stroke, and Type 2 Diabetes Mellitus." *Archives of Internal Medicine*, 165(22), 2644–2650. <https://doi.org/10.1001/ARCHINTE.165.22.2644>

- Winkels, H., Ehinger, E., Vassallo, M., Buscher, K., Dinh, H. Q., Kobiyama, K., ... Wolf, D. (2018). "Atlas of the immune cell repertoire in mouse atherosclerosis defined by single-cell RNA-sequencing and mass cytometry." *Circulation Research*, 122(12), 1675–1688. <https://doi.org/10.1161/CIRCRESAHA.117.312513>
- Wright, S. D., Ramos, R. A., Tobias, P. S., Ulevitch, R. J., & Mathison, J. C. (1990). "CD14, a receptor for complexes of lipopolysaccharide (LPS) and LPS binding protein." *Science*, 249(4975), 1431–1433. <https://doi.org/10.1126/science.1698311>
- Wynn, T. A., & Barron, L. (2010). "Macrophages: Master Regulators of Inflammation and Fibrosis." *Seminars in Liver Disease*, 30(3), 245. <https://doi.org/10.1055/S-0030-1255354>
- Wynn, T. A., Chawla, A., & Pollard, J. W. (2013). "Origins and Hallmarks of Macrophages: Development, Homeostasis, and Disease." *Nature*, 496(7446), 445–455. <https://doi.org/10.1038/nature12034>
- Wynn, T. A., & Vannella, K. M. (2016). "Macrophages in Tissue Repair, Regeneration, and Fibrosis." *Immunity*. <https://doi.org/10.1016/j.immuni.2016.02.015>
- Xing, Y., Yao, X., Li, H., Xue, G., Guo, Q., Yang, G., ... Meng, G. (2017). "Cutting Edge: TRAF6 Mediates TLR/IL-1R Signaling-Induced Nontranscriptional Priming of the NLRP3 Inflammasome." *The Journal of Immunology*, 199(5), 1561–1566. <https://doi.org/10.4049/jimmunol.1700175>
- Yamada, M., Naito, M., & Takahashi, K. (1990). "Kupffer Cell Proliferation and Glucan-Induced Granuloma Formation in Mice Depleted of Blood Monocytes by Strontium-89." *Journal of Leukocyte Biology*, 47(3), 195–205. <https://doi.org/10.1002/jlb.47.3.195>
- Yeh, F. L., Wang, Y., Tom, I., Gonzalez, L. C., & Sheng, M. (2016). "TREM2 Binds to Apolipoproteins, Including APOE and CLU/APOJ, and Thereby Facilitates Uptake of Amyloid-Beta by Microglia." *Neuron*, 91(2), 328–340. <https://doi.org/10.1016/j.neuron.2016.06.015>
- Yi, C.-X., Walter, M., Gao, Y., Pitra, S., Legutko, B., Kälén, S., ... Tschöp, M. H. (2017). "ARTICLE TNF $\alpha$  drives mitochondrial stress in POMC neurons in obesity." *Nature Communications*, 8. <https://doi.org/10.1038/ncomms15143>
- Yona, S., Kim, K. W., Wolf, Y., Mildner, A., Varol, D., Breker, M., ... Jung, S. (2013). "Fate Mapping Reveals Origins and Dynamics of Monocytes and Tissue Macrophages under Homeostasis." *Immunity*. <https://doi.org/10.1016/j.immuni.2012.12.001>
- Zach, F., Mueller, A., & Gessner, A. (2015). "Production and Functional Characterization of Murine Osteoclasts Differentiated from ER-Hoxb8-Immortalized Myeloid Progenitor Cells." *PLOS ONE*, 10(11), e0142211. <https://doi.org/10.1371/journal.pone.0142211>
- Zani, I. A., Stephen, S. L., Mughal, N. A., Russell, D., Homer-Vanniasinkam, S., Wheatcroft, S. B., & Ponnambalam, S. (2015). "Scavenger receptor structure and function in health and disease." *Cells*. <https://doi.org/10.3390/cells4020178>
- Zhou, Y., & Ness, S. A. (2013). "Myb proteins: angels and demons in normal and transformed cells." *Front Biosci*, 16, 1109–1131.
- Zitvogel, L., Kepp, O., & Kroemer, G. (2010, March 19). "Decoding Cell Death Signals in Inflammation and Immunity." *Cell*. Elsevier. <https://doi.org/10.1016/j.cell.2010.02.015>

## Appendix

### The gene set enrichment analysis GSEA



## **Acknowledgements**

My sincere gratitude goes to my supervisor Prof. Dr. med. Christian Schulz who gave me the opportunity to work with him on this project, his scientific advice, knowledge and all the insightful discussions and suggestions were indispensable for the success of this project. I would also like to extend my gratitude to my thesis advisory committee members Prof. Dr. Barbara Schraml and Prof. Dr. rer. nat. Jörg Renkawitz and formal thesis advisory committee member Dr. rer. nat. Julia von Blume. I also wish to thank Mr. Michael Lorenz for all the suggestions and the scientific support during my PhD training. Many thanks to Elisabeth Raatz for all the professional and personal support. I want to as well thank my colleagues: Julia Winterhalter, Shaza El Nemr and Filip Prica who also helped, encouraged and contributed in various ways during my PhD. I also acknowledge, the support and contributions of Tien Cuong Kieu, Dr. Stephanie Regenfelder, Dominic van den Heuvel, Zeljka Sisic and Dr. Susanne Sauer. I would also like to acknowledge, Dr. Elke Hammer and Ms. Josefine Plocke for their efforts in generating the proteomic data, and their support in the data analysis, presentation and interpretation. As well as AG Lauber, AG Jastroch, AG Walzog and Dr. Tobias Straub for their productive collaboration. I would also like to thank the DFG for the funding during my Doctoral training and Dr. Verena Kochan for her support and guidance. Finally, my deepest gratitude goes to my family for their support and to my best friends for always being there for me.

## **Publications and scientific presentations**

### **Publications**

**Elhag, S.**, Stremmel, C., Zehrer, A., Plocke, J., Hennel, R., Keuper, M., ... Schulz, C. (2021). "Differences in Cell-Intrinsic Inflammatory Programs of Yolk Sac and Bone Marrow Macrophages." <https://doi.org/10.3390/cells10123564>

### **Scientific presentations**

June 2018	1 <sup>st</sup> TAC Meeting	Oral Presentation
November 2019	Scientific Retreat of IRTG914, Günzburg, Germany	Oral Presentation
October 2019	2 <sup>nd</sup> TAC Meeting	Oral Presentation

# Affidavit



## Affidavit

Elhag, Sara Rahamatalla Mohamed

\_\_\_\_\_  
Surname, first name

\_\_\_\_\_  
Address

I hereby declare, that the submitted thesis entitled

**The developmental origins of macrophages define their metabolic and inflammatory properties**

is my own work. I have only used the sources indicated and have not made unauthorised use of services of a third party. Where the work of others has been quoted or reproduced, the source is always given.

I further declare that the dissertation presented here has not been submitted in the same or similar form to any other institution for the purpose of obtaining an academic degree.

Munich, 20.05.2022  
\_\_\_\_\_  
Place, Date

Sara Elhag  
\_\_\_\_\_  
Signature doctoral candidate

\_\_\_\_\_  
Affidavit

20.05.2022

# Confirmation of congruency between printed and electronic version of the doctoral thesis



## Confirmation of congruency between printed and electronic version of the doctoral thesis

Doctoral Candidate: Sara Rahamatalla Mohamed Elhag

Address:

I hereby declare that the electronic version of the submitted thesis, entitled

**The developmental origins of macrophages define their metabolic and inflammatory properties**

is congruent with the printed version both in content and format.

Munich, 20.05.2022

Place, Date

Sara Elhag

Signature doctoral candidate

Congruency of submitted versions

Date: 20.05.2022